

# Free Water in Helicopter Fuel Tanks

Simon Koenig

# Lock Flag

This scientific work contains confidential data and information belonging to AIRBUS HELICOPTERS DEUTSCHLAND GmbH. Any transmission, publication or reproduction of this material – regardless of type, format or extent – without the prior express written consent of AIRBUS HELICOPTERS DEUTSCHLAND GmbH and the author is prohibited.

Simon Koenig  
31<sup>st</sup> October 2019

# Free Water in Helicopter Fuel Tanks

## A Computational Prediction Study

By

**S. Koenig**

in partial fulfilment of the requirements for the degree of

**Master of Science**  
in Aerospace Engineering

at the Delft University of Technology,  
to be defended publicly on Tuesday November 19, 2019 at 09:00.

Supervisors:	Dr. Alexis Bohlin	TU Delft
	Dr. Lionel Lollini	Airbus Helicopters
Thesis committee:	Dr. Piero Colonna	TU Delft
	Dr. Marc Gerritsma	TU Delft

An electronic version of this thesis is available at <http://repository.tudelft.nl/>.



# Preface

This thesis project would not have been possible without the consistent, prompt and thorough support of the principal supervisors at TU Delft (Dr. Alexis Bohlin) and Airbus Helicopters (Dr. Lionel Lollini), as well as the entire fuel systems engineering team at Airbus Helicopters, first and foremost the team facilitator, Kornelius Krahl. Therefore I would like to extend my sincere thanks to everyone who has made this project possible.

Furthermore I would like to thank my friends and family for their support and encouragement during what has proven to be one of my most challenging projects to date.

*S. Koenig  
Donauwörth, October 2019*

# Abstract

Water accumulating in the fuel tanks of any aircraft presents an unacceptable safety hazard and must therefore be removed by draining a sample from the tank sump daily, thereby removing any contamination. The accumulation of free water inside helicopter fuel tanks, which is due to a combination of physical phenomena, is difficult to assess and therefore not well known.

The purpose of this project is the development of a computational prediction method for water accumulation in helicopter fuel tanks. This model will deliver a better understanding of the physical mechanisms involved and allow prediction of the accumulated water quantity under given conditions. Ultimately, this may be used to substantiate a potential extension of the drainage interval.

A review of relevant literature delivered an overview of the parameters influencing water accumulation within the tank: ambient temperature and humidity, tank size and fill level and mission profile. Additionally, a model of the variation of ambient humidity with altitude was reviewed and incorporated into the newly developed model. During development of the model, it became apparent that in addition to the aforementioned parameters, the accumulation of water is also influenced by the fuel blend, specifically the degree of solubility of water in a particular blend.

The new model, given data corresponding to the parameters, is able to estimate the quantity of water accumulating in a helicopter fuel tank over any time frame, whether the helicopter is on the ground, flying, or a combination of both. A choice of climate types is offered to the user to represent the four most common mission types. The model was validated thoroughly by comparing its results to those produced by alternative models, among other techniques, as it was not possible to validate the model experimentally within the scope of a master thesis.

Using the model it was found that of the helicopter mission types considered, the most critical for water accumulation are transfer flights between land and oil/gas platforms, due to the high humidity, low altitude and low fuel levels during the return flight. The most significant parameters by far are the ambient humidity and fuel level. While maintaining an appropriate safety margin, the results strongly suggest that extending the drainage interval from daily to weekly would be feasible without impacting flight safety.

The body of this report consists of 100 pages with 63 figures and 28,012 words, equivalent to 40,612 words per the TUD thesis instructions.

# Contents

Lock Flag .....	2
Abstract .....	5
Contents .....	6
<b>1</b> Introduction .....	9
1.1 Context .....	9
1.2 Motivation .....	10
1.3 Research Objective .....	10
1.4 Structure .....	10
<b>2</b> Water Contained in Fuel .....	11
2.1 Dissolved Water .....	11
2.2 Free Water .....	15
2.3 Entrained Water .....	17
<b>3</b> Atmospheric Humidity .....	18
3.1 Humidity Metrics .....	18
3.2 ICAO Standard Atmosphere .....	22
3.3 NATO Climate Categories .....	23
3.4 Vertical Humidity Profile .....	25
3.5 Humid Air-Fuel Interaction .....	26
3.6 Surface Condensation .....	31
<b>4</b> Effects on Helicopter Systems .....	35
4.1 Gauging .....	35
4.2 Ice .....	38
4.3 Microbiological Contamination .....	38
<b>5</b> Water Avoidance and Management .....	40
5.1 Scavenging .....	40
5.2 Additives .....	41
5.3 Proposed Methods .....	42
<b>6</b> Mission Profiles .....	46
6.1 Fuel Temperature .....	46
6.2 Altitude and Range .....	50
<b>7</b> Certification Regulations .....	54
7.1 Paragraph 951c .....	54
7.2 Paragraph 971 .....	55
<b>8</b> Associated Models .....	56
8.1 Airbus Helicopters Step 1 Model .....	56
8.2 Triton .....	58
8.3 Wetterwald .....	59
8.4 Oreshenkov .....	60
<b>9</b> Interim Summary and Research Questions .....	61
9.1 Conclusions from Existing Research .....	61
9.2 Research Questions .....	62
<b>10</b> Modelling Overview .....	64
10.1 Specification .....	64
10.2 Approach .....	64
10.3 Architecture .....	65

<b>11</b>	Physical Model.....	66
11.1	Nomenclature.....	66
11.2	Assumptions.....	67
11.3	Theory.....	71
11.4	Verification & Limitations.....	77
<b>12</b>	Temporal Model.....	79
12.1	Theory.....	79
12.2	Assumptions.....	84
12.3	Limitations.....	85
<b>13</b>	Validation.....	86
13.1	Similarity.....	86
13.2	Degeneracy.....	90
13.3	Face validity.....	91
13.4	Sensitivity analysis.....	93
13.5	Summary of Validation.....	102
<b>14</b>	Results, Conclusions and Recommendations.....	103
14.1	Results.....	103
14.2	Conclusions.....	106
14.3	Recommendations.....	107
<b>15</b>	Bibliography.....	109
	Appendix.....	113





# 1

## Introduction

It is of critical importance that the supply of fuel to helicopter engine(s) be free of contamination; one of the most common contaminants encountered in aviation fuels is water [1]. The present study will therefore investigate the phenomena leading to the presence of water in helicopter fuel tanks. This chapter introduces the subject area, motivation and objective of the research project, as well as providing an overview of the report structure.

### 1.1 Context

All current production helicopters are powered by internal combustion engines, either reciprocating (piston), or gas turbine. Reciprocating engines are primarily used for single-engine training and personal helicopters such as the Robinson R22 [2], for their lower cost, while turbine engines are used in larger designs with one, two or three engines due to their better power to weight ratio. The standard fuel for turbine helicopters is Jet A-1, the most commonly used civil aviation fuel around the world [3].

The presence of water in a fuel tank can lead to a number of negative effects ranging in severity from inconvenient (fuel gauge failure) to hazardous (filter blockage by ice). The effects are described in detail in chapter 4. It is therefore important that the generation mechanisms are well understood.

To limit this contamination, helicopter fuel tanks must be checked for the presence of water by draining a small quantity of liquid from the drain valve of each fuel tank, before the first flight of each day [2] [4]. This procedure was introduced without publishing any supporting research and presents many inherent problems, including confirmation bias or even noncompliance. Confirmation bias refers to the human tendency of interpreting an observation as supporting the expected outcome, when objectively this is not the case. As a result of these two effects, accidents stemming from water in fuel tanks continue to occur. The frequency of these incidents appears inversely correlated with operator size (an operator is a person or organisation that owns or uses an aircraft). It has been theorized that this stems from daily checks being the pilot's responsibility in small (especially single-aircraft) operations; time pressure and lack of oversight encourage cutting corners.

## 1.2 Motivation

Even in 2019, fundamental understanding of the causes and controlling factors of water accumulation in fuel tanks is uncertain for airplanes [5], and practically zero for helicopters. No research has been published studying the topic with a focus on rotorcraft. This situation is described as a knowledge gap or research gap: an area of research which is both interesting and not fully understood.

With a deeper understanding of the processes and conditions leading to water accumulation, further research can eventually lead to the replacement of the rigid scheduled drainage interval, either by a different fixed interval depending on conditions, or by a variable interval calculated by on-board computers. The latter strategy is in use in the automotive sector, for estimating when certain engine maintenance actions are required based on the usage profile (as an example, stop-and-go city driving produces significantly more wear than a cross-country journey).

## 1.3 Research Objective

The objective of this research project is to review the available research concerning the interaction of water and jet fuel inside aircraft fuel tanks (the majority of which resulted from a 2008 accident involving a Boeing 777 due to fuel icing [6]), followed by the development of a model to predict the accumulation of water in a helicopter fuel tank based on knowledge of the ambient conditions.

The study will test the following hypothesis:

**“Developing a computational analysis can contribute to closing the knowledge gap surrounding the accumulation of water in helicopter fuel tanks by estimating the relationship between ambient conditions and accumulation”**

Estimates of the relationships between the conditions a helicopter is used in and the quantity of water accumulated within its fuel tanks will lead to an assessment of whether further research on this topic is of interest.

## 1.4 Structure

In chapters 2 through 9, the available literature on the subject of water accumulation in helicopter fuel tanks is examined. The chapters sequentially address the questions of **what** the subject is, **why** it is a problem, **how** it can be mitigated, **when** it occurs, **how much** water is allowed, and **who** has been researching it. In chapter 9, the literature is summarised and interim conclusions are drawn; from this, the research questions are formulated.

Chapters 10 through 14 present the assumptions, logic, performance and results of the model. Conclusions are drawn on the project, and recommendations for further research are made.

# 2

## Water Contained in Fuel

Water may exist in kerosene fuel as dissolved, free or entrained (emulsified) water [1]. Dissolved water refers to water that occupies the intermolecular spaces between fuel molecules [7]; the quantity of water that can be dissolved by a given quantity of fuel is dependent on temperature and fuel composition. Free water is an accumulation of liquid water, usually at the bottom of a fuel tank. Entrained water describes microscopic water droplets that are suspended, but not dissolved in the fuel; they may be created by agitation of a water-fuel mixture or by precipitation of dissolved water from the fuel [1] [7] [8]. A schematic representation of each form is given in Figure 1.

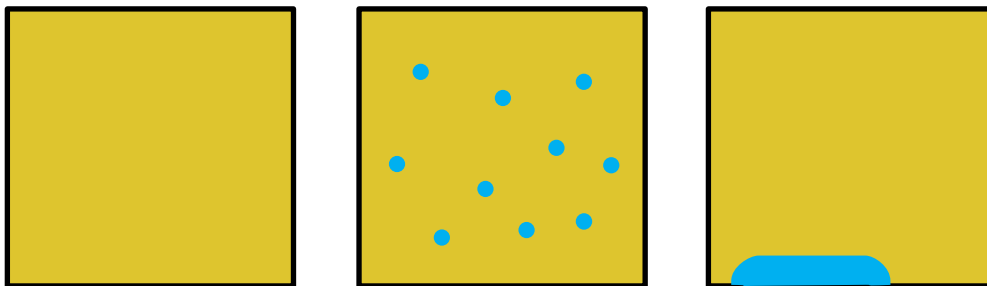


**Figure 1: From left to right: appearance of dissolved, entrained and free water in kerosene-based fuel. Entrained water gives the fuel a “hazy” or opaque appearance, while neither dissolved nor free water affect the translucent appearance of pure kerosene fuel.**

In this chapter, these three categories of water found in kerosene fuel and will be discussed, along with their respective interaction mechanisms with the fuel. An understanding of the physics underlying the presence of water is crucial to correctly predicting the evolution of water content over time, as the rate of transfer between the three states depends on the surrounding conditions.

### 2.1 Dissolved Water

Water dissolved in the fuel cannot be filtered or settled out, but a dehydration method involving onboard inert gas generating systems (OBIGGS), used in fixed-wing aircraft for fuel tank inerting, has been proposed [9]. Dissolved water is considered a normal trace content of kerosene fuel and evaporates during combustion; it is invisible to the naked eye. In steady state, the relative saturation level of the fuel will be proportional to the relative humidity of surrounding air; this is elaborated upon in section 3.5.

### 2.1.1 Degree of Solubility

Water is slightly soluble in hydrocarbon fuels [10], with a solubility ranging from approximately 10 to 150 ppmv (parts per million by volume) in the temperature ranges encountered within helicopter fuel tanks (Figure 2). The result of this phenomenon is that warm, water-saturated fuel releases free water as it cools, and may absorb water again when warmed. This was one of the subjects researched by Lam et al. [11].

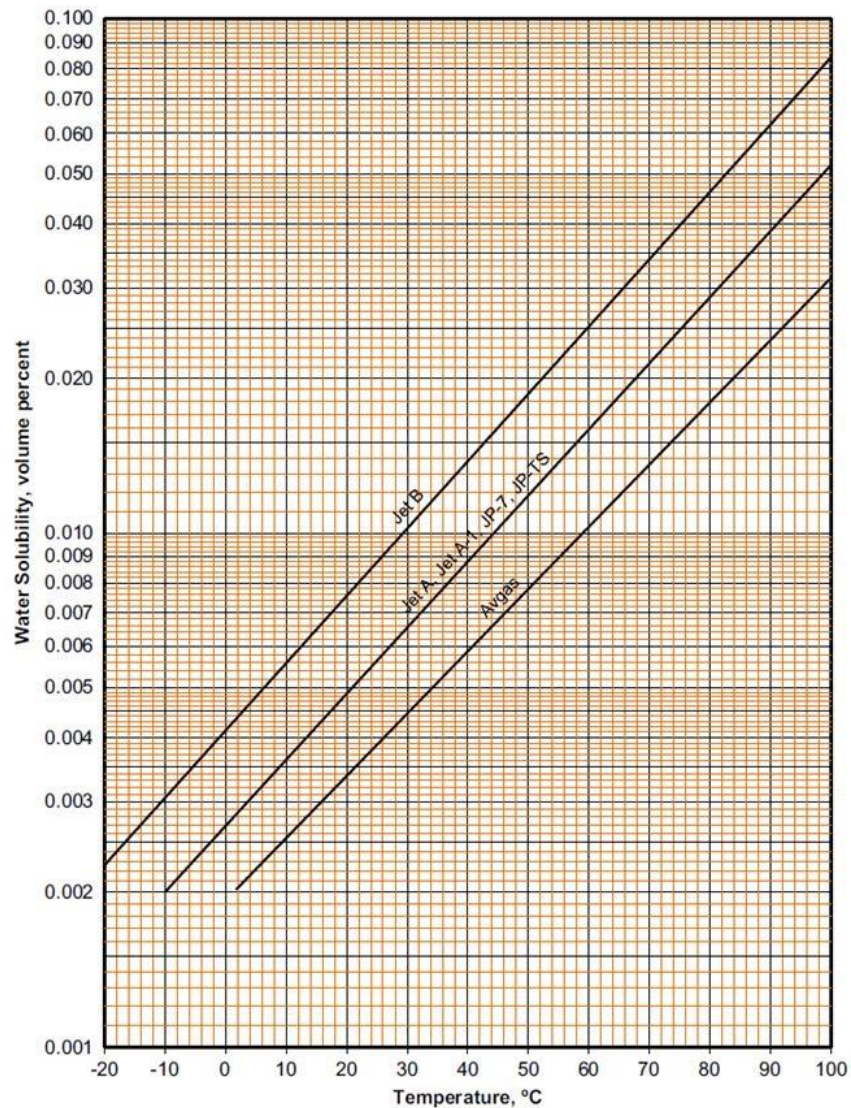


**Figure 2: Solubility of Water in Aviation Fuels as given by the Coordinating Research Council (CRC) [10]; average values for the given fuel types.**

The research studied jet fuels manufactured to several different specifications, namely:

- Jet A-1 (three suppliers, including one synthetic blend)
- No.3 Jet Fuel (Chinese equivalent to Jet A-1)
- TS-1 (Russian Jet A-1 substitute with better low-temperature properties and higher vapour pressure)
- JP-4 (equal mixture of kerosene and gasoline for low-temperature use) [3] [11]

After conditioning and dehydrating the fuel samples over silica gel, they were rehydrated to saturation and the water content measured at a range of temperatures from -5°C to 25°C. The results of these measurements, including the measurement uncertainties, are shown in Figure 3; for the Jet A-1 samples (Coryton, Air BP and Sasol), the solubility at 0°C ranges from 19.9 to 35.7 ppmm (parts per million by mass), compared to the standard value of 33.2 ppmm given by the CRC.

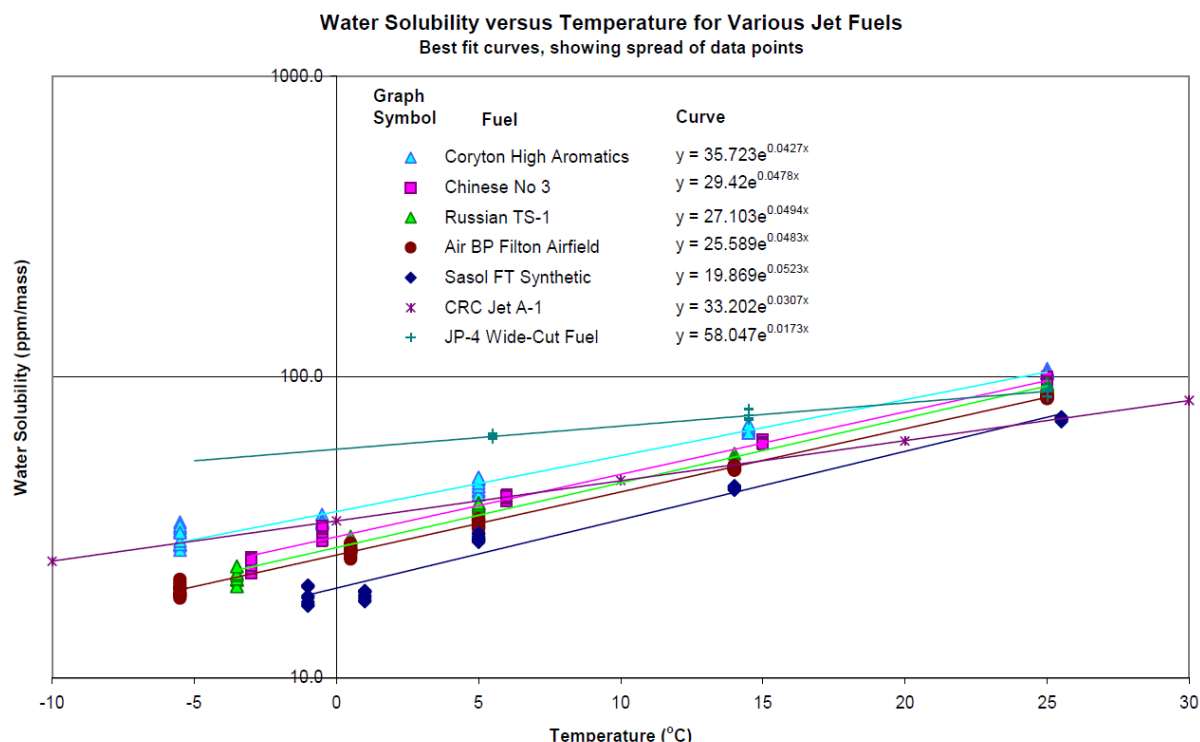


**Figure 3: Water solubility measurement results by Lam et al. [11], showing a large range of solubility (more than 100% variation in some cases) depending on fuel blend.**

The Sasol fuel, which is a synthetic blend, exhibits the lowest water solubility across nearly the entire range of temperatures tested. Research suggests that this is due to the composition of the fuel [10] [11] – the proportion of aromatic hydrocarbon species in synthetic fuels is typically lower than in natural fuels.

### 2.1.2 Significance of Fuel Composition and Synthetic Blends

An aromatic hydrocarbon is one which includes a number of carbon atoms connected in a ring, the simplest example of which is benzene ( $C_6H_6$ ). Low aromatic content is an inherent attribute of the Fischer-Tropsch process used to produce the Sasol fuel [1]. The aromatic content of kerosene-based aviation fuels ranges from 12% to 25% in practice; a minimum value of 8% is generally considered necessary. Below this threshold, elastomeric seals within the fuel system and engine may shrink, causing fuel leaks.

The solubility of water in aromatic hydrocarbons is not only generally higher than in other hydrocarbons, but also correspondingly more sensitive to temperature. Table 1 gives a comparison between benzene and iso-octane, a noncyclic hydrocarbon.

**Table 1: Water solubility in Iso-Octane and Benzene [7], showing the higher solubility of aromatic hydrocarbons**

Species name	Type	Formula	Sol., 10°C (ppmm)	Sol., 20°C (ppmm)
Iso-octane	Paraffin	C <sub>8</sub> H <sub>18</sub>	37	55
Benzene	Aromatic	C <sub>6</sub> H <sub>6</sub>	400	570

In this example, when cooled from 20°C to 10°C, one kg of saturated iso-octane would precipitate 18 mg of free water, while benzene would precipitate 170 mg under the same conditions. Therefore, fuels with a greater content of aromatic hydrocarbons exhibit correspondingly increased sensitivity of water solubility to temperature.

Figure 4 gives a comparison of the water solubility data given by the CRC [10], Lam [11], and Zhrebtsov [12]. The aromatic content of each fuel sample is given in the legend.

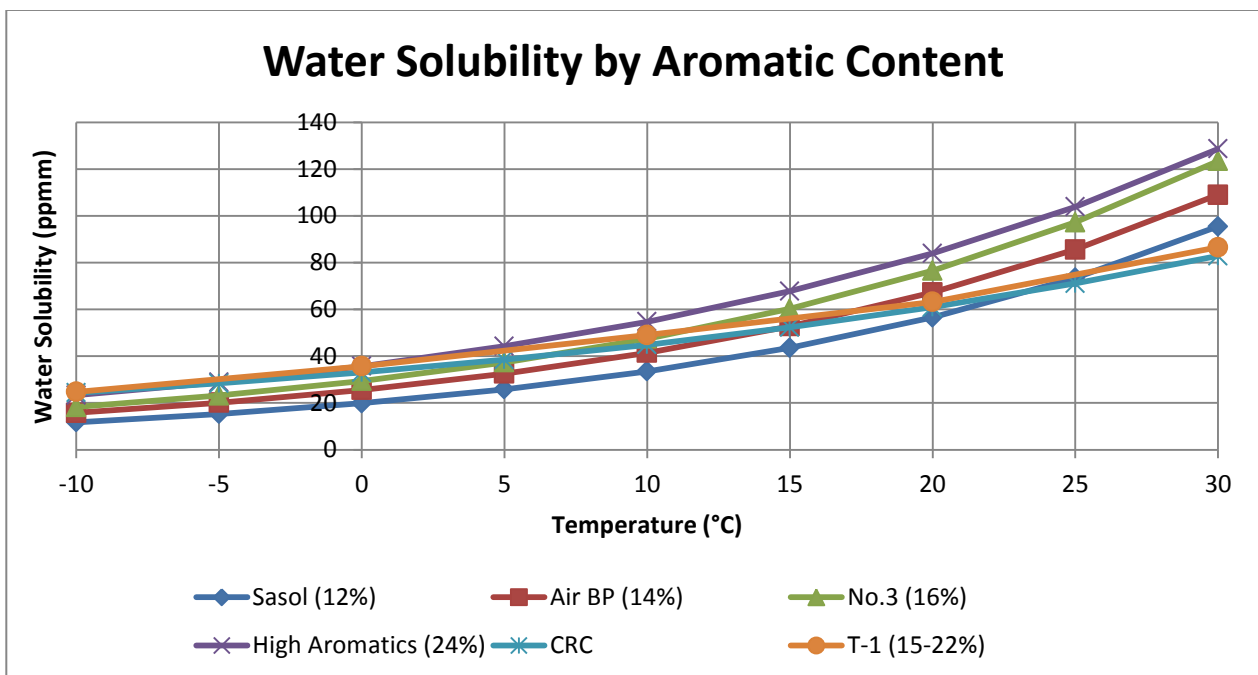


**Figure 4: Water solubility data for kerosene fuels with different aromatic content from several sources, showing positive correlation between aromatic content and water solubility.**

An important result of comparing the experimental data to that provided in the CRC handbook is that there is a strong indication of the solubility of water in jet fuels being significantly higher than presented by the CRC at moderate temperature. The difference reaches up to 50% at 30°C. This directly impacts the quantity of water entering a helicopter fuel tank when refuelling with warm, saturated fuel.

Although Zhrebtsov's experiment was conducted with fuel produced according to the Russian T-1 specification, this consists of kerosene with 15-22% aromatic content [12], and should therefore be comparable to the range of fuels tested by Lam with an aromatic content of 12-24%. In Figure 4, it can be observed that the T-1 results agree most closely with the gradient given by the CRC handbook, yet still suggest higher water solubility across the entire temperature range.

Another effect, suggested by recent research by Tien et al. [13] is that in the presence of free water, aromatic compounds from turbine fuels have a tendency to be partitioned into the free water phase, although the study was conducted on the aspect of ground water pollution by leaching compounds from jet fuels. Their results indicate that aromatic compounds partition into free water to different extents depending on the specific compound, but all exhibited a steady-state partitioning quantity of magnitude 0.1% or lower, so this is not a concern for the safe operation of helicopter engines.

When the quantity of water present in a fuel tank is greater than that which can be dissolved by the fuel, the excess exists in liquid form, either as free or entrained water.

## 2.2 Free Water

Free water refers to droplets of water too large to be suspended in an emulsion with fuel, which therefore accumulate at low points in the fuel system, primarily the fuel tank sump. It can be produced from a variety of sources including coalescence of entrained water (smaller droplets meeting and combining into larger drops), condensation of aerial humidity on cold tank walls, and rainwater ingress through leaking or poorly designed tank fittings.

### 2.2.1 Interfacial Tension

Interfacial tension (or interfacial energy) is a force present at the interface of two liquids, which acts to minimize the interface area; the magnitude of this force controls the rate of interaction between liquid water and fuel in a fuel tank. Its units are  $\frac{\text{force}}{\text{length}}$  or  $\frac{\text{energy}}{\text{area}}$ .

The origin of this phenomenon is explained with reference to Figure 5, which shows a liquid water phase bounded at the bottom by the tank wall, and at the top by a volume of fuel. In the middle of the water phase, molecule A has  $N_{bulk} = 6$  neighbouring molecules; if each intermolecular interaction has the energy  $-u$ , the total interaction energy  $U_{bulk} = -N_{bulk} \times u$ .

At the interface, molecule B has  $N_{surf} = 4$  neighbouring molecules; the total interaction energy  $U_{surf} = -N_{surf} \times u$ . Although the number of neighbouring molecules varies depending on particle size, a surface molecule will always have fewer neighbours than a continuum molecule.

Therefore, an excess energy  $\Delta U = U_{surf} - U_{bulk}$  exists at B, which represents the surface or interfacial energy. As an example, the interfacial energy between benzene and water is approximately  $35 \text{ mJ m}^{-2}$ . This is equivalent to the work that must be added (by agitation) to increase the interfacial area (e.g. to form an emulsion) [14].

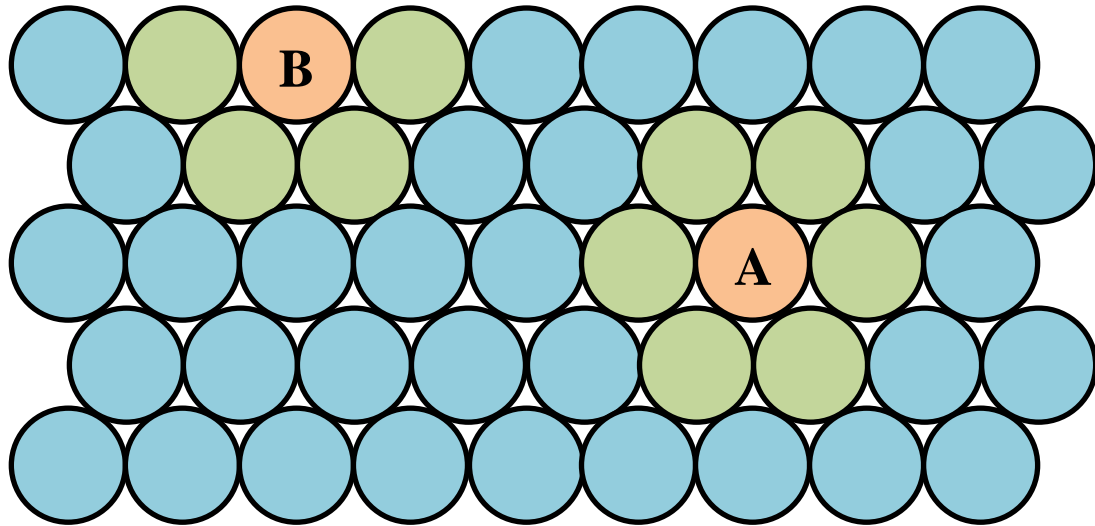


**Figure 5: Illustration of interfacial tension, showing a bulk molecule (A) and a surface molecule (B). Molecule B has fewer neighbouring molecules, leaving excess energy to produce surface tension.**

The addition of a surfactant reduces the interfacial tension [8], thereby encouraging miscibility. This is presumably the mechanism used by Aquarius (section 0).

The CRC handbook [10] states that interfacial tension is “*important to the movement of water into and out of turbine fuel, and is a key topic in fuel handling*”, but this statement is neither substantiated nor quantified. The interfacial tension between water and kerosene has been measured experimentally [15] but no research was found quantifying the relationship between the interfacial tension and the ability of water to be absorbed into the (unsaturated) fuel.

In 1970 Smith noted:

*“Contaminants in the fuel or water may change the interfacial tension ... from its normal value of 35 to 45 dynes/cm to 20 dynes/cm or lower. This makes it easier for the water to disperse into finer suspensions”.* [8]

( $\text{dyn cm}^{-1} \equiv \text{m} \text{m}^{-2}$ ).

As a finer suspension will exhibit greater stability and therefore a longer settling time, this may increase the ability of water to be re-dissolved into the fuel. At steady state, “*If undissolved water is present in the fuel or on the tank bottom, then the fuel will become fully saturated with water*” [8]. While this is a fundamentally interesting statement, it is crucial to know the associated time frame; if this process took place over the course of several weeks, it would not be relevant to changes occurring during a single flight. The rate of interaction across the interfacial boundary is discussed in the following section.

### 2.2.2 Rate of Interaction

The rate of interaction between free water and fuel is of interest as it dictates the degree of water saturation of the fuel at any given time. A very high rate of interaction implies that the presence of a small number of drops of free water in the tank might keep the fuel saturated at all times, while a low rate of interaction would reduce the importance of this effect.



Wetterwald et al. [9] make the assumption that free water cannot be re-dissolved in jet fuel once separated, based on this being prevented by interfacial tension; Wetterwald states in personal communication that this was supported by prior experience of his co-authors. The calculations therefore only consider humidity interaction between the fuel and air phases. For that particular study, neglecting water re-absorption was a conservative assumption because this increased the calculated free water quantity, causing a conservative under-estimation of water control effectiveness (M. Wetterwald, personal communication, 10th April 2019).

In 1962, Schatzberg [16] found that the dissolved water concentration in kerosene fuel stored over a layer of pure water reached steady state after 3-4 days, while bubbling dry air through the sample reduced this time to approximately 16 hours. This suggests that moisture transfer between air and fuel is indeed significantly faster than between liquid water and air, with the caveat that this comparison does not consider the agitation (mixing) effect provided by the air bubbles in the latter case. This is a very interesting result because it supports Wetterwald's reasoning that the interfacial tension impedes solution to such a degree as to make it negligible over the course of a flight of a few hours. Later, Polak similarly found that a period of 2-4 days was required to reach water saturation when storing fuel over a layer of water [17].

## 2.3 Entrained Water

Entrained water refers to droplets of water of microscopic scale, suspended within the fuel. This situation occurs either when free water and fuel are agitated, for example by being sucked through a fuel pump, or when water dissolved in the fuel precipitates out as the mixture cools. Entrained water droplets typically measure (much) less than 100  $\mu\text{m}$  in size and give the fuel sample a "cloudy" appearance [9].

At below freezing temperatures, these water droplets may freeze to form ice crystals which can block fuel handling equipment in severe cases. Entrained water does not pose a hazard to fuel systems and engines as long as it is homogeneously mixed, at low concentrations (chapters 4 and 7) and in liquid form.

The settling rate is positively correlated with the particle size, and is typically below  $1 \text{ m h}^{-1}$  in the context of an aircraft fuel tank [1], but is affected by the presence of surfactants to a degree where under certain conditions, a stable emulsion will be formed which does not settle at all. An emulsion implies greater interface area than two fully separated phases (section 2.2.1), which increases the rate of solution of water by the fuel, if the fuel is unsaturated. This will affect the location of the equilibrium formed between fuel, water and humid air, which will be discussed further in the following chapter.

# 3

## Atmospheric Humidity

When the helicopter is not being refuelled, humidity contained in the ambient air is the dominant pathway by which water enters a helicopter fuel tank. The relative significance of water entry via saturated fuel and via atmospheric humidity depends on both the usage of the helicopter (frequency of refuelling) and the ambient conditions; therefore, it is necessary to examine the range of ambient conditions encountered on the ground as well as inflight.

In this chapter, the variation of atmospheric composition over time as well as altitude will be discussed, followed by an overview of the processes leading to water transfer between the fuel tank and atmosphere. The vertical profile of atmospheric humidity is not as straightforward as it initially seems; particularly in the low altitudes at which the majority of helicopter missions take place, humidity is largely driven by local weather phenomena.

### 3.1 Humidity Metrics

Humidity refers to the presence of water vapour in air, and the maximum amount of water vapour that a given quantity of air can absorb is temperature-dependant. There are several ways to specify humidity, among them vapour pressure, specific humidity, relative humidity and dew point. These are introduced below.

#### 3.1.1 Partial Vapour Pressure

The partial vapour pressure of water in humid air is the pressure that would be measured if all the air molecules were removed from a control volume, leaving only water molecules. It has a temperature-dependent saturation value, given by the Tetens equation:

$$p_{H_2O}^{sat} = 610.78 \times e^{\left(\frac{17.2T}{237.3+T}\right)} \quad (1)$$

Where  $T$  is in °C and  $p$  is in Pa. The coefficients of the Tetens equation vary slightly depending on the conditions; those displayed above are chosen for best accuracy at temperatures between 0°C and 35°C. In this temperature range, they are accurate to 1 Pa [18].

### 3.1.2 Specific Humidity

Specific humidity (SH) is defined as the mass of water vapour present in a given mass of air, and is constant for a given unsaturated humid air mixture. SH is frequently given both in  $\text{g kg}^{-1}$  and  $\text{kg kg}^{-1}$ ; in calculations, it is most convenient to use the dimensionless mass ratio ( $\text{kg kg}^{-1}$ ). The maximum value of specific humidity under given conditions is referred to as the saturation specific humidity or  $SH^{sat}$  and is dependent on both temperature and ambient pressure.

Equation (2) is derived from the ideal gas law; 0.622 is the ratio of the individual gas constants for air and water vapour.

$$SH = 0.622 \times \frac{P_{H2O}}{P_{total}} \quad (2)$$

### 3.1.3 Relative Humidity

Relative humidity (RH) is the ratio between the actual and saturation values of either specific humidity or vapour pressure:

$$RH = \frac{SH}{SH^{sat}} = \frac{P_{H2O}}{P_{H2O}^{sat}} \quad (3)$$

When an air mass becomes saturated, some of the water condenses on a nearby surface (ground, body of water or aerial particulates) and may form a cloud in the presence of suitable cloud nuclei (aerial particulates).

### 3.1.4 Dew Point

The dew point is the temperature to which a humid air mixture must be cooled to reach saturation; saturation is reached once the saturation specific humidity has fallen to equal the actual specific humidity of the mixture. Knowing the water vapour pressure, equation (1) can be rearranged to calculate the dew point in °C:

$$T_{dp} = \frac{\ln\left(\frac{P_{H2O}}{610.78}\right) \times 237.3}{17.27 - \ln\left(\frac{P_{H2O}}{610.78}\right)} \quad (4)$$

The water vapour pressure can be found if RH and actual temperature are known, using equations (1) and (3).

The difference between the dew point and actual temperature is termed “spread”. The relationship between spread, temperature and humidity is shown in Figure 6.

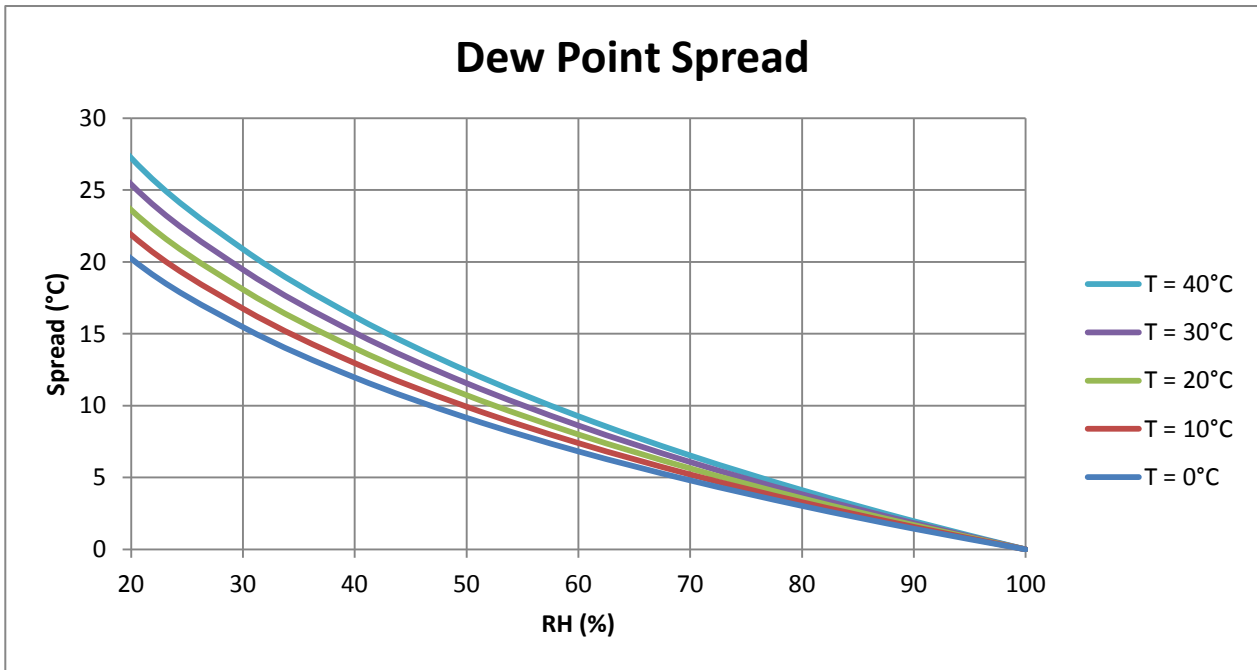


**Figure 6: Relationship between dew point spread, temperature and humidity. Spread is always zero at saturation.**

Dew point spread is important to surface condensation, discussed in section 3.6. It is an indicator for how readily condensation will occur on a nearby cool surface.

### 3.1.5 Humidity Cycle

The following cycle (Figure 7, Figure 8 and Table 2) is one mechanism how water can accumulate in fuel tanks over time; the water shed by the air during its saturated cooling collects underneath the fuel.

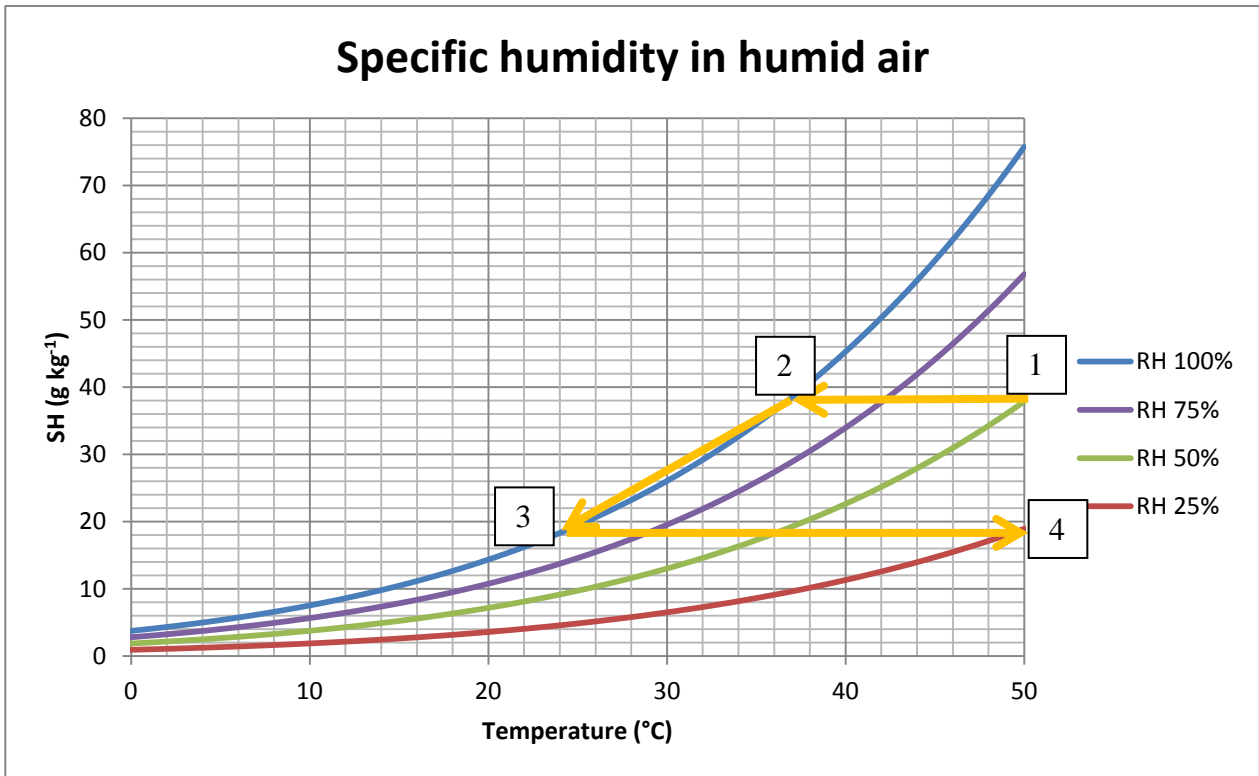


**Figure 7: Specific humidity cycle. From 1 to 4: cooling to saturation, saturated further cooling (condensation), and heating.**

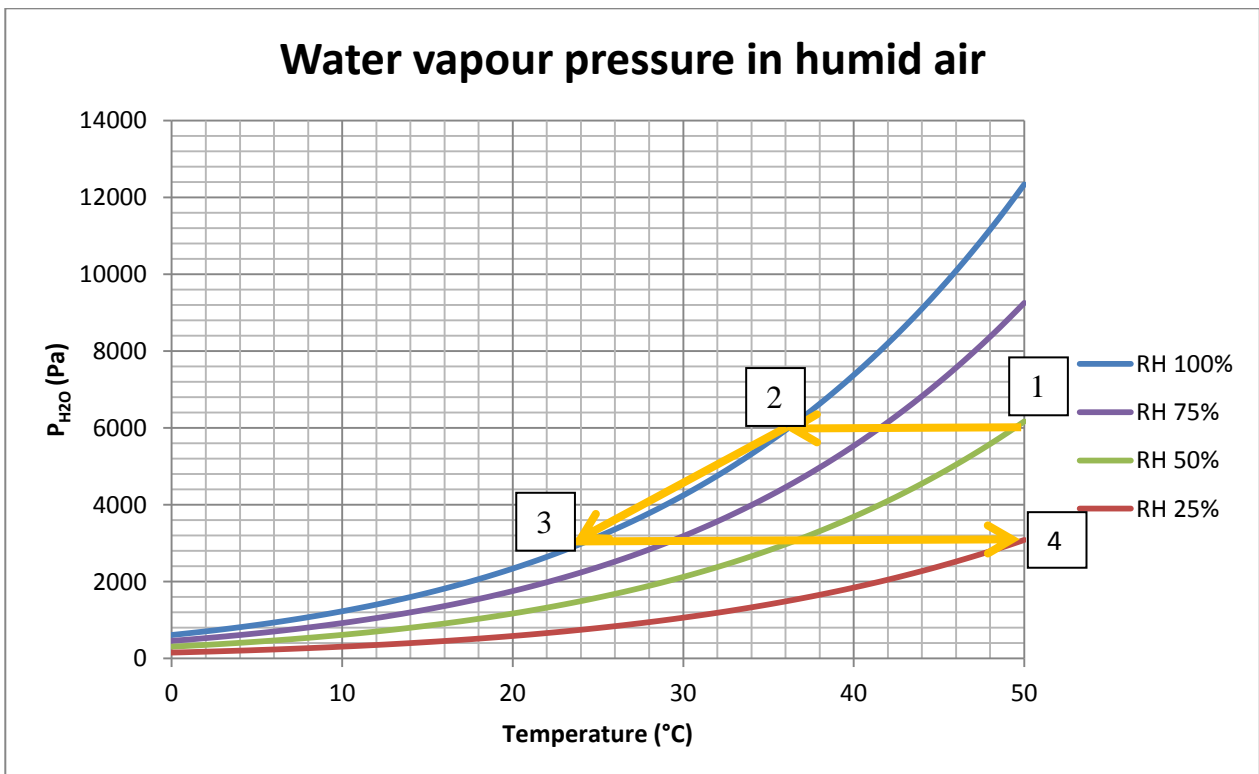


**Figure 8: Water vapour pressure cycle. From 1 to 4: cooling to saturation, saturated further cooling (condensation), and heating.**

**Table 2: Humid air cycle data**

<b>State</b>	<b>1</b>	<b>2</b>	<b>3</b>	<b>4</b>
<b>Temperature (°C)</b>	50	37	24	50
<b>Specific humidity (g kg<sup>-1</sup>)</b>	38	38	18	18
<b>Water vapour pressure (Pa)</b>	6000	6000	3000	3000
<b>Relative humidity (%)</b>	50	100	100	25
<b>Dew Point (°C)</b>	37	37	20	20

From the initial state (warm, unsaturated), the air first cools until reaching its dew point at point 2; if the air is cooled further, some of the water vapour must condense as the air can no longer “hold” it.

Relative humidity is constant at 100% from point 2 to point 3: the air is continually saturated. Although the RH is the same, the specific humidity decreases during this cooling process, as some of the vapour condenses out. If the air is now heated once more, the specific humidity is constant but the air’s ability to absorb moisture increases with temperature; the relative humidity therefore falls in accordance with equation (3).

Helicopters experience such temperature cycles both in flight (a change in altitude implies a change in temperature) and on the ground (temperature varies throughout a day). This is discussed in the following sections.

### **3.2 ICAO Standard Atmosphere**

The International Civil Aviation Organization (ICAO) defines a standard atmosphere to be used in aviation; this is used for aircraft performance calculations as well as calibrating barometric instruments. [19] This standard atmosphere describes average values of the atmospheric variables relevant to aviation, namely the altitude profiles of density, temperature and pressure; Figure 9 shows the three parameters covering the altitude range of helicopter operations.

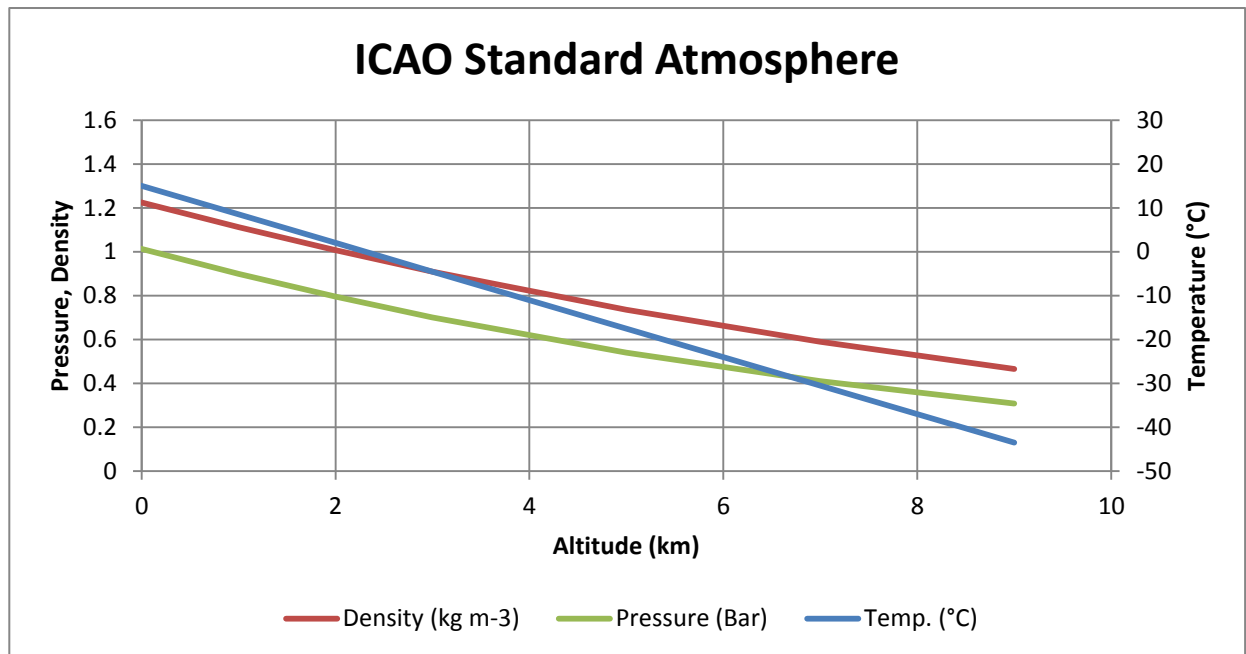


**Figure 9: Excerpt of the ICAO standard atmosphere at altitudes relevant to helicopters.**

Importantly for the subject of study, the ICAO atmosphere makes the assumption that relative humidity is always zero [19]. For aircraft performance calculations this assumption is actually non-conservative, because the presence of water vapour reduces the overall air density and thus reduces aircraft performance.

Although the impact is presumed to be small for the intended purpose of the data, knowledge of the aerial humidity is of critical importance for the subject of water accumulation in a fuel tank. It may be possible to extrapolate this when the conditions at ground level are known; some of these are discussed in the next section.

### 3.3 NATO Climate Categories

The North Atlantic Treaty Organization (NATO) defines a list of climatic conditions to be considered during the design of equipment for NATO forces [20]. At the time of writing, the document has been withdrawn without replacement, but the climatic categories are still used by Airbus internally to specify system performance requirements [21] (Figure 10).

These discrete climate categories can be useful when attempting to predict water accumulation by allowing the variable ambient conditions experienced by helicopters to be discretized into one or more climate categories per operator; many regions experience several different climate categories during the course of a year. A summary of the categories is given in Table 3; from this it follows that in geographic Europe, categories A3 and C0 will be encountered throughout, and categories C1, M2 and M3 may be encountered in certain sub-regions.

**Table 3: Summary of NATO climate categories, data extracted from [20].**

Cycle	Description	Regions	Temp. (°C)		RH (%)	
			min	max	min	max
A1	Extreme Hot Dry	Sahara, Middle East	32	49	3	8
A2	Hot Dry	Australia, Central Asia, Sahara	30	44	14	44
A3	Intermediate	Global	28	39	43	78
B1 (7d/y)	Wet Warm	Southeast Asia, Northern Brazil, Caribbean, Some Coastal Africa	24	24	100	100
B1 (358d/y)			23	32	66	88
B2	Wet Hot	Southeast USA, Brazil, China	26	35	74	100
B3	Humid Hot Coastal Desert	Red Sea Coast, Persian Gulf Coast	31	41	59	88
C0	Mild Cold	Global	-19	-6	100	100
C1	Intermediate Cold	USA, Eastern Europe, China	-32	-21	100	100
C2	Cold	Canada, Western Russia	-46	-37	100	100
C3	Severe Cold	Alaska	-51	-51	100	100
C4	Extreme Cold	Siberia, Greenland	-57	-57	100	100
M1	Marine Hot	Tropical Seas	29	48	21	67
M2	Marine Intermediate	Mid-Latitude Seas	25.5	35	53	100
M3	Marine Cold	High-Latitude Seas	-34	-23	100	100

For each of these climates, hourly values of temperature, humidity, and solar radiation are given at ground level. Some examples of this are shown in Figure 10; this information can be used to estimate water accumulation in a helicopter when it is on the ground, as well as potentially forming a basis for estimating the humidity at altitude.

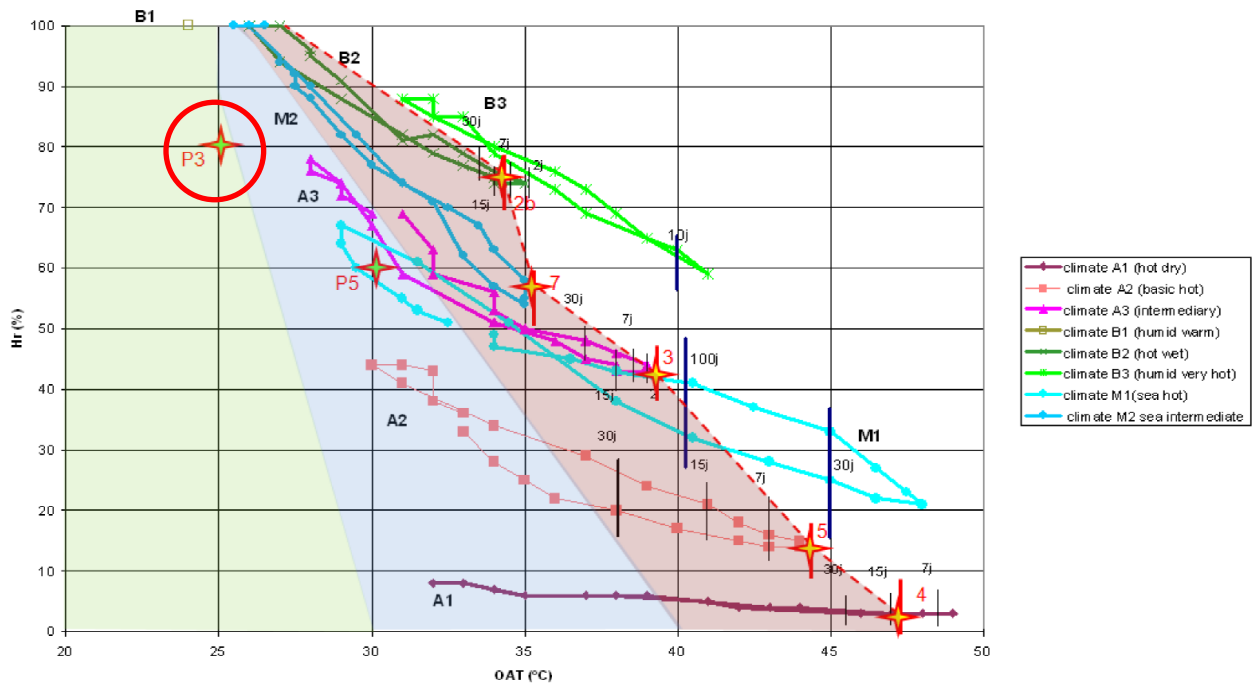


**Figure 10: Humidity-temperature diagram for several climatic categories from NATO [21]. P3 (circled red) is described as “typical north sea weather condition”, a common climate encountered by Airbus helicopters.**



The point “P3” (80% RH, 25°C) is highlighted. This condition is used within Airbus to denote typical North Sea weather, which is relevant as North Sea oil & gas platform shuttle flights are among the most popular civilian helicopter missions in Europe.

The next section will discuss the variation of humidity with altitude, which is important to modelling the conditions encountered by an aircraft in flight but not discussed in STANAG 2895.

### 3.4 Vertical Humidity Profile

It proves surprisingly difficult to find published generalised information concerning the variation of humidity with altitude, although of course one can infer the saturation humidity from the temperature profile of the ICAO standard atmosphere. It is therefore necessary to study different climates discretely.

A large proportion of helicopter missions are conducted at low altitudes (chapter 6), where humidity is strongly dependent on local weather phenomena (clouds and precipitation), so the vertical profiles are of limited applicability at low altitudes.

In 1990, Parameswaran and Krishna Murthy published a study which derived an exponential expression for the vertical profile of water vapour density [22] based on measured weather data in India. The expression is as follows:

$$\rho(h) = C \left[ (1 - \delta h_0) e^{-\frac{h}{H_1}} + \delta h_0 e^{-h_0/H_1} e^{-\frac{h-h_0}{H_2}} \right] \quad (5)$$

Where C is a surface water vapour density constant,  $h_0$  is the transition altitude,  $H_1$  and  $H_2$  are the vapour density scale height parameters above and below the transition altitude, and  $\delta h_0$  is a step function:

$$\delta h_0 = \begin{cases} 0, & h < h_0 \\ 1, & h \geq h_0 \end{cases} \quad (6)$$

With the exception of the step function, the parameters are location-specific and vary depending on the season, which limits the possibility of generalising their findings. The paper provides coefficient values pertaining to the profiles at several Indian weather stations, in which the transition altitude ranges from 1.8 to 2.3 km, while pointing out that Reitan in 1963 found the transition altitude to range from 2.2 to 3.0 km for stations in the USA. Reitan himself states that the parameters “*can be thought of as a characteristic of the area, and uniformity among areas in different climatic regimes would not be expected*” [23]. The parameters vary strongly even over the course of a single day; for example, for Delhi in May,  $H_1$  ranges from 2.9 to 3.4 km<sup>-1</sup>.

As an example, in order to make this model fit the data for a tropical ocean climate (see appendix) the values of C,  $h_0$ ,  $H_1$ , and  $H_2$  must be set to 24 g m<sup>-3</sup>, 0.6 km, 6.00 km<sup>-1</sup>, and 2.05 km<sup>-1</sup> respectively; compared to the values given by Parameswaran, this represents a much lower transition altitude and a much shallower high-altitude gradient. Standard atmosphere conditions are assumed for pressure and temperature. The results are shown below:

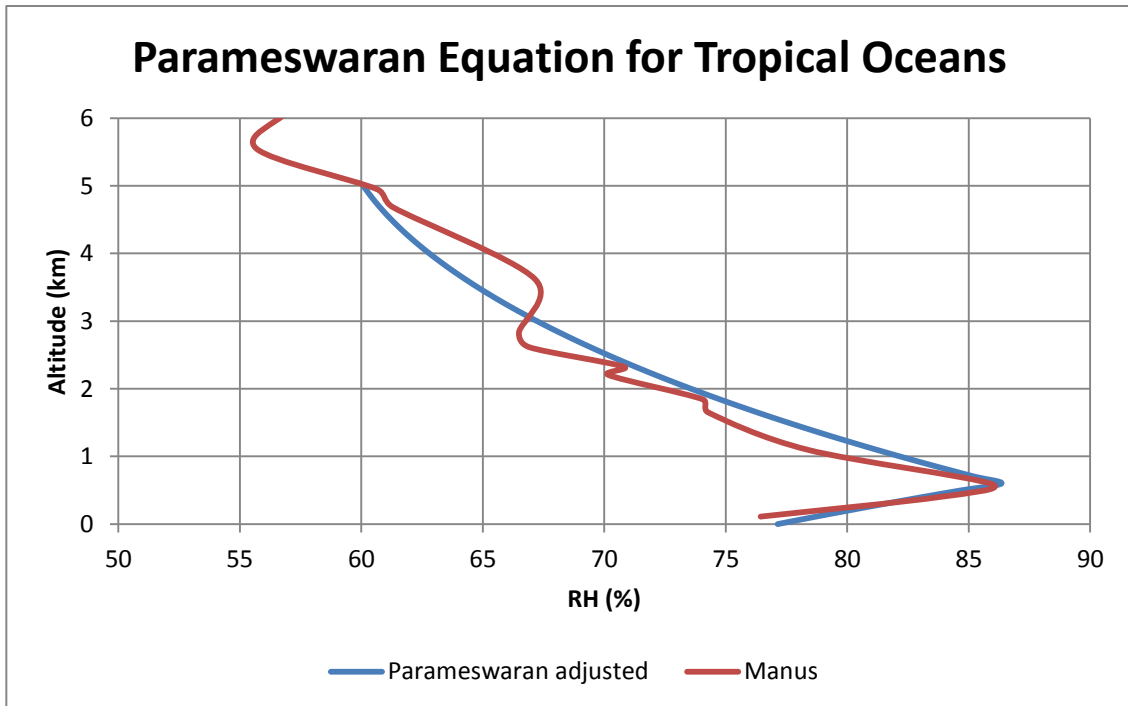


**Figure 11: Parameswaran relationship with coefficients to match tropical ocean climate (Manus island – see appendix).**

The large deviations in the required input parameters between the Indian and marine climates serve to illustrate the difficulty of generalising the vertical variation of humidity. However, it is possible to discretize the vertical profile for each climate category specified by NATO, by using Parameswaran’s equation and the ground-level humidity and temperature from NATO. It is important that the most reliable data possible is used, as the free water generation depends significantly on the ambient humidity, as explained below.

### 3.5 Humid Air-Fuel Interaction

Kerosene fuel exhibits reversible hygroscopicity, meaning it has the ability to both attract moisture from surrounding air and release moisture back to the air depending on the relative saturation of both phases [1]. This is an important mechanism that affects the production of free water within the fuel tank, as the fuel can be both hydrated if ambient humidity is high, and dehydrated if it is low. Both the location of the equilibrium and the time taken to reach it are of interest for modelling this process.

#### 3.5.1 Equilibrium

If warm, saturated fuel encounters cooler, non-saturated air (such as it might following a climb to cruise altitude), a continuous process may occur in which water evaporates from the fuel and increases the relative humidity of the air, which then condenses on cool surfaces within the fuel tank and runs down into the tank sump; water vapour from the fuel continually replenishes the humidity in the air until fuel and air have equal relative humidity [1]; depending on the magnitude of interfacial tension, the condensation may or may not accumulate in the tank sump.

The CRC states:

*“The quantity of water dissolved in aircraft fuels is determined by the partial pressure of water in the vapour space above the fuel. At relative humidity values less than 100%, the amount of water dissolved in fuel will be correspondingly less than saturation values in accordance with Henry’s Law.” [10]*

Henry’s law asserts that at equilibrium, the quantity of a gas dissolved in a liquid is proportional to the partial vapour pressure of the same species in the gas phase above the liquid [24]. This means that if the relative humidity of the air above the fuel were only 50%, then the amount of water dissolved within the fuel would also be 50% of its saturation quantity at steady state [1]; this is also supported by Smith [8], but applies only at uniform temperature. The CRC refers to vapour pressure equilibrium rather than relative humidity equilibrium, which is true also when temperature is not uniform.

When the two phases have different temperatures, the saturation vapour pressures are different, so the RH values may differ even though the vapour pressures are equalized. An example of this is shown in Figure 12:

$T_{\text{air}} = 27^{\circ}\text{C}$ $\text{RH}_{\text{air}} = 59\%$ $P_{\text{H}_2\text{O}} = 2093 \text{ Pa}$
$T_{\text{fuel}} = 20^{\circ}\text{C}$ $\text{RH}_{\text{fuel}} = 90\%$ $P_{\text{H}_2\text{O}} = 2093 \text{ Pa}$

**Figure 12: Illustration of fuel-air equilibrium with differing fuel and ullage temperatures**

In the case of different saturation vapour pressures, it is important to consider that the actual vapour pressure in air may be higher than the saturation pressure in fuel or vice versa; this might appear to indicate that warm, saturated air could force cooler fuel to become supersaturated. However Terada states that this is not the case: once one phase has reached saturation, net humidity transfer will be zero [25], as shown in Figure 13.

$T_{\text{air}} = 27^{\circ}\text{C}$ $\text{RH}_{\text{air}} = 90\%$ $P_{\text{H}_2\text{O}} = 3186 \text{ Pa}$
$T_{\text{fuel}} = 20^{\circ}\text{C}$ $\text{RH}_{\text{fuel}} = 100\%$ $P_{\text{H}_2\text{O}} = 2326 \text{ Pa}$

**Figure 13: Illustration of fuel-air equilibrium limited by fuel saturation**

It can be seen in this example that although the vapour pressure in air is far higher, the fuel has reached saturation and therefore no further (net) transfer will occur. This is important, as the rate of transfer is proportional to the difference in water vapour pressure between the phases; in this

example, the limiting vapour pressure difference is that between the actual and saturated vapour pressures in fuel, which is currently zero.

### 3.5.2 Rate

Smith, referring to 1963 work by Winter, Lewis and Larsen, claims that completely dry fuel in a shallow tank reaches equilibrium with the air above in a period of 3-4 hours [8]; the journal article referred to was unavailable for review, so this claim should be treated with caution.

Much more recently, Terada et al. [25] analytically determined a correlation to calculate the rate of water transfer between partially saturated fuel and air based on the interface area, water partial pressures in both phases, and a constant; equation (7).

$$\dot{n}_{H_2O} = KA\Delta p_{H_2O} \quad (7)$$

Where  $\dot{n}_{H_2O}$  is the rate of water transfer in moles per second,  $K$  is the transfer constant,  $A$  is the interface area and  $\Delta p_{H_2O}$  is the difference in partial pressure of water in fuel and air. Terada et al. estimate  $K$  to be in the order of magnitude of  $5e^{-7}$ .

Calculating the value of vapour pressure difference to be used requires some logic; Terada states for transfer from fuel to air:

$$\Delta p_{H_2O} = \begin{cases} p_{H_2O}^{fuel} - p_{H_2O}^{air}, & p_{H_2O}^{fuel} < p_{H_2O}^{air,sat} \\ p_{H_2O}^{air,sat} - p_{H_2O}^{air}, & p_{H_2O}^{fuel} \geq p_{H_2O}^{air,sat} \end{cases} \quad (8)$$

Essentially, the partial pressure of water in air can never exceed the saturation level, and the transfer rate is proportional to the difference between the vapour pressure in air and to the smaller of the saturation vapour pressure and the vapour pressure in fuel.

In the paper, only transfer from fuel to air is considered. However, in the case of helicopter fuel tanks, bidirectional transfer must be taken into account; this increases the logical complexity as there are now four pressures to consider (actual and saturation pressures in fuel and air respectively), with the selection of pressure difference depending on the relative magnitude of all four pressures. The saturation pressures of water in air and fuel differ if the two phases are at different temperatures as mentioned in section 3.5.1. A 2-level decision tree with 5 possible outcomes is required, shown in Figure 14.

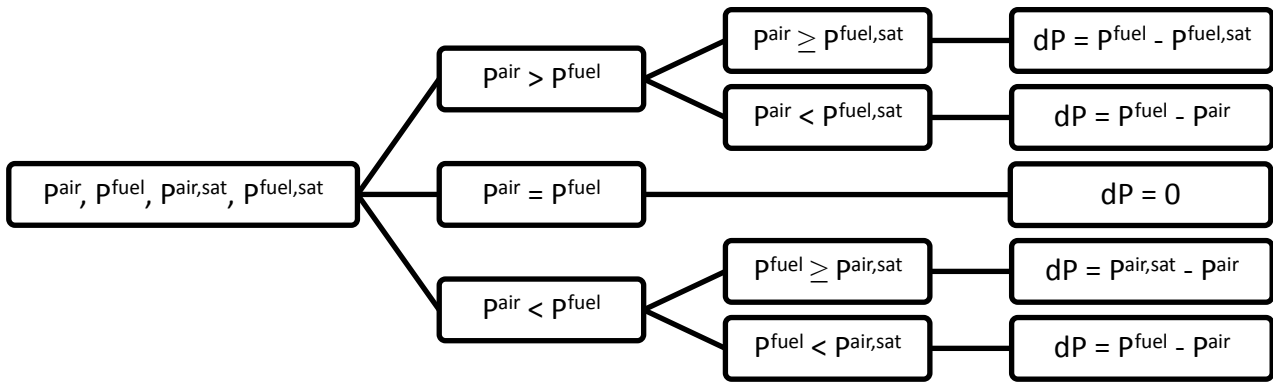


**Figure 14: Decision tree for vapour pressure difference between fuel and air, to be used when calculating fuel-ullage humidity exchange.**

The value of partial pressure difference (whether it is positive or negative) indicates the directionality of transfer. Importantly, this relationship cannot be directly used to calculate the rate of mass transfer between a bulk of fuel in contact with a bulk of air, due to the fact that diffusion of water within the fuel and air phases will not be instantaneous and therefore quickly become a limiting factor. The water vapour pressure in both phases will very quickly reach equilibrium close to the interface, at which point mass transfer slows as it is limited by the rate of water transport within each phase.

To estimate the rate of transfer when considering bulk fuel, it is useful to refer to the 2011 work of Merkulov et al. [26], who conducted an experiment with a fuel column of 96 cm height (which is representative of a small helicopter tank at ~50cm), above which dry air was maintained. Measuring the relative humidity of the fuel at various depths over time, the following results were found:

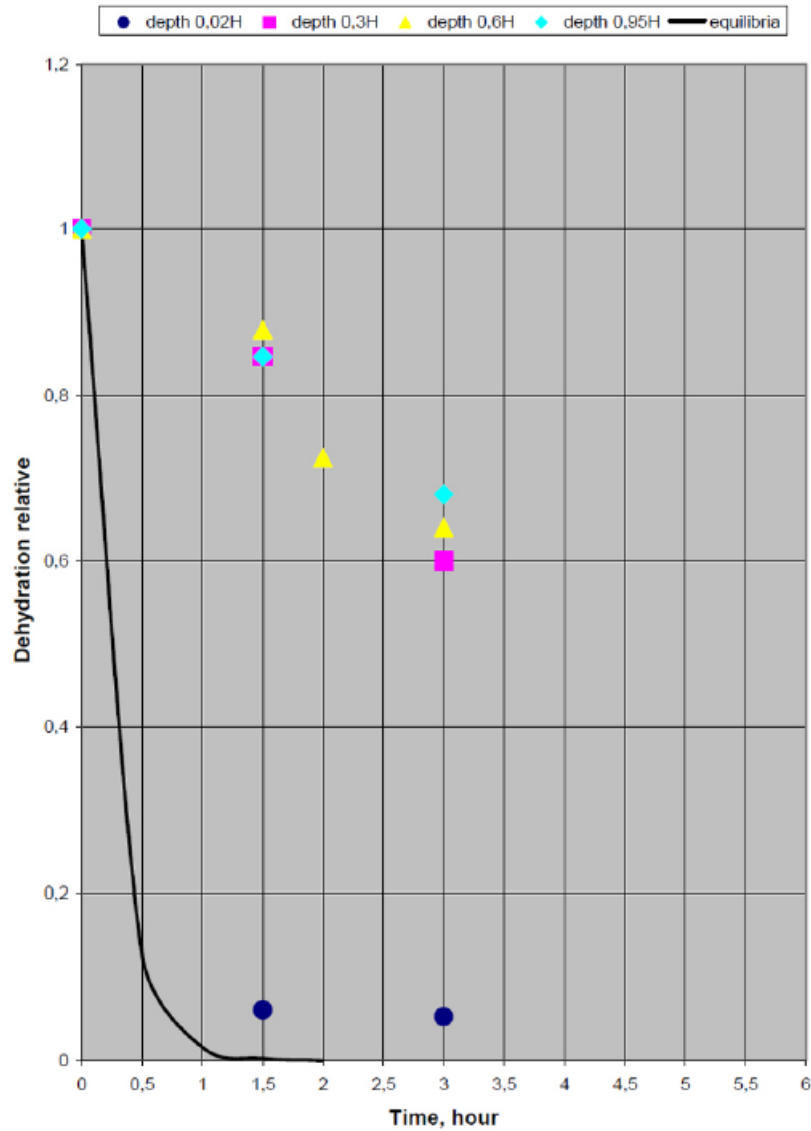


**Figure 15: Experimental data on the rate of fuel dehydration at several depths from Merkulov et al. [26]**

The results suggest that the dehydration rate is nearly constant at depths greater than 30% of the total depth, and that the bulk dehydration rate is in the order of 14 times slower than the surface rate. Combined with the findings of Terada et al., this provides the basis for a humidity interaction model in the proposed thesis project. Converting Terada's equation from  $\text{Mol s}^{-1}$  to  $\text{kg s}^{-1}$  and applying a scaling factor based on Merkulov's results, the equation becomes:

$$\dot{m}_{H_2O} = KA\Delta p_{H_2O} \times \frac{0.0180}{14} \quad (9)$$

The accuracy of this equation is unknown, as it has not been validated experimentally; Merkulov's results merely give an indication. Terada suggests that  $K$  might range from  $4e^{-7}$  to  $6e^{-7}$  depending on the exact composition of the fuel. Considering the combined uncertainties of  $K$  and the scaling factor, an overall accuracy to within one order of magnitude can conservatively be assumed.

### 3.6 Surface Condensation

In the vicinity of a cold surface, the boundary layer air temperature is lower than in the surrounding air, and therefore the local RH can reach 100% even if the bulk RH is far below saturation. Excess water vapour condenses and forms dew on the surface, an effect which can be observed when a drink is removed from a refrigerator and placed in a warm room as shown in Figure 16. The rate of condensation can be limited either by thermal or diffusion characteristics [27].

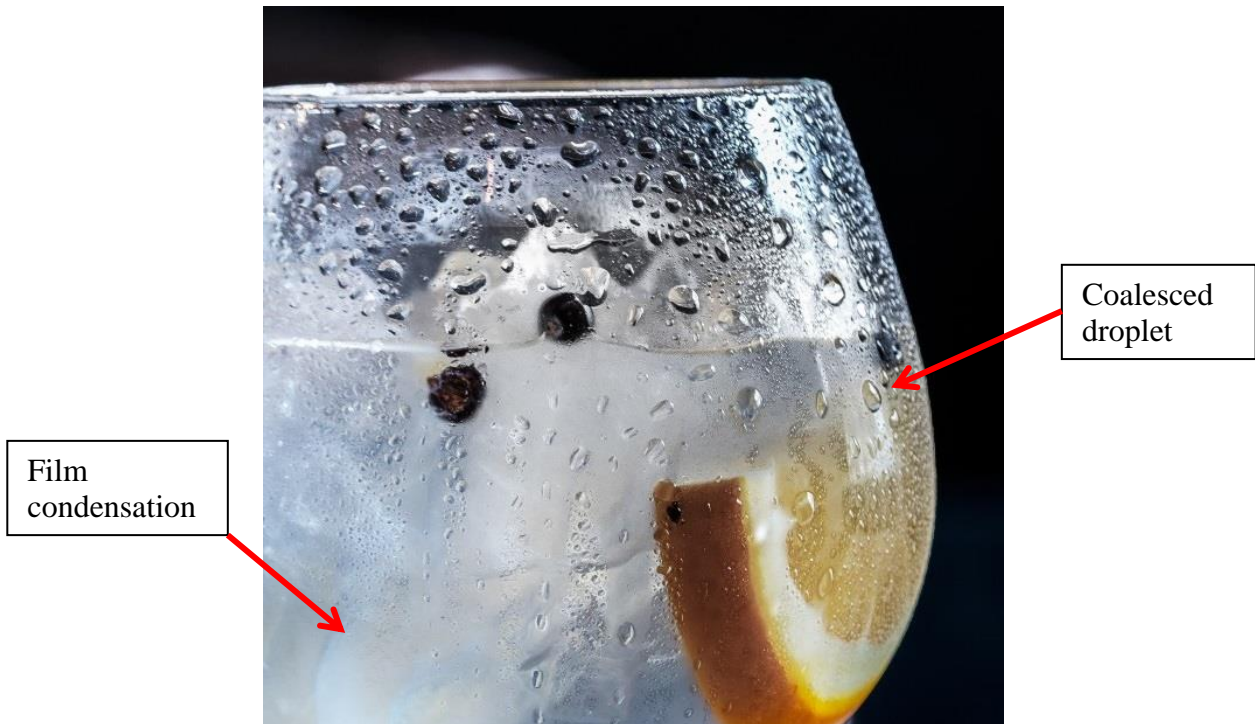


**Figure 16: Surface condensation on a cold beverage [28], showing both film condensation (initial stage) and coalesced droplets (developed stage).**

It is important to at least estimate the order of magnitude of liquid water produced this way, as it may contribute to the accumulation of free water in a fuel tank. Unfortunately, it is not easy to accurately predict this effect without resorting to a finite element method, due to the complexity of the thermal conditions and geometry.

Surface condensation refers only to condensation forming on a cold surface when the bulk humidity is not saturated. The amount of water condensed when the bulk air reaches saturation is treated separately.

#### 3.6.1 Thermal Factors

The most important prerequisite for the formation of surface condensation is that the surface temperature is below the dew point of the air within the tank. No condensation can occur if this condition is not met, as the air will not reach saturation in the boundary layer. Condensation of water vapour is an exothermic process; The quantity of energy released during the process is

known as the latent heat of condensation. Due to the law of conservation of energy, this heat contributes to warming the condensed water and its immediate surroundings. Experiments suggest that nearly all of the latent heat is transferred to the substrate rather than to the surrounding air. This can have profound effects, for example raising the temperature of a chilled drink can by 8°C in just 5 minutes [29].

Depending on the geometry and properties of the substrate material, the energy will be partially conducted away from the interface and partially transferred to enthalpy of the material (warming the substrate). Rubber has a very low thermal conductivity but a high specific heat capacity compared to aluminium, so the energy will tend to heat up the rubber tank bladder (and the condensed liquid water) rather than being conducted away through the material. Condensation will continue until the surface temperature and local dew point have converged (the surface temperature rises while the dew point falls).

Of course, latent heat is not the only thermal process concerning a fuel tank bladder. Heat will also be exchanged to or from the ullage air, the surrounding air and structure, and the fuel. The amount of water that can condense before the tank wall exceeds the dew point temperature depends on the rate of heat transfer, and therefore on each of the thermal pathways. An overview of the heat transmission pathways (excluding heat storage interactions) is shown in Figure 17.

Empirically, it is known that dew is far more likely to form on metal surfaces (e.g. car body) than on rubber (e.g. tyres). The thermal conductivity of rubber is two orders of magnitude lower than that of steel.

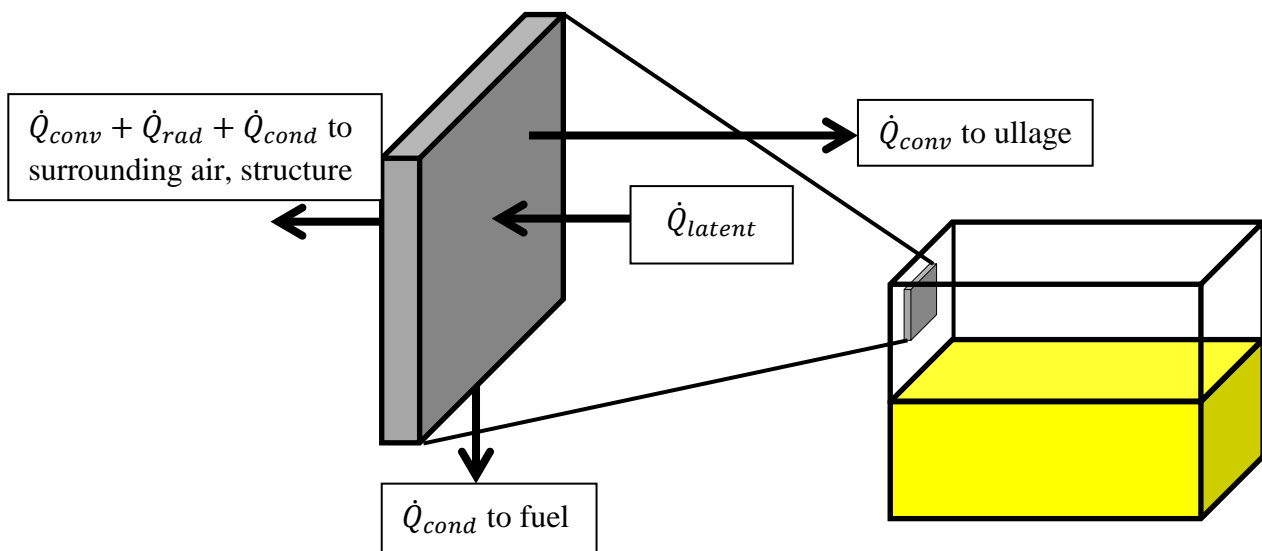


**Figure 17: Thermal process overview of surface condensation, energy storage terms not shown (enthalpy of fuel, condensate, bladder material)**

The transfer of heat to sinks outside of the tank are extremely difficult to calculate as this would require knowledge of the design of surrounding structure, as well as the temperature that this structure will have reached after a flight of a given duration. In addition, this would be different for every helicopter model and even vary substantially from location to location along the circumference of the tank. Substantial model differences between helicopter models would be contrary to the project goal of building a generalised model.



### 3.6.2 Diffusion

Once some vapour has condensed out of the air, the local dew point near the surface is reduced and will eventually descend below the substrate surface temperature. Condensation then cannot continue as the boundary layer air is unsaturated. Additional humidity is supplied by diffusion from outside the boundary layer.

The rate at which this diffusion process occurs is dependent on the flow regime (static, laminar, or turbulent), flow velocity, and vapour pressure gradient. Figure 18 shows an example of the temperature and dew point profiles that might be found near a surface on which diffusion-limited condensation is occurring; the mixture is exactly saturated at the surface, and grows increasingly unsaturated with distance. The relative humidity (degree of saturation) is indicated by the dew point spread.

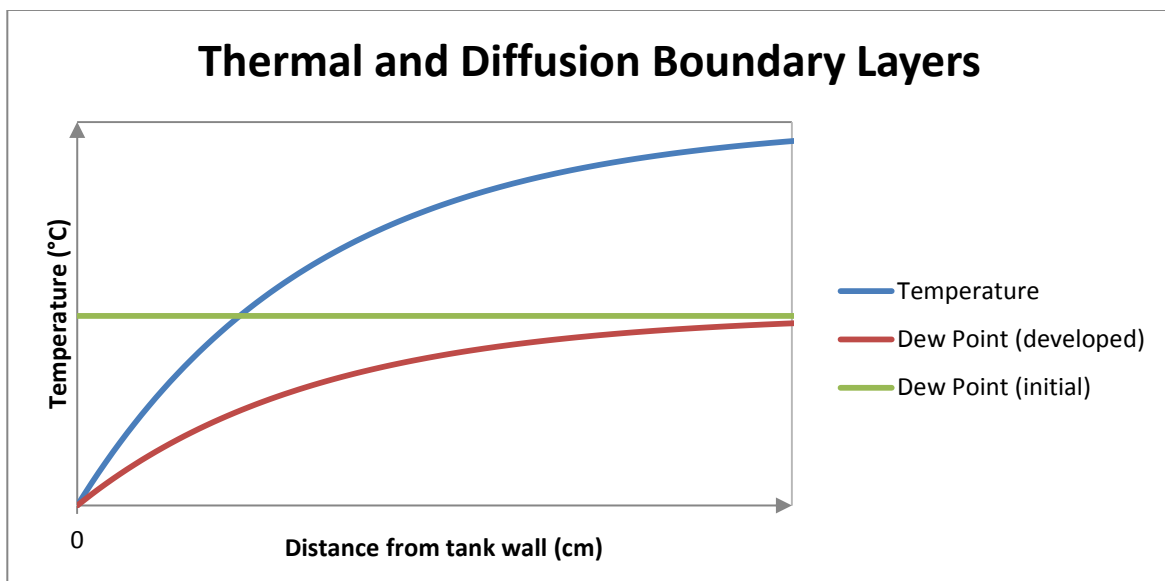


**Figure 18: Thermal and diffusion boundary layers at the tank wall. Condensation occurs at the tank wall when the ullage dew point is higher than the wall temperature. At steady state, the ullage dew point matches the tank wall temperature.**

The figure illustrates that initially, the dew point in the mixture is uniform, and the actual temperature is below the dew point, causing condensation to occur at the surface. The local dew point then begins to drop as vapour is condensed.

The flow conditions within the tank strongly affect the diffusion behaviour. In quiescent conditions, the diffusion boundary layer will be stable and very thick; the resulting small vapour pressure gradient leads to a low rate of diffusion and therefore limited condensation. If the flow is turbulent, near-perfect mixing can be assumed [9], which tends to accelerate humidity transport.

In summary, the diffusion characteristics are difficult to predict with any reasonable degree of accuracy. In the following section, an attempt is made at empirically assessing the degree of significance of the surface condensation phenomenon when analysing free water accumulation.

### 3.6.3 Applicability

In the previous section it was stated that better mixing within the tank accelerates the transport of humidity to the surface by producing a steeper vapour pressure gradient. However, in this condition, the temperature gradient will also be steeper; the surface air temperature will be closer to the bulk temperature. Therefore, the probability and rate of condensation are not expected to increase as strongly with flow velocity as implied by the higher diffusion rate. This phenomenon can be empirically observed by pointing a fan at a fogged-up window or mirror: the condensed water quickly evaporates, unless the ambient air is close to saturation. Airflow therefore lowers the risk and rate of condensation build-up; some air movement is always to be expected in a helicopter fuel tank due to the presence of one or more vents.

Terada et al. neglected sub-saturation surface condensation entirely, and their calculated results were remarkably close to experimental data [25]. Wetterwald et al. made the same assumption but commented,

*“Tank walls are assumed to have the bulk ullage temperature for simplicity. This assumption neglects the effect of cold surfaces on condensation that underestimates the overall condensation. Using a relatively lower bulk ullage temperature may compensate the effect.” [9]*

It is unclear from the article whether or not a lower bulk ullage temperature was ultimately considered in Wetterwald’s model; in any case, any attempt at estimating how much the temperature should be lowered by would be an educated guess at best.

Even after determining the quantity of condensation formed on the surfaces of a fuel bladder, the question remains of what happens to this water. On the vertical surfaces, it will readily run down into the tank sump after reaching a critical film thickness [9]; underneath the horizontal ceiling of the tank, it is conceivable that even after coalescing to large droplets, water does not drip down into the fuel. This delay introduces the possibility of re-evaporation.

Re-evaporation can occur if the film remains attached as the substrate temperature increases towards ambient temperature. As the surface temperature is now above the dew point, the water will evaporate. The rate of evaporation is dependent on the flow velocity and degree of saturation of the surrounding air.

In summary, surface condensation is almost impossible to predict to any reasonable degree of certainty without an in-depth study of the surrounding structure of the particular helicopter model under consideration, and the flow conditions within the fuel tank. Following this, a finite element method would be required in order to model condensation, which is dependent on both time and location within the tank. This most likely would require the use of computational fluid dynamics. Due to the small mass of condensation and large mass of the fuel tank and fuel, it is likely not feasible to determine the condensation rate experimentally with the required resolution. Bespoke experiments for each new helicopter type would be contrary to the project goal.

Additionally, there are empirical and literature indications that condensation in fuel tanks, especially those made of rubber, is not a significant contributor to water accumulation in said tanks. Therefore, it may be justified to neglect this phenomenon.

# 4

## Effects on Helicopter Systems

Water in fuel (in liquid or solid form) can produce a number of effects, both beneficial and detrimental. Examining the potential impact of the presence of water demonstrates the importance of adhering strictly to the prescribed water drain interval and of ensuring thorough validation of any analysis, model or simulation before an extension of the interval is considered. Furthermore, an understanding of the effects is relevant when assessing which physical phenomena are or are not relevant to the analysis.

### 4.1 Gauging

All Airbus helicopters currently use capacitive fuel level sensors. Such sensors consist of two concentric, electrically conductive cylindrical tubes, between which there is either fuel or air, which acts as the dielectric medium of the capacitor. As the dielectric constants of fuel and air are significantly different, the fuel level determines the capacitance, normally given in picofarad (pF), which is then used by the onboard electronics to conclude the fuel level in the tank [30]. Figure 19 presents a diagram of such a fuel probe. An electrically independent low level sensor is affixed to the probes in the supply tanks to redundantly warn the pilot once the available fuel supply drops below a certain level, normally 20 minutes of remaining endurance.

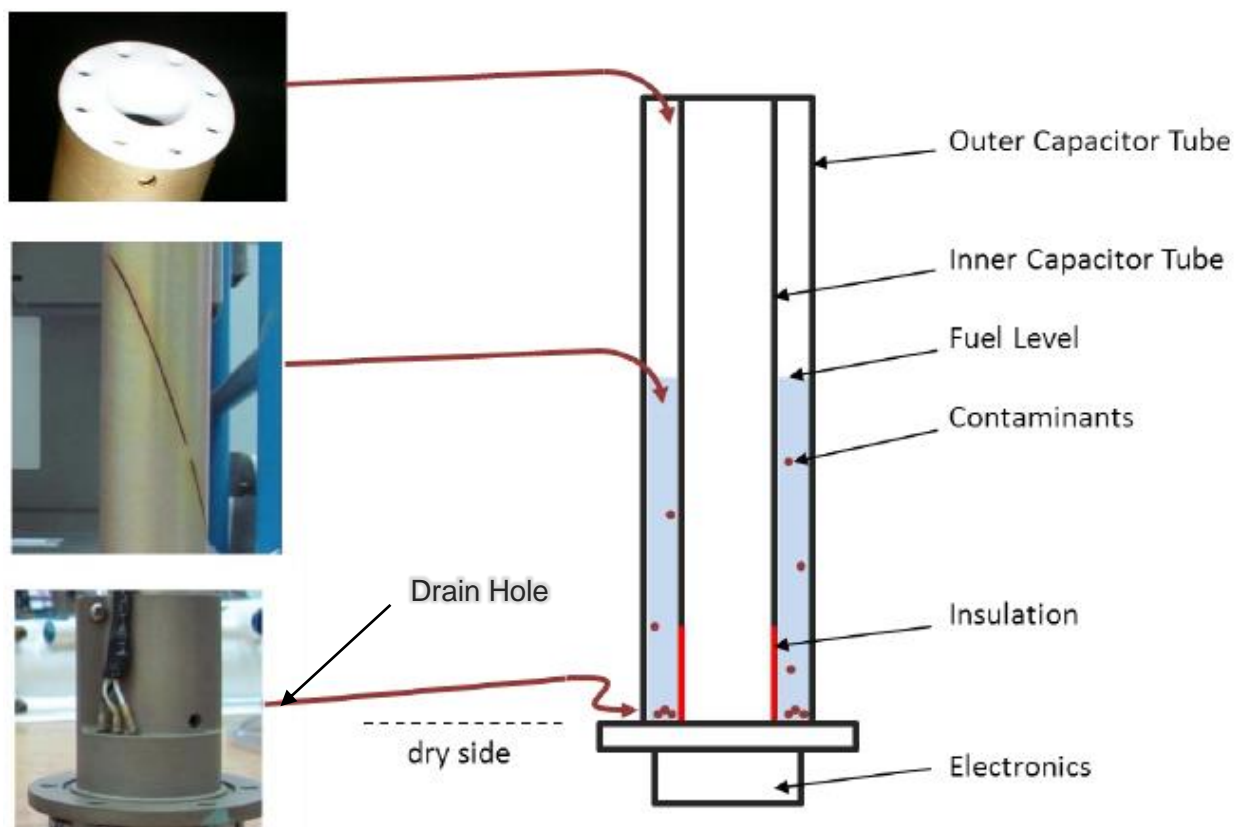


**Figure 19: Diagram of Airbus Helicopters capacitive fuel level probe [31].**

As the dielectric constant of water is in the order of 40 times greater than that of aviation fuel, the presence of even minute quantities of water between the sensor electrodes affects the fuel quantity reading; the probe tends to over-read [32] [33]. In 2013, contradictory fuel indications were reported on an Airbus helicopter, namely that the supply tanks showed as full, although the independent low level warnings had been activated.

Airbus investigated this incident; it was found to be caused by water trapped between the electrodes. Two very small holes are provided in the external electrode to allow fuel to rise up and down the inner cavity with fuel level variations in the tank; water droplets became trapped in the cavity due to the surface tension around the drain hole. This is shown in Figure 19 (drain hole, lower left of figure) and Figure 20. The presence of this water caused the sensor to over-read [33].

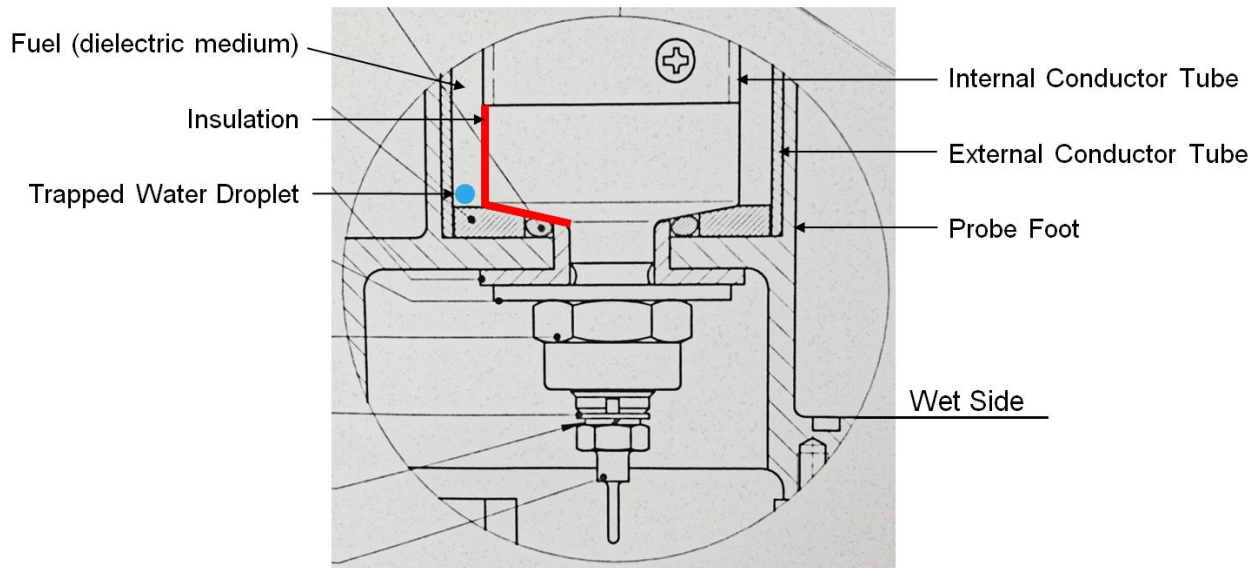


**Figure 20: Water droplet trapped in fuel level probe [30]**

In response to the findings, a project to redesign the probe was started; the most recent design is shown in Figure 21. The drain holes were significantly enlarged to encourage water droplets to exit the probe:

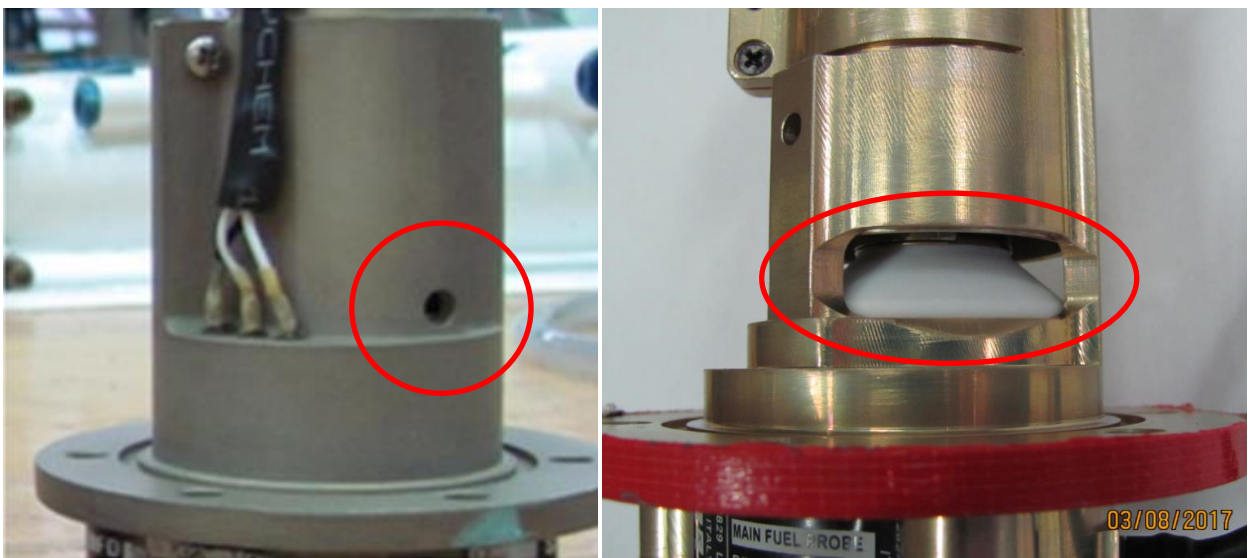


**Figure 21: Old (left) and new (right) fuel probe foot design [31]. Drain holes circled, showing enlarged hole on new probe design.**

A related problem is that in the presence of entrained water, microscopic water droplets adhere to the electrode surfaces (this is thought to be due to electrostatic attraction), and remain there unless the helicopter is completely drained of fuel and the probes allowed to dry. Over time, the fuel quantity indication becomes increasingly inaccurate, which may not be noticed as it is a gradual change (H. Mendick, personal communication, 3<sup>rd</sup> April 2019).

Although the independent low level sensor exists to prevent running out of fuel in flight, incorrect or contradictory fuel quantity information is a major concern; for example, if the pilot has relied on the indicated quantity and is flying over water or mountainous terrain, an unexpected low level warning may prompt a dangerous ditching or landing manoeuvre.

Fuel level sensors may also be affected by microbial growth on the sensor itself; in this case a failure of the fuel quantity measuring system would be indicated to the pilot, who should then initiate a precautionary landing [34]. This could for example occur if water-retaining biological growth created a short circuit between the electrodes of a capacitive fuel level sensor.

## 4.2 Ice

The hazards associated with the presence of ice in aircraft fuel systems are well understood; however, the accident of Boeing 777 G-YMMM in 2008 showed that even small quantities of ice may accumulate and block a heat exchanger, restricting the fuel supply to the engine and causing a dramatic loss of power [6]. In this particular incident, small quantities of ice accumulated during the course of the flight on the interior surfaces of fuel hoses and were dislodged by the variation of flow during final approach. This ice then blocked fuel-oil heat exchangers in both engines.

Figure 22 illustrates the danger associated with fuel icing, showing ice accumulation on a H135 fuel pump strainer:

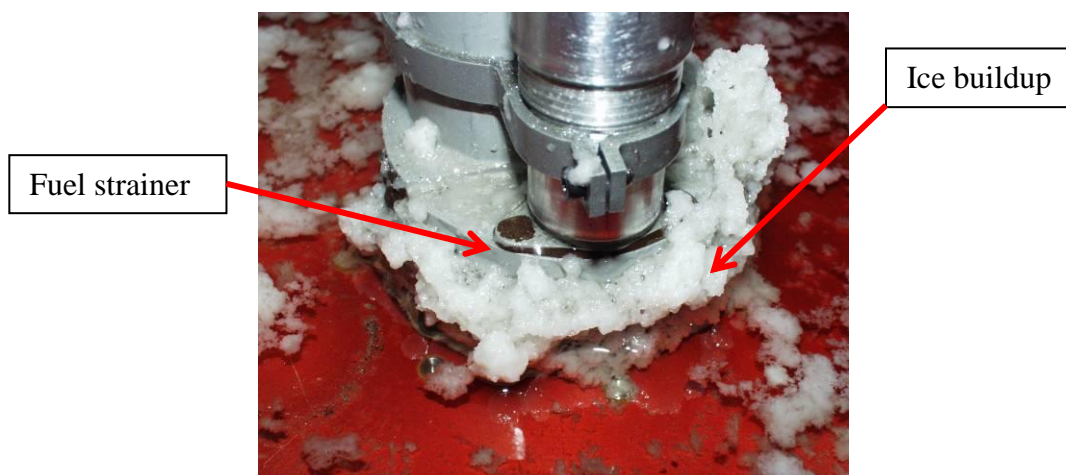


**Figure 22: Ice accumulation on a helicopter fuel pump strainer after a high-concentration laboratory test [30]**

As helicopter missions are much shorter (the maximum endurance of any Airbus helicopter is 4.5 hours without reserve [30]) than the intercontinental flight by G-YMMM, the problem of successive ice accumulation in fuel hoses should be diminished. Nonetheless, fuel filters and jet pumps (a jet pump uses the Venturi effect to produce a pressure gradient) with nozzle diameters of only a few millimetres may be blocked by very small quantities of ice (Figure 22); therefore it is especially important to minimise water accumulation when freezing ambient conditions exist.

## 4.3 Microbiological Contamination

The International Air Transport Association (IATA) states that the microbes found in fuel grow within the water phase using hydrocarbons as nutrients, therefore growing both at the water-fuel interface and in condensation on tank walls [35]; they are able to grow at temperatures from -4 to 55°C in any hydrocarbon fuel. The substances excreted by some microorganisms are corrosive or

exhibit surfactant properties; this leads to corrosion of metallic fuel equipment and the increased absorption of free water into the fuel phase, respectively.

If growth is allowed to accumulate, large coherent mats may be dislodged and block filters and pumps [36], potentially leading to an engine flameout (extinguishment of combustion due to fuel starvation) in extreme cases. Alternatively, microbes may grow on filter elements themselves, eventually blocking the element.

Once microbial contamination has developed, biofilms present on tank walls retain a significant amount of water (over 90% of the biofilm consists of water) [36]; this means that once microbial growth is present in a fuel tank, continuing to drain water is not an effective means to control the problem – the tank must be mechanically cleaned and treated with biocide.

Finally, some microorganisms also produce surfactants; this increases the capacity for water and other contaminants to be suspended in the fuel. Entrained water therefore will settle more slowly or not at all [35] [36], which makes it impossible to drain and perpetuates the growth of further microbes.

# 5

## Water Avoidance and Management

Several additives are currently in use to protect helicopter fuel systems against the detrimental effects of water presence, and additional strategies have been proposed to treat the problem at the root by preventing the build-up of water in the first place. In this chapter, the main existing and proposed methods will be reviewed and assessed on their applicability to helicopters; none of the options are entirely free of downsides.

This assessment contributes to the justification for extended research into free water prediction, as there is currently no real alternative to the tedious and inexact daily drainage.

### 5.1 Scavenging

On commercial airplanes, a water management method named “water scavenging” has been in use for several years. The technology consists of aspirating any accumulated free water from the sump of each fuel tank and mixing it into the fuel supplied to the airplane’s engines [37]; this ensures that accumulated water quantities are kept very low. Peak water concentration in the engine fuel supply is reached during taxi and take-off, when water accumulated during parking must be disposed of.

As discussed in chapter 7, fixed-wing aircraft can tolerate far higher water concentrations than helicopters. Combined with the presence of a water scavenging system, this enables drain intervals to be significantly extended, for example to 7 days on the Airbus A380; still, water drain operations account for nearly 75% of fuel system maintenance effort on wide-body aircraft [38].

A water scavenging system consists primarily of an additional jet pump per sump, to aspirate the accumulated water, and some hoses to route the water into the engine fuel supply. Installing such a system on a helicopter would cause a number of problems, chief among which are space concerns and jet pump sizing.

Helicopter fuel tanks are very small compared with commercial aircraft; in most cases, there is already a large amount of fuel equipment within the fuel tanks leaving no space for any additional components for water drainage.

Additionally, the low water concentration limits applicable to helicopters would demand a jet pump with an extremely small nozzle in order to not exceed 200 ppmv. Taking the Airbus



Helicopters H135 as an example with a fuel consumption of approximately  $130 \text{ l h}^{-1}$  per engine in cruise, this is equivalent to  $26 \text{ ml h}^{-1}$  per engine. A jet pump with a nozzle diameter below 1 mm would be required; such a small nozzle could very easily clog with the smallest of contaminant particles, causing a hazardous free water accumulation once more. Susceptibility of scavenging systems to dormant (unnoticed) failures has been frequently observed in fixed-wing aircraft.

## 5.2 Additives

### 5.2.1 Fuel System Icing Inhibitor

Fuel system icing inhibitor (FSII) additives may be used to avoid the ice-related detrimental effects of free water. The current industry standard is diethylene glycol monomethyl ether (DiEGME), approved in concentrations of 700 to 1500 ppmv. DiEGME is a hygroscopic substance that lowers the freezing temperature of water [39] similarly to ethylene glycol used in automotive coolants.

Due to its hygroscopic nature, DiEGME tends to concentrate in free water phases, raising toxicity concerns when handling water drained from a treated fuel tank. This property also potentially lowers the concentration in the remaining fuel below the minimum effective level, thereby once again producing an icing risk.

The CRC states, “*Undissolved FSII can damage elastomers and other materials in the aircraft.*” [10]. The implication of this, particularly with regard to the elastomeric fuel bladders employed on helicopters, is that great care must be taken to pre-mix the additive into the fuel strictly within concentration limits specified by the manufacturer. It also raises concerns regarding the previously-discussed tendency of DiEGME to accumulate in higher concentrations in the free water phase, locally exposing tank bladder material to higher than specified concentrations. Experience within Airbus shows that in such cases, the bladder may begin leaking in a matter of weeks [30].

DiEGME has been demonstrated to reduce (but not eliminate) the rate of microbiological growth in kerosene fuel [40].

### 5.2.2 Biocides

As FSII does not eliminate the risk of microbiological contamination in turbine fuels, dedicated biocidal additives may be required in certain situations, depending on climate (warm, humid climates promote biological activity) and intended storage time. Biocides may be the only reasonable option in cases where an aircraft is to be stored unattended, allowing a significant quantity of free water to accumulate in fuel tanks.

### 5.2.3 Aquarius

Neither FSII nor biocides address the root cause of the undesired effects they are respectively targeted at. Aquarius is an additive currently being evaluated for approval which aims to prevent the precipitation of dissolved water from turbine fuels.

One molecule of Aquarius bonds to one molecule of water, and may be added to fuel up to 250 ppm. When the water concentration exceeds the concentration of Aquarius, free water is once again formed, providing a habitat for microbes and the potential for fuel system icing. An in-service evaluation was successfully started in July 2018 on a Lufthansa A340 flight between Munich and San Francisco [41].

Aquarius must be added during every refuelling process, implying both initial (mixing equipment) and ongoing costs [38]. Like any additive, this disproportionately impacts small (e.g. single-aircraft) operators.

## 5.3 Proposed Methods

### 5.3.1 OBIGGS Fuel Dehydration

On-board inert gas generating systems (OBIGGS) were first seriously considered on large passenger aircraft in the aftermath of TWA flight 800, a Boeing 747 whose center fuel tank exploded in flight in 1996. Such systems “*supply dry warm Nitrogen Enriched Air (NEA) to fuel tanks to reduce flammability*” [9]. Essentially, the air and fuel vapour within the ullage is displaced by NEA with a low enough oxygen content to prevent the formation of a flammable mixture.

Wetterwald et al. proposed using this system to bubble dry NEA through the fuel in order to dehydrate it; a schematic is provided in Figure 23. The modelling method and assumptions are similar to those used in the Airbus Helicopters step 1 model (section 8.1).

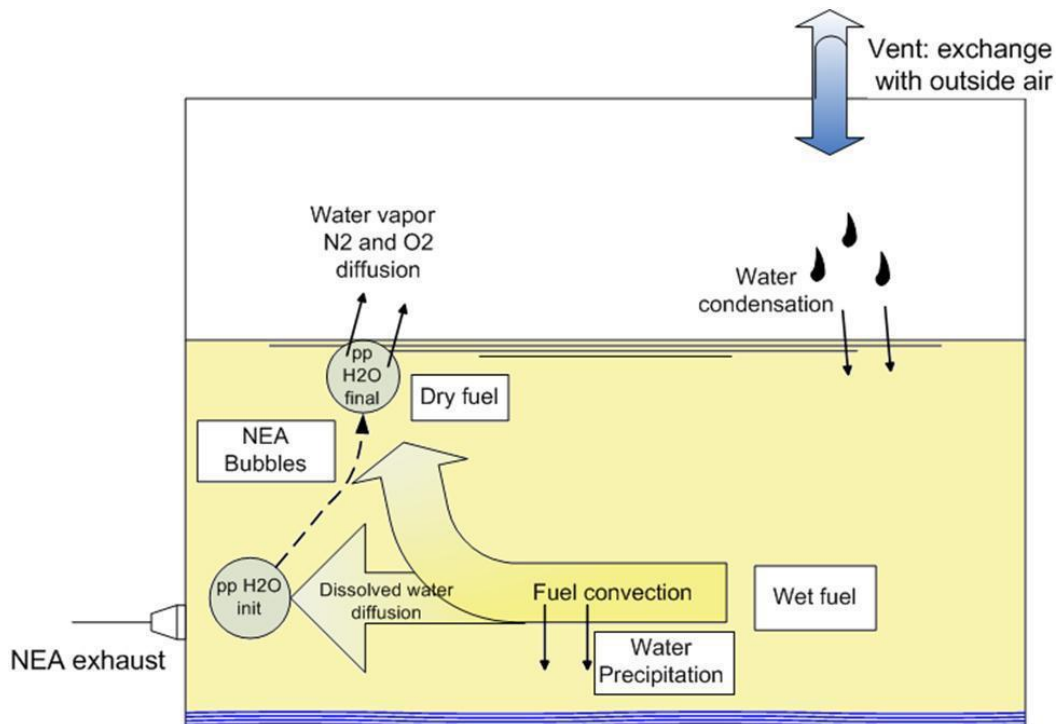


**Figure 23: Diagram of proposed OBIGGS fuel dehydration system [9], showing water transport processes**

The NEA bubbles, introduced at the left of Figure 23, initially have a near-zero water vapour pressure within; this leads to a significant pressure difference which causes water to evaporate from the fuel into the bubble as explained by Terada. An uncertainty once again arises surrounding the diffusion behaviour: in this case, there can be a convection current within the fuel tank, driven by the rising bubbles, in addition to diffusion of water through the fuel.

The model used by Wetterwald et al. indicates that the proposal has potential in reducing water accumulation inflight. It was later validated against experimental data by Merkulov et al. [26] and found to deliver accurate results when replicating the conditions of a laboratory test; it remains unclear how close these conditions are to those encountered during a real flight. The lack of reliable input data is a limitation across all attempts to model water accumulation in aircraft fuel tanks, more details are to be found in section 8. A further limitation is that OBIGGS only works when the aircraft engines are operating, so water will still accumulate when the aircraft is on ground.

This topic was also investigated by Frank and Drikakis in 2018 [42] using computational fluid dynamics (CFD). Similarly to Wetterwald et al., their research reached the conclusion that on aircraft with existing NEA systems, they can be used for fuel dehydration with little or no modification to the system.

Currently, OBIGGS systems are only available as optional equipment on one Airbus helicopter model – the Tiger (military) [30]; therefore water control using OBIGGS is not currently a possibility for civil helicopters, although it is potentially interesting for military operators. The research paper is interesting for its approach to modelling the water accumulation in the non-inerted case; unlike the Airbus step 1 model, Wetterwald et al. accounted for an entire mission profile, albeit a very simple one with three uniform phases – climb, cruise and descent. Wetterwald’s model is discussed in more detail in chapter 8.3.

### 5.3.2 Dry Vent System

A dry vent system refers to preventing the entry of water into the fuel tank via humid air; it does not address water entering via fuel. Airbus has a patent on such a system [43], consisting of a desiccant dehumidifying device placed into the fuel tank vent line(s), which can be regenerated by blowing hot air from the wing anti-icing system (WAIS) through the dehumidifier. The system is presently at a low technical readiness level [38] and in the context of a helicopter, raises the question of where to source hot air for desiccant regeneration as rotor anti-icing systems (equivalent to WAIS) are not common, especially on smaller helicopters and on those operated in the warm climates which are most at risk of water accumulation.

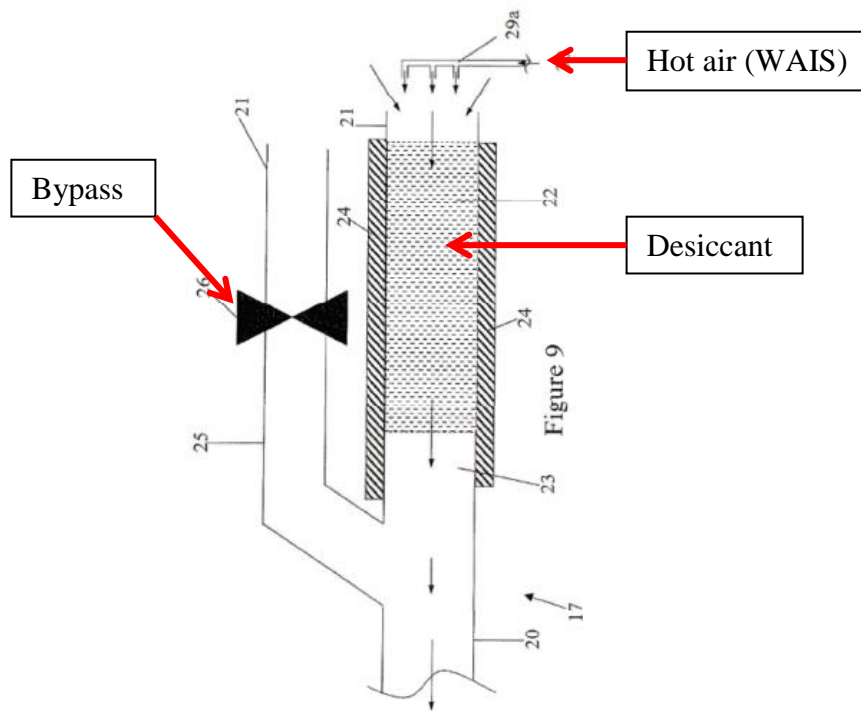
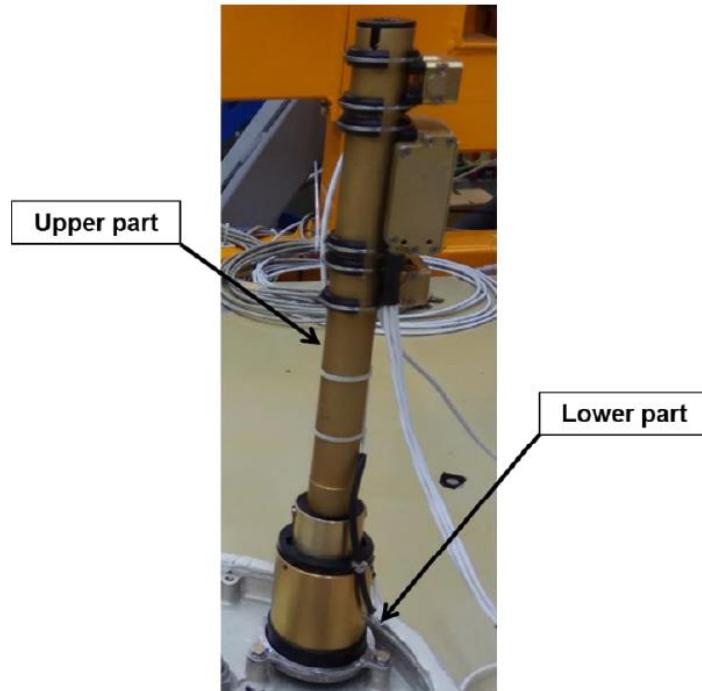


Figure 24: Diagram of the dry fuel tank vent system with desiccant regeneration feature [43]. Hot air from WAIS is used to dry the desiccant when it becomes saturated. Bypass is used in case of desiccant clogging.

### 5.3.3 Free Water Detection

The earliest method of free water detection used by Airbus Helicopters was an optical sensor placed into the sump of each supply tank of the helicopter; water is differentiated from fuel by its different refractive properties. Water levels as low as 1-2 mm could be detected reliably. The disadvantage of this strategy is the requirement for a dedicated sensor and the associated space and wiring (M. Hebensperger, personal communication, 5<sup>th</sup> April 2019).

Subsequently, a strategy was introduced to detect free water using a combined capacitive probe for fuel and water level measurement (Figure 25), relying on the fluids' respective dielectric constants as described in section 4.1.



**Figure 25: Combined capacitive fuel and water level probe [44]**

This proved to be a step back in terms of sensitivity, as the combined tasks of the probe require significantly different resolutions; there must be a compromise between accurate calculation of fuel level and water level. Finally, free water can be detected only in the range of 8 to 25 mm; above this range, a sensor failure is indicated (M. Hebensperger, personal communication, 5<sup>th</sup> April 2019). In the context of the NH90 helicopter model (for which this system is destined), 8 mm represents a free water quantity of about 200 ml per tank [44], corresponding to more than 600 ppm of free water even when the tanks are full. The NH90 is a purely military helicopter and thus not subject to the certification requirements given in chapter 7.

# 6

## Mission Profiles

The temperature history experienced by a fuel tank is a crucial piece of information in order to estimate water accumulation, which is the result of temperature cycles experienced by both the air and fuel. Both of these thermal parameters are directly related to the mission profile (altitude vs. time) flown by an aircraft.

In this chapter, the limited available data regarding helicopter missions will be presented and their relevance to free water prediction evaluated, along with a discussion of the differences between airplanes and helicopters.

### 6.1 Fuel Temperature

The evolution of fuel temperature over the course of any period of time (inflight or on the ground) depends primarily on two parameters: the rate of heat transfer into or out of the fuel tank, and the thermal mass of the fuel contained therein.

#### 6.1.1 Comparison between Airplanes and Helicopters

In the wing tanks of fixed-wing aircraft, the fuel is generally separated from the transonic flow of very cold air (below  $-50^{\circ}\text{C}$ ) only by the wing skin, made of aluminium a few millimetres thick (high thermal conductivity). As a result, the fuel temperature follows the ambient air temperature quite quickly; Figure 26 shows an example of this.

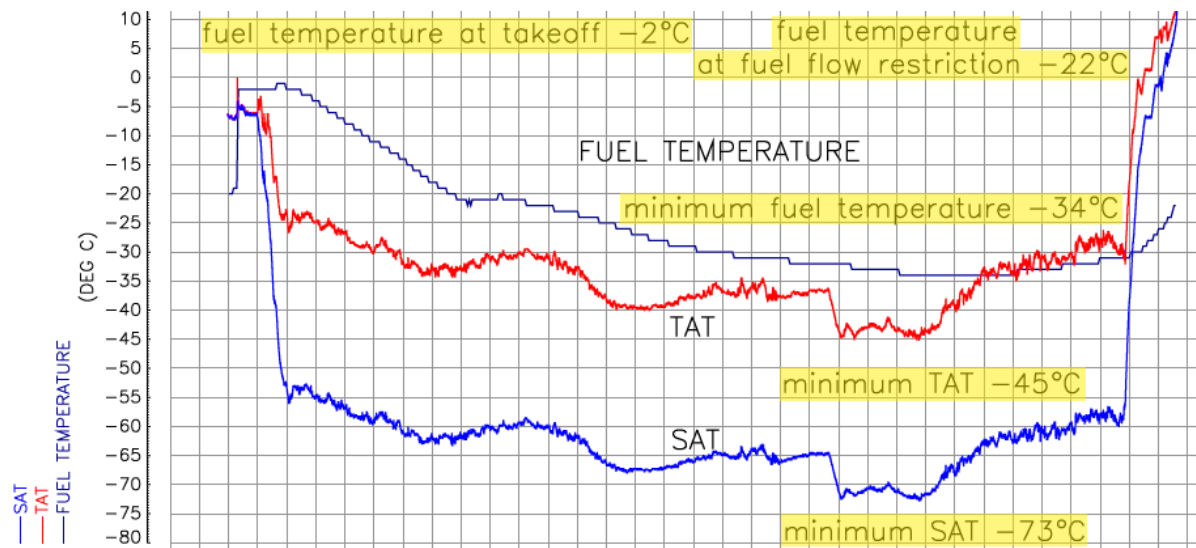


Figure 26: Fuel and air temperatures on British Airways flight no. 38, 17<sup>th</sup> January 2008 [6] (one square = 20 mins). Total ambient temperature (TAT, red) and static ambient temperature (SAT, blue) shown.

The fuel temperature on BA038 fell by 20°C during the initial 2 hours of cruise flight, with full fuel tanks (large thermal mass). In the final 2 hours of the flight, the now nearly empty fuel tanks displayed an even faster response to ambient temperature changes, as the thermal mass was reduced.

The fuel temperature on helicopters displays a slower response to ambient temperature; this has two reasons:

1. Helicopters use rubber fuel bladders separated from the fuselage skin by crash-resistant foam blocks (thermal conductivity:  $\sim 0.03 \text{ W m}^{-1} \text{ K}^{-1}$  for foam [45] vs.  $\sim 240 \text{ W m}^{-1} \text{ K}^{-1}$  for aluminium [46])
2. Helicopter missions are shorter and at lower altitude (smaller temperature gradient)

An example of fuel temperature evolution during a flight test on an Airbus helicopter is shown in Figure 27; the test helicopter's fuel tank was less than half full at the beginning of the flight. Although the temperature difference between fuel and ambient air is nearly triple the difference at the beginning of BA038, the rate of cooling is only 70% higher ( $0.28^\circ\text{C min}^{-1}$  for the helicopter,  $0.17^\circ\text{C min}^{-1}$  for the airplane).

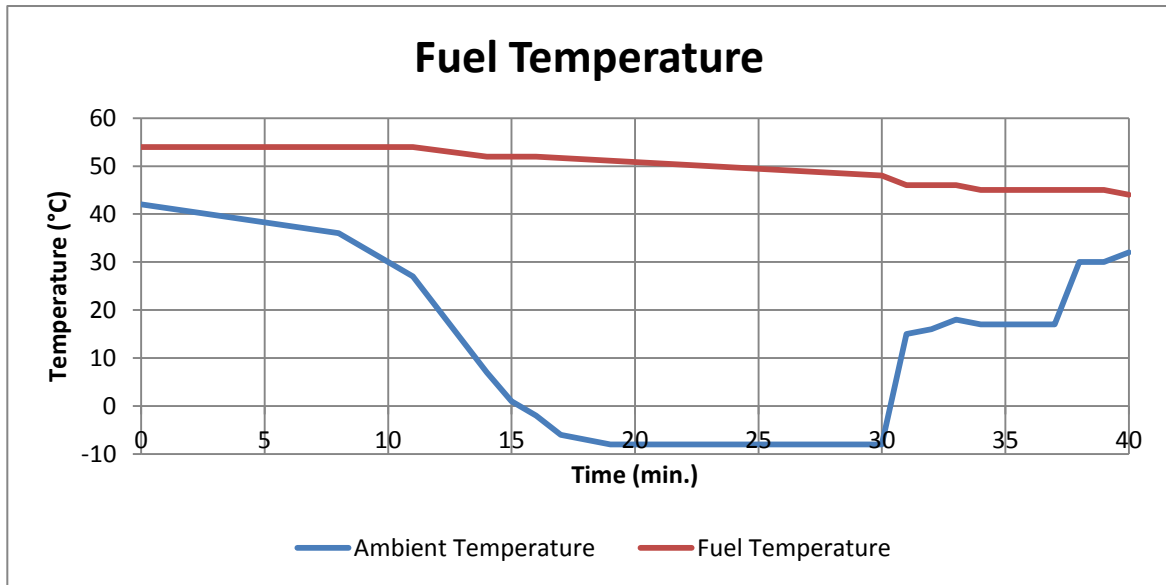


**Figure 27: Fuel temperature response to ambient temperature on BK117D2 flight no. F1242**

Similar results are available for a flight test with the H160; the fuel quantities at the start and end of the flight were 500 and 200 kg respectively. The fuel temperature, ambient temperature and altitude are shown in Figure 28 and Figure 29.

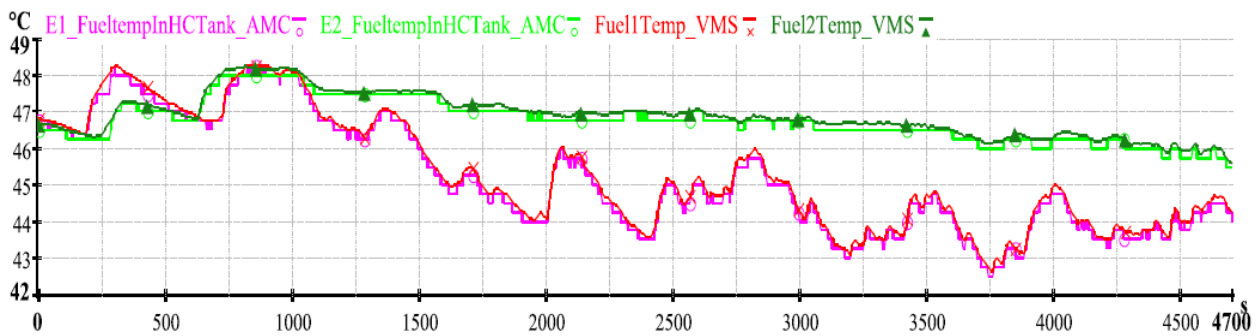


**Figure 28: Fuel temperature against time (seconds) during H160 flight no. F0228 [47]**



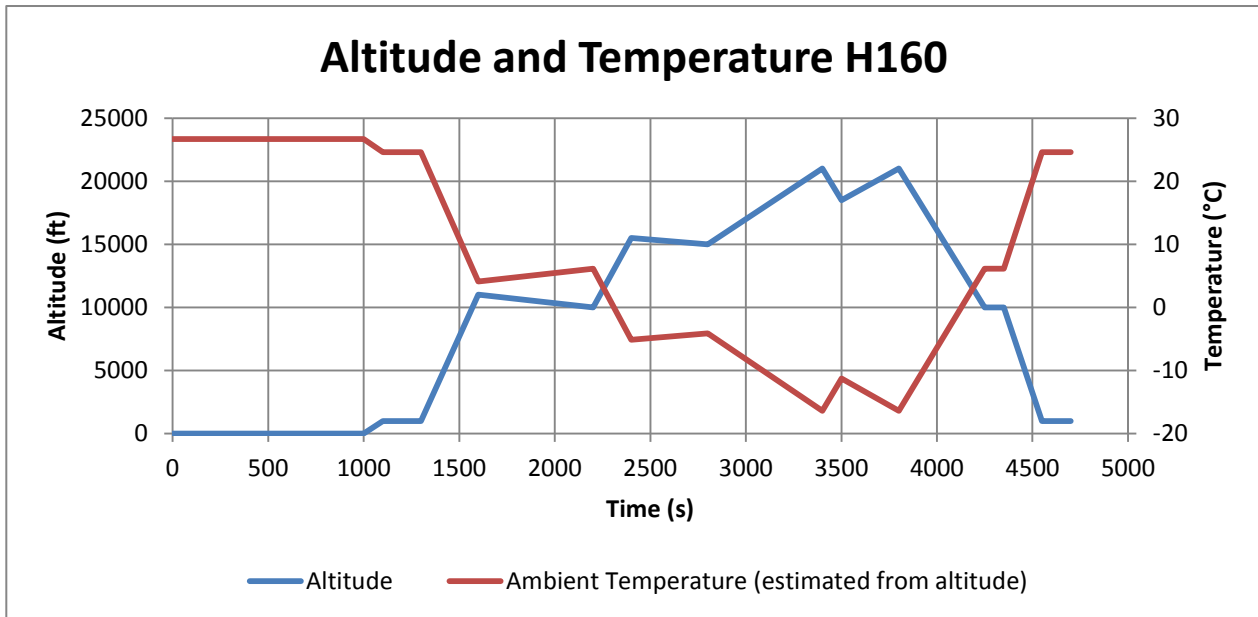


Figure 29: Measured altitude and approximate (ICAO) ambient temperature during H160 flight no. F0228

Again it can be seen that although the temperature difference between the inside and outside of the fuel tank is up to 60°C, the fuel temperature decreases only by around 2°C over the course of nearly an hour at altitude. This indicates that helicopters are less susceptible than airplanes to free water generation due to thermal cycling of the fuel. Using the known data, it is possible to determine the overall heat transfer coefficient.

### 6.1.2 Fuel Temperature Modelling

Considering that the cooling (or heating) rate of the fuel in a helicopter fuel tank is proportional to both the temperature difference and the fuel mass, it is possible to infer a correlation from existing experimental data to roughly estimate the fuel temperature evolution during any given mission profile.

The data shown in Figure 27 and Figure 28 stem from certification flight tests at 20,000 ft (6100m) - for certification, operation in the full flight envelope must be demonstrated. It is rare for helicopters to operate at such altitudes (see section 6.2); a temperature difference of 60°C between the fuel and ambient air is therefore also not a regular occurrence. Combined with the afore-mentioned factor of helicopter missions being limited in duration (the maximum endurance of helicopters is between 3 and 4.5 hours [30]), this would justify the consideration of constant inflight fuel temperature in modelling, but it is not necessary to make this simplification as the correlation is simple to determine.

The fuel temperature is considered to follow an implicit relationship: the rate of change of fuel temperature depends on the temperature difference across the tank wall and therefore on the fuel temperature itself. Other parameters will be the fuel mass and the surface area, material type and thickness of the outer shell, crash-resistant foam and tank bladder. As these are not always known with certainty, an overall heat transfer constant  $K_f$  can be derived from experimental data which is particular to the helicopter model; its units are  $\text{kJ K}^{-1} \text{s}^{-1}$ , or transferred energy per unit of temperature difference and time.

$$\frac{dT_{fuel}}{dt} = \frac{K_f}{m_f \times c_{pf}} \times (T_{fuel} - T_{amb}) \quad (10)$$

Using flight test data in which the fuel temperature, ambient temperature and fuel mass were recorded over time (such as Figure 30), the value of  $K_f$  can be calculated. The specific heat capacity ( $c_p$ ) value used is the average value for Kerosene:  $2.01 \text{ kJ kg}^{-1} \text{ K}^{-1}$ .

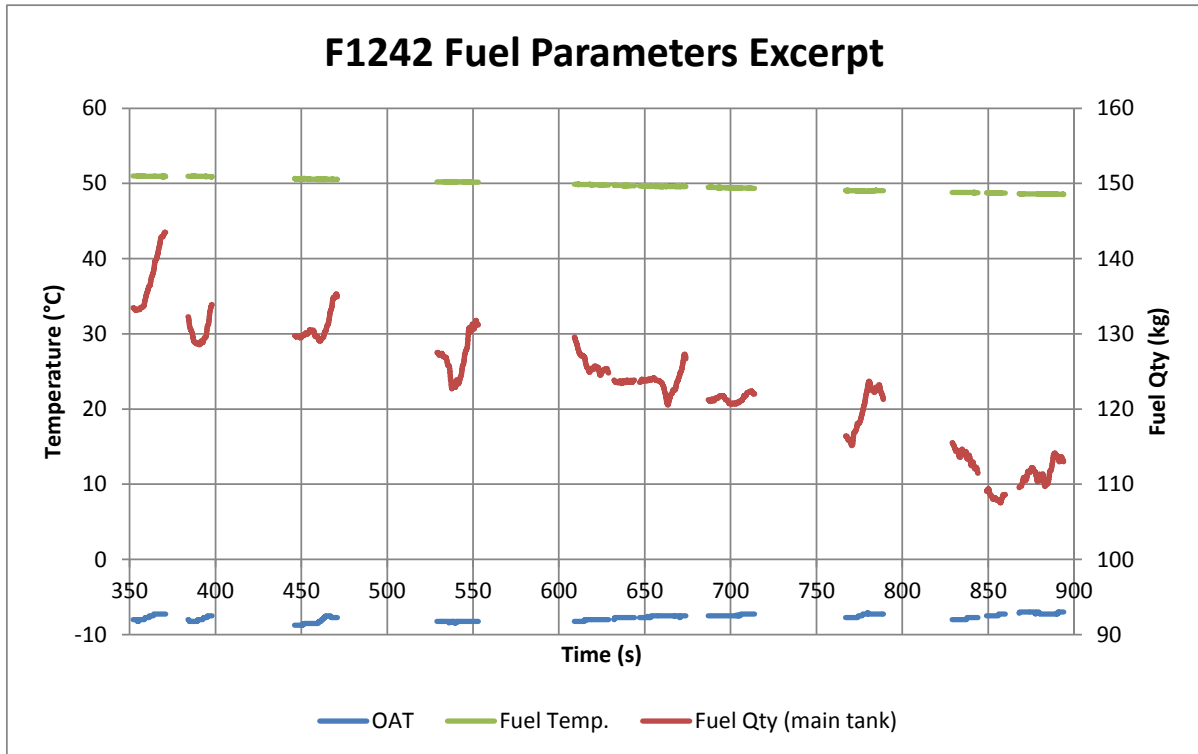


Figure 30: Excerpt of fuel quantity, fuel temperature, and ambient temperature (OAT) from a flight test.

Analysis of data from several helicopter types showed the value of  $K_f$  varying from  $0.010$  to  $0.035 \text{ kJ K}^{-1} \text{ s}^{-1}$ ; the primarily carbon-fibre H160 exhibited the slowest heat transfer while the aluminium-skinned H135 showed the highest value. Besides geometrical differences, this may be due to the fact that carbon fibre composites have a thermal conductivity at least one order of magnitude lower than that of aluminium [46] [48].

## 6.2 Altitude and Range

Information about the habits of helicopter operators in terms of altitude and duration provides valuable insight into the ambient temperatures typically encountered by these helicopters, which is necessary in order to estimate the thermal conditions within the fuel tank.

The altitude and track of helicopters differ significantly between different operator types; it is not reasonable to make a generalisation across all helicopter operators. Two main sources of data can be considered: data held by Airbus customer support and publicly accessible air traffic control radar records. Information pertaining to North Sea oil & gas transfers, law enforcement and air ambulance operations is presented in this section, as they are the most common categories.

## 6.2.1 North Sea Oil & Gas

Figure 31 and Figure 32 depict the speed and altitude profile of a return flight from Esbjerg (Denmark) to an oil platform in Danish waters, flown by an Airbus Helicopters H175. Based on the speed and duration, the distance appears to be approximately 260 km; the cruise altitude was 5000 ft (1500 m) outbound and 7500 ft (2300 m) during the return leg – far below the helicopter’s service ceiling of 15000 ft (4600 m) [49].

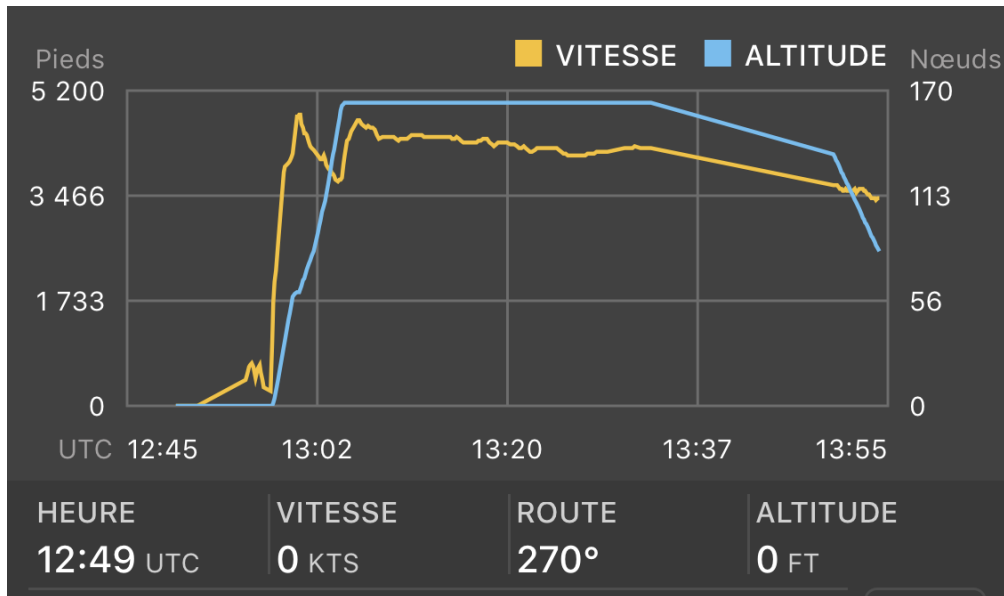


**Figure 31: Outbound flight from Esbjerg (Denmark) to Drop 609 oil platform**

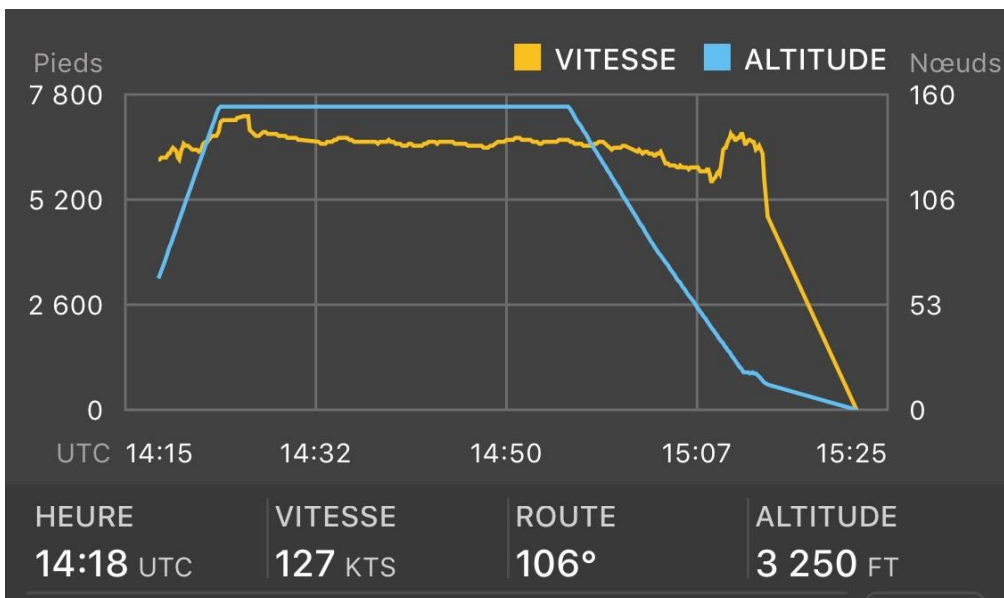


**Figure 32: Return flight from Drop 609 oil platform to Esbjerg (Denmark)**

Additional mission information can be obtained from Flightradar24, which provides radar data for past flights of any aircraft with a compatible transponder. Although no statistical information is provided, it is possible to review the last 7 days of radar data for a given aircraft; for example, a H175, registration PH-NHV flew at least 7 legs between North Sea oil platforms and Den

Helder (in the Netherlands) on 18<sup>th</sup> April 2019; the maximum altitude was 5000 ft (1500 m) with a range of approximately 200 nmi (370 km), shown by the example in Figure 33:



Figure 33: Selected radar data of PH-NHV on 18<sup>th</sup> April 2019 [50]

### 6.2.2 Law Enforcement

A useful demonstration of the difference in mission profile depending on the operator is provided by analysis of the flight path followed by a H135 operating a police surveillance flight in Scotland. This flight lasted 98 minutes, during which an altitude of 3000 ft (900 m) was never exceeded, with more than half of the flight taking place around 1000 ft (1000 m) [51], Figure 34. Temperature was reportedly 6°C at ground level and 0°C at 3000 ft (900 m), corresponding to the standard ICAO temperature lapse rate. Based on the information in section 6.1, there is likely to have been no measurable change in fuel temperature during the flight.

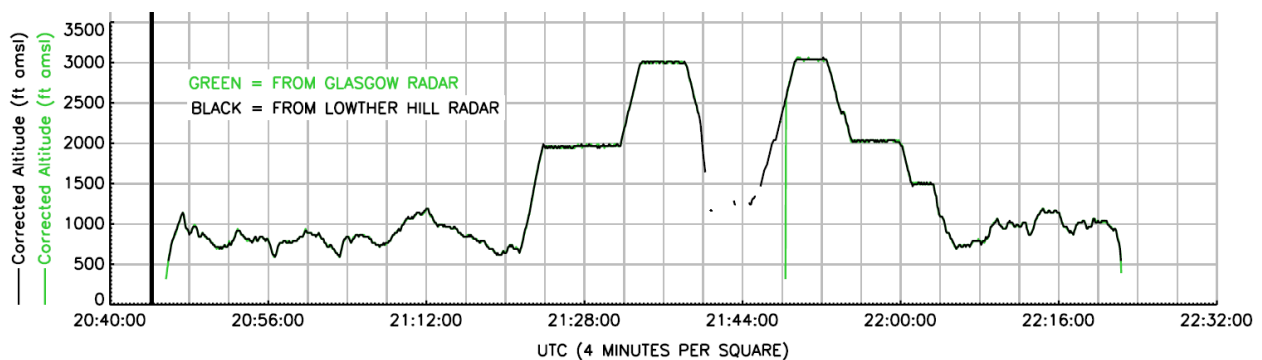


Figure 34: Altitude of police H135 in November [51]

### 6.2.3 MEDEVAC

Air ambulance flights are unique among civil helicopter applications as they are typically both short and spontaneous. As an example, the H135 PH-HVB can be considered; in the week of 17<sup>th</sup> to 24<sup>th</sup> April 2019, it flew 100 legs primarily to or from hospitals in Rotterdam. Only 20 of these flights exceeded 15 minutes in duration and the maximum altitude was 2000 ft (600 m). An example is shown in Figure 35.



**Figure 35: PH-HVB flight from a field to the nearby Rotterdam university hospital, 24<sup>th</sup> April 2019 [50], showing the very low altitude generally flown by emergency response helicopters.**

# 7

## Certification Regulations

Certification regulations provide a legal framework for the design of aircraft and their systems, among them helicopter fuel systems. An understanding of the requirements set by these regulations is important when analysing free water accumulation, because they dictate how much water the system must be able to demonstrably tolerate, which in turn determines the maximum safely allowable accumulation.

In this chapter, which focuses on regulations for the European Union, the applicable rules will be examined, along with the regulatory differences between helicopters and airplanes which have enabled the tolerance of much higher water quantities in airplane fuel tanks.

The European Aviation Safety Agency (EASA) is the authority responsible for setting and enforcing airworthiness requirements for aircraft to be registered in its jurisdiction. The regulations applicable to helicopters are CS27 (small rotorcraft, max. takeoff mass  $\leq 3175$  kg) [52] and CS29 (large rotorcraft) [53].

The paragraphs applicable to water in fuel tanks are similar between the two specifications; they are paragraphs 951c and 971 in each case, which will be subsequently discussed.

### 7.1 Paragraph 951c

Paragraph 951c is worded in CS27 as follows:

*“Each fuel system for a turbine engine must be capable of sustained operation throughout its flow and pressure range with fuel initially saturated with water at 27°C (80°F) and having 0.198 cc of free water per litre (0.75 cc per US gallon) added and cooled to the most critical condition for icing likely to be encountered in operation.” [52] pp. 1-E-4*

Due to the cooling of the fuel, the total free water concentration is increased by the amount released from the cooling fuel. This change will be in the order of magnitude of 50 ppmv – the CRC states an approximation of 1 ppmv per °F [10].

The value of 198 ppmv (CS29 refers to 200 ppmv) is neither justified nor substantiated by EASA; it appears to have been duplicated from the US Federal Aviation Administration (FAA)

regulations. The corresponding Federal Aviation Regulation section 29.951c, amendment 29-10 [54] was made effective as of 31<sup>st</sup> October 1974 and based on Notice of Proposed Rulemaking (NPRM) 71-12; however this NPRM does not provide any justification for the choice of concentration and temperature [55].

Although the basis for this value cannot be determined, it is certainly not current, having been in force for 45 years. The specifications for large aeroplanes feature the following similar text:

*“Each fuel system must be capable of sustained operation throughout its flow and pressure range with fuel initially saturated with water at 26.7°C (80°F) and having 0.20 cm<sup>3</sup> of free water per litre (0.75 cm<sup>3</sup> per US gallon) added and cooled to the most critical condition for icing likely to be encountered in operation.” [56] pp. 1-E-5*

This similarity suggests that the requirement in CS27 and CS29 may have been simply duplicated from airplanes, with an unknown level of applicability validation.

## **7.2 Paragraph 971**

Unlike paragraph 951c, paragraph 971 differs substantially between the two rotorcraft categories. For small helicopters, the requirement specifies a fuel tank sump *“with an effective capacity in any ground attitude ... of 0.25% of the tank capacity or 0.24 litres, whichever is greater”* while for larger helicopters, 0.10% or 0.24 litres is required [52] [53].

In this case, the specifications for large aeroplanes permit an exemption that is not present in either helicopter specification: *“Each fuel tank must have a sump...unless operating limitations are established to ensure that the accumulation of water in service will not exceed the sump capacity.”* [56]. This statement likely refers to the application of water scavenging as outlined in chapter 5, which eliminates the need for a large sump volume as long as the scavenging system is functional.

# 8

## Associated Models

In order to gain an overview of the possible approaches to an aircraft fuel tank analysis, this chapter presents and reviews existing models and analysis related to the subject of water accumulation in fuel tanks and to the work intended in this research project. Based on the sometimes limited information on the analysis methods, previous work appears to fall into the following categories: basic numerical analysis and physical modelling.

### 8.1 Airbus Helicopters Step 1 Model

A spreadsheet was previously developed within Airbus Helicopters, which is able to perform preliminary calculations of the quantity of free water generated in a fuel tank of given volume during the change from an initial to a final state [57]. This preliminary numerical analysis appears to be a good basis for the development of a more sophisticated analysis program. Its accuracy in calculating the volume of water accumulation is estimated to be within one order of magnitude.

#### 8.1.1 Inputs and assumptions

As inputs, the spreadsheet requires the volumes of the fuel tank and of the fuel itself (which is considered constant), the initial and final ambient temperatures and pressures, and the initial relative humidity.

The following assumptions are known:

1. Fuel always saturated with water
2. Constant fuel volume
3. Temperature decreasing from initial to final state (no provision for temperature increase)
4. Uniform pressure throughout the tank
5. Constant water density
6. No humidity exchange between existing air and aspirated air volume
7. No fuel dissolved in water
8. No fuel vapour
9. Temperature equilibrium between all phases



The assumption of fuel always being saturated with water is not justified and requires further research (which is one of the present MSc project's goals). As stated in section 3.5, the relative humidities of fuel and air should equalize over time, but on the other hand, in the presence of a volume of free water underneath the fuel, more water might continually be absorbed by the fuel if it is not saturated – section 2.2. In this situation, the fuel would be functioning as a wick, transporting water from the free water phase to moisture in the air by means of solution. It is likely that the equilibrium reached in this condition is dependent on the ratio of fuel surface area exposed to air and water, respectively, among other factors such as temperature and agitation.

The most critical limiting assumptions are 2, 3 and 6. Assumption 2 (constant fuel volume) was likely made in order to simplify the calculation of air ingress and speed up development of this basic prediction. Assumption 6 is particularly relevant with regard to the equilibrium of humidities between air and fuel discussed above.

Importantly, the spreadsheet does not take into account mission profile, fuel consumption or ullage temperature differing from fuel temperature. These are the main factors limiting its usefulness to estimating accumulation within an order of magnitude.

### 8.1.2 Calculation Steps

The step 1 model calculates the accumulated water quantity according to the following steps:

1. Calculation of initial conditions: Using the given inputs, the model calculates the initial values of
  - a. fuel and air density
  - b. specific humidity of the air
  - c. degree of water solubility in fuel (a curve of water solubility in fuel is used, which may be modified to account for different fuel blends as discussed in section 2.1)
  - d. mass and volume of dry air, water vapour and dissolved water
2. Calculation of new air RH considering new temperature and pressure
3. Calculation of final quantities of water vapour (considering relative humidity) and dissolved water (considering 100% saturation)
4. Determination of free water quantity from difference between steps 1 and 3
5. Calculation of aspirated air volume from difference of initial and final total volumes

This approach is very simplistic and although certainly useful in determining whether serious research on the topic is warranted, it is likely to be more resource-efficient to build a new program from the ground up rather than to attempt adapting the Excel architecture to a more complex algorithm.

### 8.1.3 Example Cases

A series of sample situations were entered into the step 1 model to generate an elementary sensitivity analysis. These were 2 each ground and climb cases, detailed in Table 4.

**Table 4: Sample results of Airbus Helicopters step 1 model**

Climate	Description	Initial conditions			Final conditions		Water qty./ml	
		Temp. °C	RH %	Press. Pa	Temp. °C	Press. Pa	90% full	10% full
<b>A3</b>	European summer	39	43	101325	28	101325	110	12
<b>A3</b>	Climb SL to 2km	39	43	101325	26	79495	126	14
<b>B2</b>	Wet hot SE USA	35	74	101325	21	101325	125	71
<b>B2</b>	Climb SL to 2km	35	74	101325	22	79495	115	40

It is distinctly noticeable that the free water quantities calculated are largest when the fuel tank is almost full of fuel (a tank of 500l capacity was considered). This is due to the assumption made in the model, that the fuel is always saturated with water; therefore any minimal reduction in temperature immediately leads to the generation of free water. Ragozin concurs, stating “*The greatest quantity of water will have accumulated on the bottom of the tank in which there was the least free space and the most kerosene.*” [7].

For the 90% full cases, the water production is equivalent to 244-280 ppmv; for the 10% cases, the concentrations are 240-1420 ppmv, up to 7 times the amount demonstrated to be safe according to chapter 7.

Additionally, among the ground cases, the free water production is observed to be higher in the more humid climate; this is in line with operator feedback (L. Lollini, personal communication, March 2019). A significant contributing factor in this observation is the fact that air in the B2 climate cycle reaches saturation on a daily basis (Table 3 and Figure 10), therefore producing significant amounts of condensation every evening as the air cools below its dew point; air saturation is not reached in cycle A3.

Ragozin’s observations do not appear consistent with the latter operator feedback – he claims that an empty fuel tank will not accumulate any water, and in partially-filled tanks, the accumulation will be proportional to the quantity of fuel present, which implies that air-space condensation either plays no role, or is self-compensating. However, Ragozin refers to a sealed tank, rather than a vented one as found on helicopters.

## 8.2 Triton

An existing MATLAB®-Simscape based model named “Triton” was developed for Airbus Commercial Aircraft; it is a full fuel storage system model. Triton uses a physical model of each subdivision inside the fuel tanks, known as bays, and even considers the non-instantaneous flow between the bays due to baffles and other restrictions as well as flow restrictions in pumps, hoses, valves and other equipment. The modelling of water accumulation is only a small subset of its capabilities.

Triton is able to predict the accumulation of free water during a given mission of an A330-200. Input data were taken from measurements during actual flights operated by KLM between Amsterdam and the Dutch West Indies. Its results are promising [5], but it has not been validated; for this it would be necessary to record the quantities of water drained after the mission. As new

airplane designs incorporate water scavenging which largely eliminates the physical need for water drainage, Triton is more intended as a design tool to evaluate the distribution of water between the various tanks, than as an evaluation method to demonstrate water accumulation behaviour to airworthiness authorities.

The scope and level of detail in the model far exceeds that which could be achieved in an MSc graduation project, and Triton is not likely to be adaptable to helicopters (M. Yahyaoui, personal communication, 25 March 2019) due to the extensive architectural differences between fixed-wing aircraft and rotorcraft. It follows that the effort required to adapt this model to helicopters is higher than that required to build a new analysis from the ground up; the latter option is therefore preferable. The existence of this model does, however, indicate the feasibility of such modelling methods.

### 8.3 Wetterwald

In order to evaluate the potential of using OBIGGS to control water accumulation (chapter 5.3.1), Wetterwald et al. developed a MATLAB® model [9]. This functions as a time step model; at each time step, calculations are performed on the ullage and fuel humidity to determine whether any free water is generated during that time step.

Assumptions were made for the mission profile and fuel temperature:

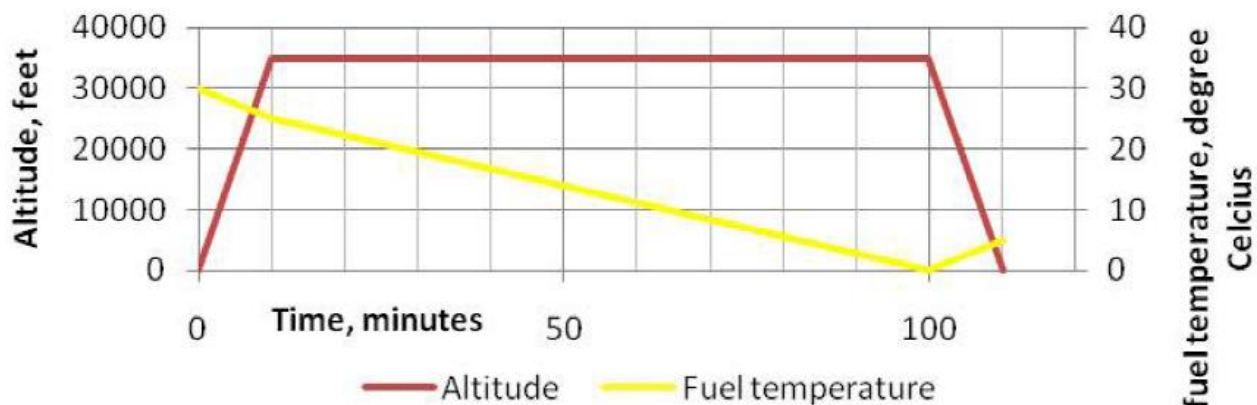


Figure 36: Wetterwald model mission profile and assumed fuel temperature profile [9]

In addition to using an assumed fuel temperature profile, Wetterwald further simplifies his model by assuming perfect mixing in both the fuel and ullage phases, and that the tank walls have the same temperature as the ullage. The latter assumption means that surface condensation is not considered.

Unlike the AH step 1 model, Wetterwald does consider fuel dehydration by the ullage (this is the object of the OBIGGS study). Also, the Parameswaran equation for humidity at altitude is used, albeit with only one fixed set of coefficients given by Parameswaran for Port Blair (India).

There may be an opportunity for partial validation of a new model to be developed by comparing it to the results presented by Wetterwald et al. for the non-inerted cases, as the paper documents the assumptions and inputs very thoroughly. An excerpt of the results is shown in Figure 37.

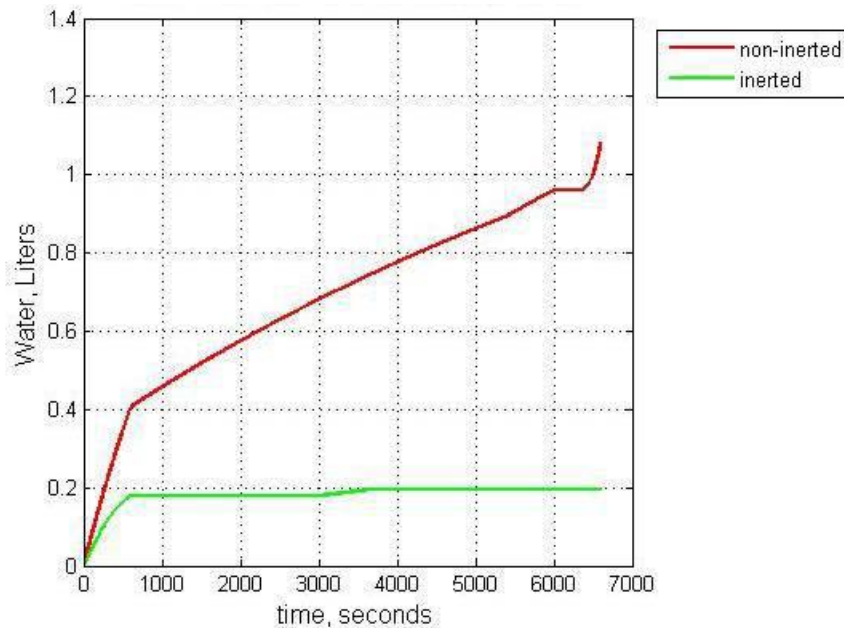


Figure 37: Free water quantity in a Boeing 747 centre wing tank (50% fuel load) [9], numerical model data

## 8.4 Oreshenkov

In 2004, Oreshenkov [58] published results of a partially validated mathematical model for the accumulation of free water in jet fuel storage tanks; the model achieved an error of below 10% for TS-1 storage tanks of 25 and 50 m<sup>3</sup> over one year. The measurement results were in the order of 100 ppmv of free water over the course of the year; however it is unclear how applicable this is to helicopters. The storage tanks have a much greater thermal mass leading to less temperature variation, and Oreshenkov does not give the values of the climate data used. For reliability, the model would also need to be validated against multiple measured results in different climatic conditions and tank sizes.

Similarly to Wetterwald et al. (section 5.3.1), Oreshenkov also attempts to model the accumulation of free water inflight by dividing an airplane flight into three rudimentary phases (climb, cruise and descent). Although the results are promising, with an error of 15% to measured results, only a single data point is shown for validation. The tank wall temperature and wall-fuel heat transfer coefficient are used to model fuel temperature over time; no values or measurement methods are provided for any variable but it can be reasonably assumed that a large commercial aircraft is being considered, again limiting its applicability to helicopters due to tank size and construction as well as ambient conditions and mission profile.

# 9

## Interim Summary and Research Questions

In this section, the existing research will be summarised, the knowledge gap highlighted and research questions formulated.

### 9.1 Conclusions from Existing Research

In chapter 2, the types of water found in helicopter fuel tanks were presented, along with the physical processes underpinning their creation, entry, retention and exit from the fuel system. Here it can be concluded that all of the effects which lead to the existence of water in airplane fuel tanks are applicable also to helicopters to some degree, but that no research has yet been published investigating the degree of similarity.

Additionally, in chapter 3 the vertical profile of temperature, pressure, density, and humidity were examined based on aviation industry standard values, measurements, and computational models. This highlighted the problem that the atmospheric conditions are difficult to generalise; although models exist which can calculate the vertical distribution of humidity to a sufficient degree of accuracy, the profile appears to always depend on the ground-level conditions, as well as the geographic location of the site. This is further complicated by the effect of local weather phenomena on the conditions at low altitudes, particularly temperature and humidity.

NATO provides a potential way to bypass this generalisation problem, by discretizing the world's climate into 12 categories. Using these discrete categories combined with the available vertical humidity profile data, the ambient conditions encountered by a helicopter during a given mission can be approximated if the duration, altitude, and location of the mission are known and low-altitude weather effects neglected. This leaves the uncertainty of what happens when travelling through clouds, where the air is sometimes super-saturated.

In chapters 4 and 5, the detrimental effects of water in helicopter fuel tanks and the unsatisfactory prevention, avoidance and curative methods were outlined. The combination of potentially dangerous and/or expensive consequences and the present lack of any satisfactory water management or avoidance technology applicable to helicopters serve to demonstrate the importance of this aspect of helicopter operations; without detailed investigation of water build-

up, it is unavoidable to perform the drain operation daily. As with the airworthiness requirements, the physical justification of once daily as the required drain frequency is not readily apparent. As an extension of the ambient condition data in chapter 3, the missions performed by helicopters are discussed in section 6, with respect to the inputs likely to be required when modelling the water accumulation. The presented fuel temperature measurements from flight tests, combined with an example of a helicopter mission showing the tendency for helicopters to fly at altitudes below their already relatively low service ceilings, support the suggestion that fuel temperature could be considered constant during a helicopter flight. If implemented, this would remove one unknown variable from the model.

A brief review of airworthiness authority requirements in chapter 7 showed that there is an absence of physical justification for the requirements applicable to water in the fuel supply; certainly, none has been published. The present research aims to quantify the actual water accumulation encountered in helicopter fuel tanks, which will provide as-yet non-existent contextual information to aid in understanding this requirement. The results could, after further validation, be used as a basis for adjusting or rephrasing the requirement, for example by referring to a fraction of sump volume instead of a concentration within the fuel.

In chapter 8 it becomes apparent that no sufficiently sophisticated water accumulation model yet exists for helicopters. This is the knowledge gap that will be addressed by the new model. The theory applied in some of the existing models will be synthesized, augmented where possible, and packaged in a user-friendly and broadly applicable MATLAB program.

## 9.2 Research Questions

It has been demonstrated that a knowledge gap exists surrounding the computational prediction of free water accumulation in helicopter fuel tanks. The literature study generated a large number of research questions; only a subset of these can be investigated within the scope of the present MSc thesis project owing to resource constraints (e.g. no experiments can be performed, time limit of 9 months).

The overarching research question to be answered by the thesis project is as follows:

***Is it possible to improve understanding of the physical phenomena causing water accumulation in helicopter fuel tanks, by developing a computational prediction model?***

The following sub-questions will need to be answered to conclude on the main research question:

1. Which criteria must an analysis or model fulfil in order to be considered validated, in this context?
2. Which factors most strongly influence the free water quantity in a helicopter fuel tank?
3. To what degree of certainty and accuracy is it possible to computationally predict the free water quantity in a helicopter fuel tank?
  - a. Which types of data are required in order to predict water accumulation?
  - b. Is this data available and reliable?
  - c. Can helicopter missions be sufficiently grouped or generalized?
  - d. To what level of confidence can the analysis be validated?

4. To what extent does the different fuel water solubility exhibited by alternative fuel blends impact free water quantity and its predictability?
5. Are the quantities of free water encountered low enough to allow an extended drain interval without compromising safety?

# 10

## Modelling Overview

Based on the research questions, it was decided to develop a model using MATLAB<sup>®</sup> to predict the accumulation of water in a helicopter fuel tank from first principles and given ambient conditions and mission profile. This model is named the Airbus Helicopter Water Accumulation Simulation (AHWAS).

This chapter provides an introduction to the aims, approach and design of AHWAS.

### 10.1 Specification

Within the scope of a MSc thesis, the model should fulfil the following requirements:

1. Work reliably under any physically possible combination of input conditions
2. Calculate the accumulated water over the course of a single flight, a series of flights, an entire day or week
3. Employ a user-selectable time step
4. Consider the physical phenomena:
  - a. Variable fuel temperature
  - b. Variable fuel and air humidity
  - c. Temperature-variable water saturation level in air
  - d. Temperature-variable water solubility in fuel
  - e. Water exchange between fuel and air (reversible hygroscopicity)
  - f. Surface condensation of warm air on cool surfaces when bulk  $RH < 1$
5. Allow a sensitivity analysis of the water accumulation to each input parameter

### 10.2 Approach

In general terms, the approach to the modeling problem consists of calculating the evolution of physical parameters (state variables) in the fuel tank based on first principles. In some cases, either for simplification or to circumvent the use of unknown physical variables, coefficients are derived from existing flight test data; one example of this is the fuel thermal coefficient,



described in section 6.1. The fuel thermal coefficient is required to avoid the need for a CFD model of the thermal conditions within and surrounding the fuel bladder.

MATLAB<sup>®</sup> R2017a was chosen as the software environment for development of the model; some of its advantages over Microsoft Excel used for the Airbus Helicopters step 1 model are:

1. Clarity of mathematical equations due to:
  - a. use of named variables instead of cell numbers
  - b. multi-line if / elseif / else statements in place of the nested if structures required by Excel
2. The absence of enormous tables of visible data
3. The ability to stably handle larger quantities of data than Excel, especially in iteration loops (macros)
4. The ability to produce a customized user interface (e.g. data input windows)
5. Ease of error-checking and debugging due to visible code

### **10.3 Architecture**

The modelling effort is divided into two phases:

1. Development of a physical model to calculate the final state based on the initial state and the time step (similar in scope to the AH step 1 model)
2. Development of a temporal model to supply the physical model with inputs and perform calculations with non-linear variation of parameters, over an extended period of time

The physical model is similar in concept to the existing Airbus Helicopters step 1 model but more sophisticated and with fewer assumptions. Given the initial conditions, the final fuel volume and ambient conditions, as well as the time step, this model calculates the final conditions and deduces the quantity of free water accumulated over the time step.

The temporal model is able to determine the water accumulation over time given the mission profile and climate information. The time period under study is divided up into a number of time steps. Each subdivision treated as a step change and the parameters are passed to the physical model, which returns the water quantity produced during that iteration and the final values of the state variables. These state variables are then passed forward to the physical model in the next step as the initial values.

# 11

## Physical Model

The physical model performs calculations for one step-change in ambient conditions. As the time step is considered small, certain simplifications can be made (chapter 11.2). Required inputs include the initial and final conditions inside and outside of the fuel tank, as well as certain fuel system parameters such as the fuel surface area, fuel volume and tank volume.

As the flow of data within the code is relatively complex, it will be explained using a flow chart inspired by the Extended Design Structure Matrix (XDSM) proposed by Lambe and Martins [59]. With an XDSM, it is possible to specify which data are shared between which processes. This also forms the basis of validation by degeneracy checks as explained in section 13.

### 11.1 Nomenclature

A large number of symbols are required to refer to the data. These are listed in Table 5.

**Table 5: List of symbols used in XDSM**

Symbol	Name	Unit
<b>A</b>	surface area	m <sup>2</sup>
<b>C<sub>p</sub></b>	specific heat capacity of fuel	kJ kg <sup>-1</sup> K <sup>-1</sup>
<b>h</b>	altitude	ft or m
<b>K<sub>f</sub></b>	fuel thermal constant	kJ K <sup>-1</sup> s <sup>-1</sup>
<b>m</b>	mass	kg
<b>P</b>	(partial) pressure	Pa
<b>RH</b>	relative humidity	-
<b>S</b>	solubility of water in fuel by mass	-
<b>SH</b>	specific humidity	-
<b>T</b>	temperature	K or °C
<b>V</b>	volume	l or m <sup>3</sup>
<b>Δt</b>	time step	s
<b>ρ</b>	density	kg m <sup>-3</sup>

To these symbols, a number of subscripts are appended to specify which value is being referred to; these are listed in Table 6. The number 1 or 2 is appended to the following subscripts to

differentiate between the initial and final value where necessary, as well as the letter “s” to denote saturation conditions.

**Table 6: Subscripts used in XDSM**

<b>Subscript</b>	<b>Meaning</b>
<b>a</b>	ambient
<b>b</b>	base (sea level)
<b>c</b>	condensation
<b>cr</b>	critical
<b>dw</b>	dissolved water
<b>ev</b>	evaporation
<b>f</b>	fuel
<b>pr</b>	precipitation
<b>S</b>	tank bladder surface
<b>s</b>	saturation
<b>T</b>	tank
<b>u</b>	ullage
<b>v</b>	vent
<b>wv</b>	water vapour

Example:  $P_{wv1s}$  indicates the initial saturation pressure of water vapour.

In the MATLAB® code, structures are used (a structure is essentially a parameter tree). The structures “initial” and “final”, as well as “ambient” are used, with one or two sublevels.

In the second level, parameter names similar to those in Table 5 appear (“t”, “rho”), and on the third level (if present), parameter specifications similar to the subscripts in Table 6 appear. For example, the initial ullage temperature is referred to as “initial.t.ull”. More general parameters are referred to in plain text, such as “timestep” and “cp\_fuel”.

## **11.2 Assumptions**

In this section, the most important assumptions will be listed, discussed and contrasted with the approaches taken by similar models. Table 7 gives a comparison of the main assumptions between AHWAS and the Airbus Helicopters step 1 model, Wetterwald, and Oreshenkov.

**Table 7: Comparison of assumptions between associated models**

<b>Aspect</b>	<b>AHWAS</b>	<b>AH step 1</b>	<b>Wetterwald</b>	<b>Oreshenkov</b>
<b>fuel saturation (RH<sub>f</sub>)</b>	state variable	always saturated	state variable	state variable
<b>fuel volume</b>	state variable	constant	constant	constant
<b>directionality</b>	state variable	cooling only	state variable	state variable
<b>ullage/fuel humidity exchange</b>	variable rate, bidirectional	N/A	N/A	instantaneous
<b>temperature</b>	linked state variables	equilibrium	equilibrium	linked state variables
<b>surface condensation</b>	no re-evaporation	N/A	N/A	critical droplet size

Assumptions shared by all 4 models include:

- No fuel vapour in the ullage (this has no effect on the interaction between water and fuel)
- No fuel dissolved in water
- Constant water density
- Variable fuel density
- No free water reabsorption into the fuel
- Perfect mixing in both phases

The models are arranged in order of accessibility: for the AH step 1 analysis, the entire spreadsheet is available to perform calculations as required. Wetterwald provides graphical and tabulated results of his analysis, while Oreshenkov only states the relative accuracy of his model to measured data under unknown conditions.

In addition to the above basic assumptions, more complex assumptions were required to construct the model within the limitations of data availability and complexity. These are described in the following sections.

### 11.2.1 Cross-Venting

Cross-venting refers to air exchange between the tank ullage and environment even when there is no change in conditions. The fuel tanks of larger helicopters generally have at least two vent lines which exit the fuselage on opposite sides, so any pressure difference between the outlets produces airflow through the tank. Such pressure variations can be caused by wind when the helicopter is stationary or by the rotor wake during flight. (L. Lollini, personal communication, 26<sup>th</sup> April 2019). This phenomenon leads to uncertainty as to the conditions within the ullage space, as it depends on surrounding air flow and vent system design.

In flight, it could be assumed that helicopters with two vents per tank have a high degree of cross-flow.

One limitation of this assumption is that it is not known what happens if the helicopter is stored in an enclosed environment where there are no air currents, although it can be reasoned that in this situation, fuel temperature variations are lower in magnitude and that therefore the

assumption is conservative. In the context of the primarily commercial or governmental usage profiles flown by Airbus helicopters, storage in a hangar indicates longer-term storage (multiple days), after which the accumulated free water would be drained in any case before the next flight. Therefore, this assumption is not a limitation in practice.

Alternatively, it is possible to calculate a mass-weighted average temperature and specific humidity for the ullage contents, based on whether and how much air is entering or leaving the fuel tank, which is likely to more correctly represent the situation in helicopters with only one vent per tank (example: H135). This method has the result of significantly reducing the volume of condensed water as the ullage temperature variations are much smaller in amplitude, remaining close to the fuel temperature. This is the method employed by AHWAS, because it would not otherwise be possible to calculate condensation; further details can be found in section 11.3.4.

The effect of neglecting cross-venting is estimated to be small, because increased airflow, while introducing greater quantities of humidity, also decreases the formation of condensation on the bladder surface while encouraging re-evaporation.

### 11.2.2 Constant Parameters

Due to the use of a small time step, several slow-moving parameters can be considered constant across a single time step, for certain calculations. These are:

**Table 8: Constant parameter assumptions**

Parameter	Constant when calculating:	Justification
$m_f$	$T_{f2}$	fuel quantity changes very slowly compared to $\Delta t$ $T_s$ changes slowly due to thermal inertia of structure
$T_a, T_f$	$T_s$	
$P_{dw}, P_{dws}$	$\Delta P_{H2O}$	dissolved water concentration changes slowly compared to $\Delta t$
$\rho_u$ $SH_a$	$\Delta m_v$ all	ingress air quickly reaches same temperature as ullage no significant composition change over a small altitude change

### 11.2.3 Re-Absorption

Free water accumulated at the bottom of the fuel tank is assumed not to be re-absorbed (a conservative assumption). This is supported by literature (chapter 2.2); the rate of absorption is very slow (multiple days) compared to the time step used in the model, so considering this effect would have a negligible impact on the results.

## 11.2.4 Condensation

Tiwari's experiment [60] provides data on the rate of accumulation of condensation under given thermal and humidity conditions. This includes the finding that the rate of accumulation is proportional to the dew point spread, which is shown in Figure 38.

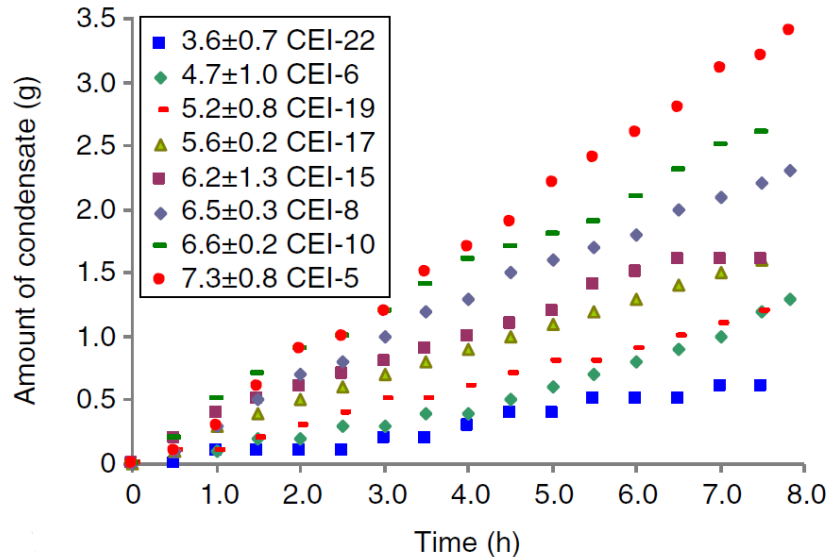


**Figure 38: Accumulation of condensate over time on a horizontal substrate, for several different dew point spreads [60]**

Within a fuel tank, the supply of humidity is finite during a small time interval, so the ullage humidity begins to decrease immediately once condensation begins. Thereafter, the rate of condensation will slow asymptotically until the dew point of the ullage matches the surface temperature. It is assumed that this process is sufficiently fast to be considered instantaneous within one time step.

Taking one example from Tiwari, at 5°C dew point spread the rate of accumulation is approximately  $100 \text{ g h}^{-1} \text{ m}^{-2}$ . The empty fuel tank of a medium-sized helicopter such as the H135 contains approximately 600 g of air at sea level and has an internal surface area of approximately  $5 \text{ m}^2$ ; the initial rate of condensation should therefore be about  $500 \text{ g h}^{-1}$ . With a saturated ullage at 30°C and a surface temperature of 25°C, the quantity of condensable humidity in the tank is  $7 \text{ g kg}^{-1}$ , equivalent to 4.2 g for the H135. Considering the initial rate of  $500 \text{ g h}^{-1}$ , this gives a thermal time constant of approximately 30 seconds, comparable to the time step used in the analysis. Therefore the assumption of instantaneous condensation is justified. Additionally, it is a conservative assumption.

Perfect mixing can justifiably [9] be assumed in the ullage, a diffusive limit therefore does not apply to the condensation process.

Due to the unpredictability of droplet formation and coalescence on the tank surfaces, it is not possible to predict whether or not any condensation formed will run down the tank wall into the sump, or remain attached and eventually re-evaporate. For this reason, the assumption is made that all condensation makes its way into the tank sump; the assumption is conservative but the degree of conservatism can only be guessed from empirical observations and is strongly

dependent on the surrounding conditions. Oreshenkov [58] claims to have modelled this behavior but does not provide any details.

### 11.3 Theory

The physical model consists of four conceptual elements, respectively analyzing:

- Thermal effects
- Humidity exchange between fuel and air
- Airflow into or out of the tank
- Condensation

The relationship between these elements is shown in Figure 39 and each element will be described in the following sections.

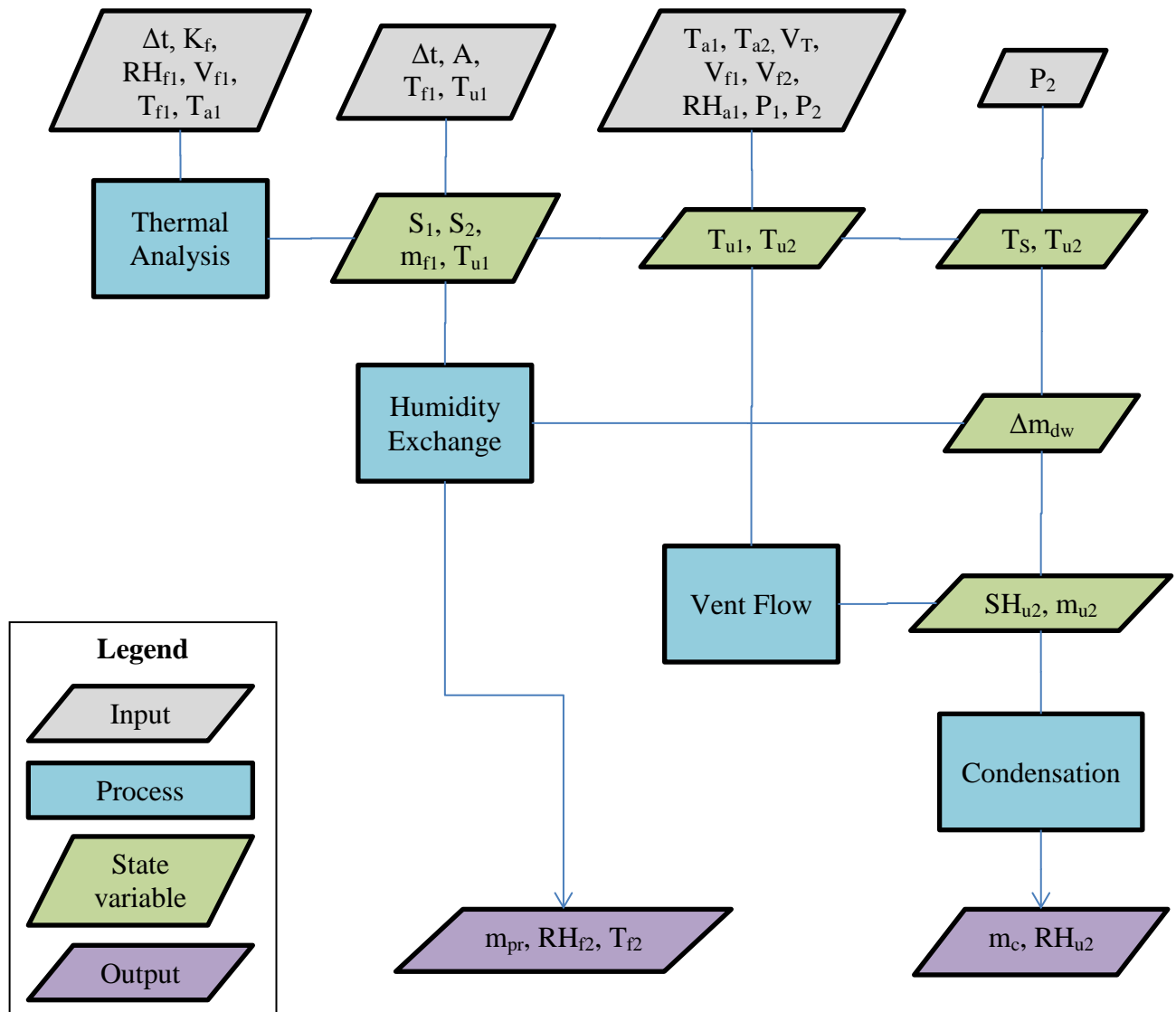


Figure 39: Schematic representation of physical model

The two outputs  $m_c$  and  $m_{pr}$  together give the quantity of free water generated during the time step, while  $RH_{f2}$ ,  $T_{f2}$  and  $RH_{u2}$  are fed back as the initial values for the following time step.

### 11.3.1 Thermal Analysis

This subsection serves to determine the initial and final temperatures of the fuel, ullage and bladder surface, as well as the initial and final solubility of water in fuel. As the time interval under consideration is small, the fuel quantity and ambient temperature can be considered constant for the calculation of fuel heating or cooling. Figure 40 gives the subsection's XDSM.

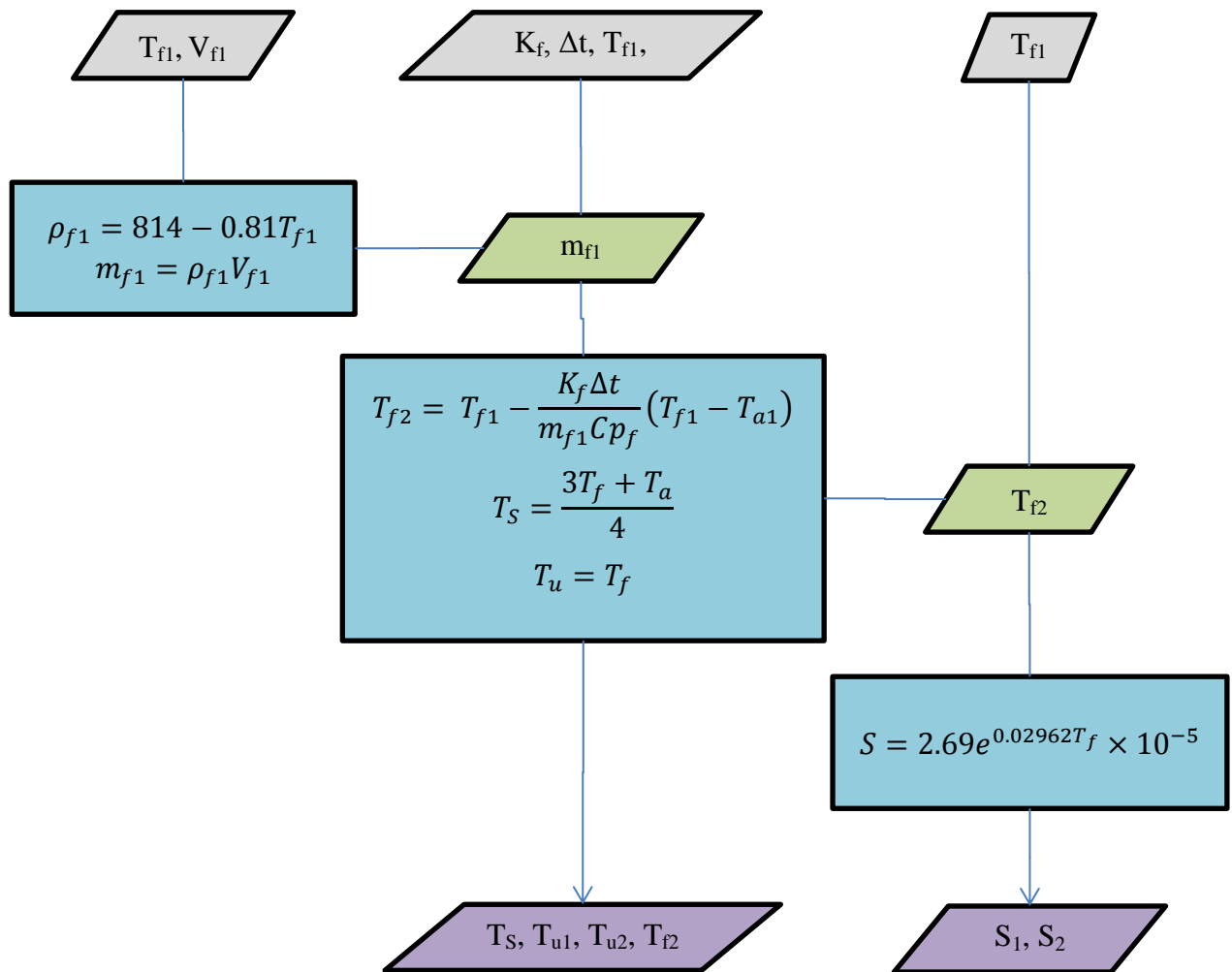


Figure 40: Schematic representation of thermal analysis

In the first step, the initial fuel volume is converted to mass, which is calculated based on the temperature-dependent density. The function linking temperature and fuel density varies slightly between fuel blends; the coefficients used here are averages given by the CRC [10].



The final fuel temperature is estimated based on equation (10); details of its derivation are given in chapter 6.1.2. Based on the final fuel temperature, the initial and final values of the bladder surface temperature  $T_s$  and ullage temperature  $T_u$  can be estimated.

A significant but conservative limitation in the accuracy is that the bladder surface temperature can only be estimated. Rubber has a very low thermal conductivity, so the temperature will vary strongly across the surface; the average temperature depends on the structure surrounding the tank. Within the project scope, it is not realistic to investigate this in detail, so a conservative estimate of bladder temperature is used, by considering it to lie between fuel and ambient temperature. The surface temperature is expected to follow fuel temperature more closely due to the previously discussed thermal insulation provided by crash-resistant foam. This approach was decided upon in discussion with Airbus experts – refer to chapter 13.3.

Lastly, given the initial and final fuel temperatures, the solubility of water in the fuel is calculated based on the experimental data discussed in chapter 2.1.1. As with the density correlation, the coefficient and exponent vary between fuel blends; those shown in Figure 40 are average values.

### 11.3.2 Humidity Exchange

The humidity exchange section performs the calculation of water transfer between humidity in the ullage air and dissolved water in fuel, based largely on the works of Terada and Merkulov as discussed in chapter 3.5. This allows the calculation of new humidity (water concentration) values for both phases, which in turn is required to calculate water precipitation.

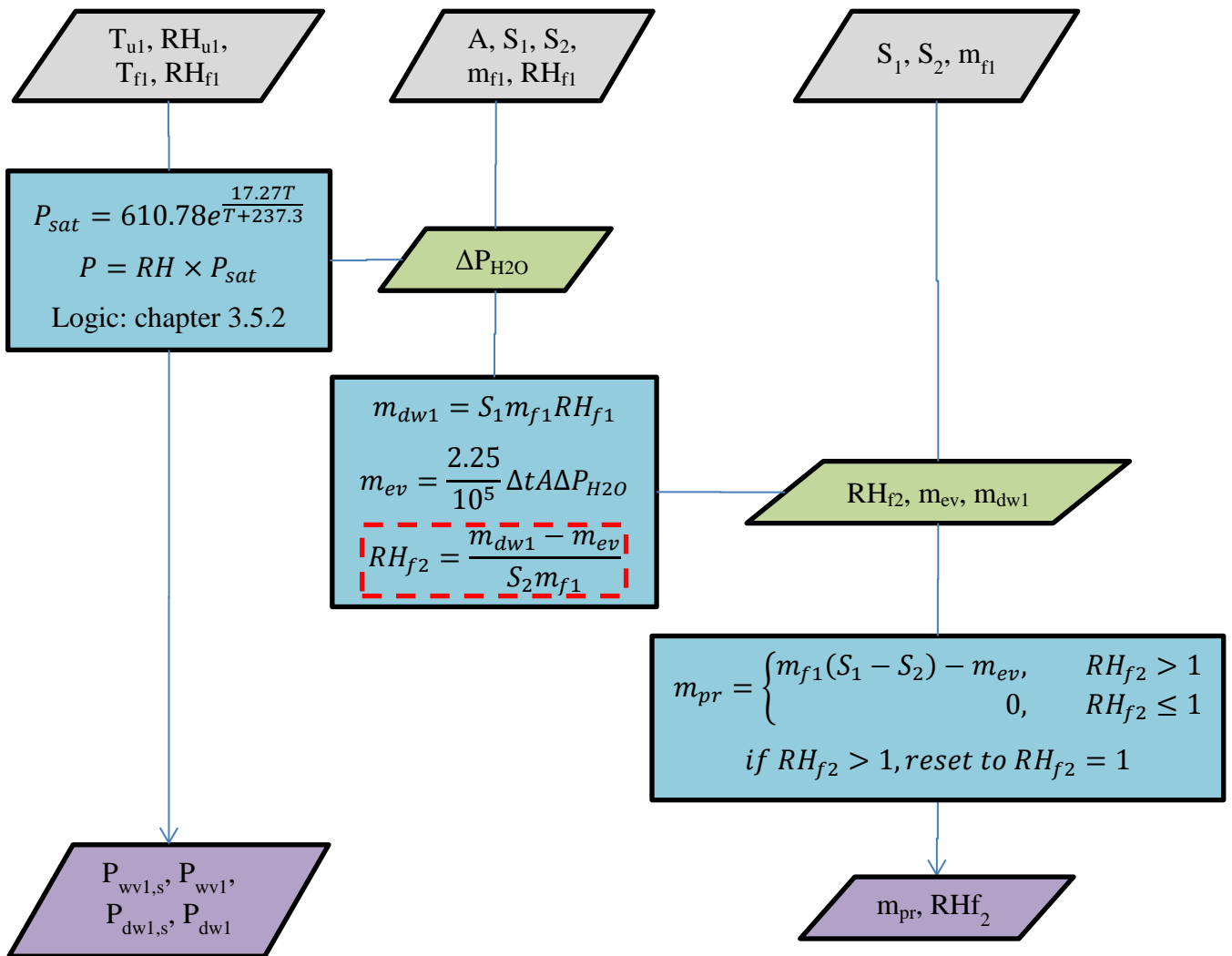


**Figure 41: Schematic representation of humidity exchange between fuel and ullage. Red highlight: this expression represents the theoretical  $RH_{f2}$  before precipitation; precipitation occurs if this is greater than 1.**

In the first step, the Tetens equation (equation (1)) is used along with some decision logic (chapter 3.5.2) to determine the vapour pressure difference  $\Delta P_{H_2O}$  between the fuel and air. This value is then used with equation (9) to calculate the quantity of water evaporating from or absorbed by the fuel.

Having calculated the quantity of water evaporated from or absorbed by the fuel, a mass balance can be constructed to determine the quantity of dissolved water precipitated as liquid droplets. It is not necessary to consider the quantity of dissolved water consumed by the engine, as (under the assumption of a homogenous water-fuel mixture) this does not affect the concentration of water in the fuel. Therefore, one must only compare the final concentration of dissolved water (taking into account transfer to or from the ullage) to the final water solubility to determine whether any precipitation occurs, and if so, how much.

### 11.3.3 Vent Flow

The vent flow calculation is independent of the humidity exchange between ullage and fuel, but the change in ullage temperature (from the thermal calculation) is required, as this temperature

variation partially drives flow through the fuel tank vent(s) by affecting the air density. Much larger flow rates are achieved when the ambient pressure changes (during climb or descent).

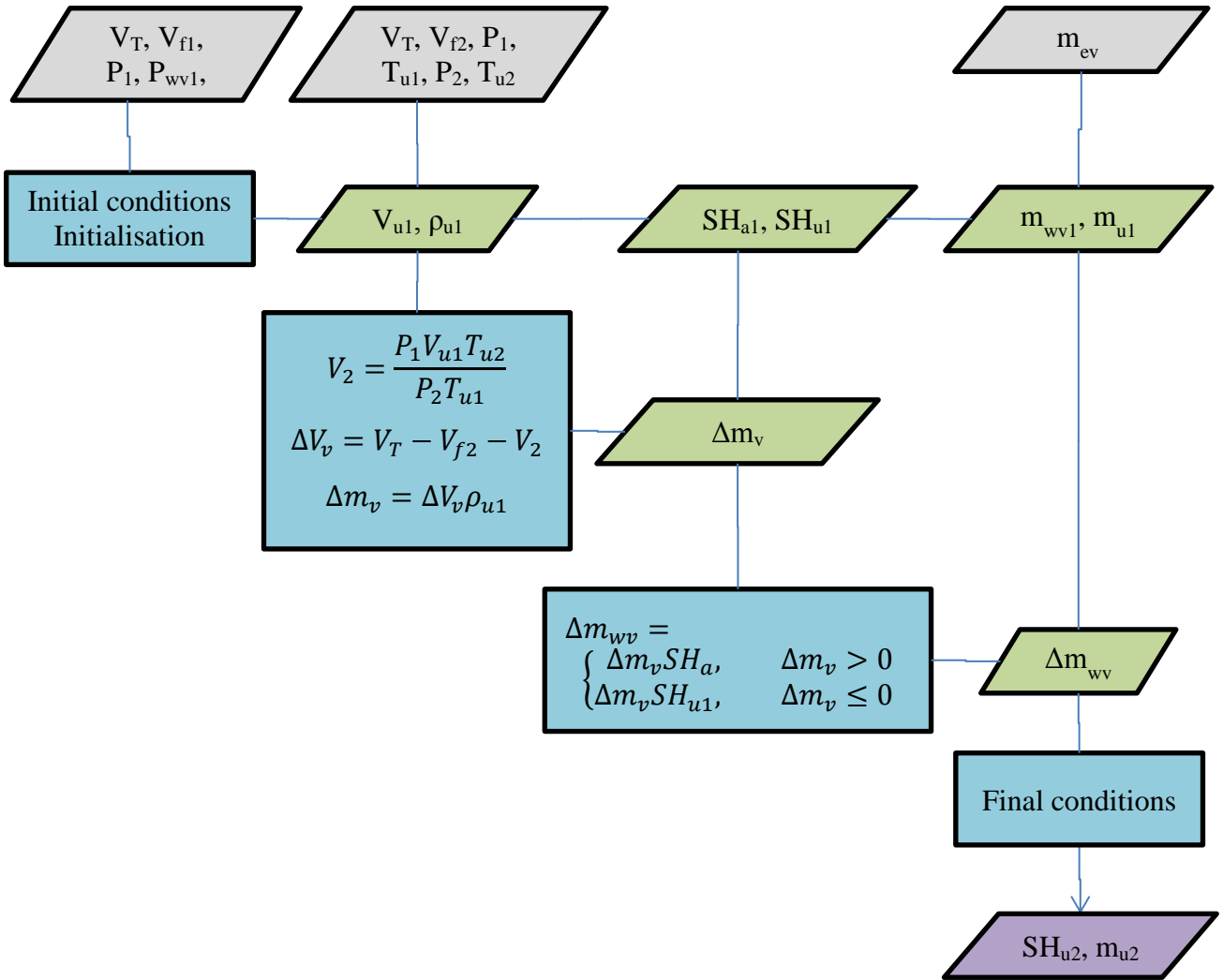


Figure 42: Schematic representation of vent flow calculation.

To calculate the air ingress or egress, the ideal gas law is used. With this law, the final volume of the initial ullage gas mass under the final conditions can be determined as shown in equation (11).

$$V_2 = \frac{P_1 V_{u1} T_{u2}}{P_2 T_{u1}} \tag{11}$$

Using a volume balance considering the tank volume  $V_T$ , final fuel volume  $V_{f2}$ , and the new air volume  $V_2$ , the volume of any ingress or egress is calculated, and multiplying by the density gives the mass of transferred air.

The amount of water vapour that is transferred along with the air depends on the direction of flow, as the specific humidity within the tank is different from that in the surrounding atmosphere. Therefore a conditional function (step 3 in Figure 42) is required to determine the

transferred water vapour mass. With this information, the total mass of water vapour is known and the final specific humidity  $SH_{u2}$  of the ullage can be calculated.

### 11.3.4 Condensation

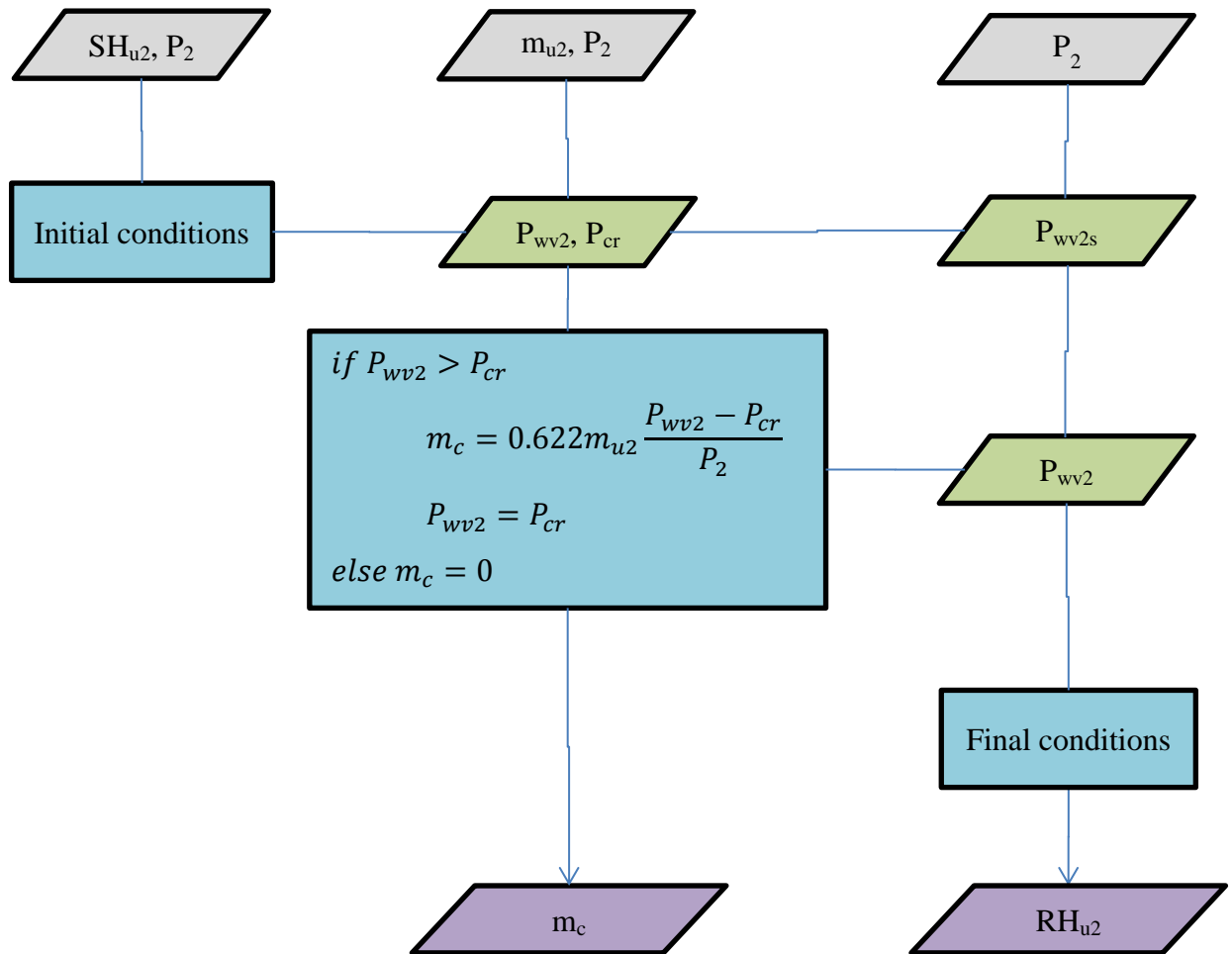


Figure 43: Schematic representation of condensation calculation

As discussed in chapter 3.6, modelling the accumulation of surface condensation in a realistic way is not trivial. The high diffusivity of the gaseous species indicates that a diffusive limit does not apply, which is supported by Wetterwald [9], and the process is instead limited thermally. This is why cross-venting cannot be used as an assumption: cross-venting would introduce an infinite supply of humidity. As stated during discussion of the thermal analysis (11.3.1), the bladder surface temperature can only be estimated conservatively and does not change due to condensation (an exothermic process). This, together with an infinite supply of humidity, would lead to an infinite quantity of condensed water.

The estimation approach therefore consists of considering the dew point of ullage air to always be at or below the bladder surface temperature. If the dew point is raised above the surface temperature by the ingress of humid air, the excess is considered to immediately condense into

liquid water, and to not re-evaporate. The partial vapour pressure associated with the surface temperature is written as  $P_{cr}$ ; the decision logic for calculation of condensation is shown in step two of Figure 43.

## 11.4 Verification & Limitations

### 11.4.1 Result similarity with associated model

Table 9 shows a comparison of water accumulation data produced by the AHWAS' physical model and the AH step 1 model. The fuel was always considered saturated, initial and final temperatures 30 and 20°C respectively, fuel tank volume 700 L. AHWAS was run with a single time step of one second, in order to eliminate the effect of humidity transfer between fuel and air, which is not considered by the AH model.

**Table 9: Result comparison of AHWAS and AH step 1 model**

	% fuel load	AHWAS water qty. (ml)			AH Step 1 model water qty. (ml)			% Diff. (total)
		Precip.	Condens.	Total	Precip.	Condens.	Total	
<b>Ambient RH = 0.5</b>	0	0.0	0.0	0.0	0.0	0.0	0.0	0
	25	2.9	0.0	2.9	3.0	0.0	3.0	-3
	50	5.9	0.0	5.9	6.0	0.0	6.0	-3
	75	8.8	0.0	8.8	9.1	0.0	9.1	-3
	100	11.7	0.0	11.7	12.1	0.0	12.1	-3
<b>Ambient RH = 0.9</b>	0	0.0	3.2	3.2	0.0	8.0	8.0	-60
	25	2.9	2.4	5.3	3.0	6.0	9.0	-41
	50	5.9	1.6	7.5	6.0	4.0	10.0	-26
	75	8.8	0.8	9.6	9.1	2.0	11.1	-13
	100	11.7	0.0	11.7	12.1	0.0	12.1	-3

Large differences are noticeable in the case with higher ambient humidity (where saturation occurs). This is due to the fact that the two models use significantly differing equations to calculate the partial vapour pressure of water. Equations (12) and (13) respectively show the formula used in the AH step 1 model and in the physical model (the latter is the Tetens equation).

$$P_{wv} = \exp\left(\frac{7.625T}{241 + T} + 2.7877\right) \quad (12)$$

$$P_{wv} = 610.78 \times \exp\left(\frac{17.27T}{237.3 + T}\right) \quad (13)$$

The source of equation (12) is not clear, but the calculated vapour pressure differs by up to a factor of 6; while the difference is partially negated when calculating specific humidity (the value of interest when determining condensation, equation (2)), evidently significant variations of up to 60% are still possible.

A further observation from Table 9 is that when the transfer of humidity between fuel and ullage is neglected, the quantity of water precipitated from the fuel is independent of ambient and ullage humidity, which corresponds to empirical expectations.

#### 11.4.2 Limitations

The physical model depends on the fuel thermal constant  $K_f$ , which is calculated from experimental data and is specific to each helicopter type. In order to calculate it numerically, knowledge of the helicopter's structure surrounding the fuel tanks would be required as an input to a finite-element thermal simulation, which is outside of the scope of the present project.

The impact of scaling on the accuracy of the model is not known; any change to the inputs which affect the assumptions listed in section 11.2 could potentially invalidate them. One example of this would be a significantly larger fuel tank, which increases the bladder surface area and decreases the justifiability of considering the entire bladder surface to have the same temperature.

However, the fuel's volume to surface area ratio is accounted for in the model; this parameter affects the rate of change of fuel relative humidity in the presence of an ullage volume with a different humidity (mass transfer rate is proportional to surface area, while rate of change of RH is proportional to fuel quantity).

Therefore it is proposed that the model is sufficiently flexible to be applied to all light and medium helicopters, for which the data required to determine  $K_f$  is available.

As already discussed in section 11.2, the model does not consider the re-evaporation of condensation or the re-absorption of free water into the fuel; both are conservative assumptions, meaning that making these assumptions leads to an over-estimation of the quantity of water found in the tank. Until laboratory experiments have been conducted to determine the rate at which these two processes take place, the assumptions cannot be relaxed.

# 12

## Temporal Model

The purpose of the temporal model is to iteratively control the physical model. Given mission profile, climate and fuel system parameters, the temporal model will run the physical model as a time-step iterative analysis to determine the water accumulation over the given time span.

### 12.1 Theory

Aside from controlling the physical model, the temporal model performs initialization of the required inputs based on the information supplied by the user; a logic diagram is shown in Figure 44.

The given mission profile (provided as a table of altitude over time) and climate (chosen from 4 STANAG 2895 climate categories) are manipulated through interpolation into a table giving the altitude, sea-level temperature and sea-level relative humidity for each iteration. Further calculations are then performed to expand this table with the ambient temperature, pressure and relative humidity at the respective altitude for each iteration. Additionally, the initial and final fuel volumes are determined based on the provided fuel consumption information.

Along with several constant parameters, this information is then passed to the physical model, which provides as outputs the quantity of free water produced during the iteration, as well as the final values of fuel and ullage temperature and relative humidity (degree of saturation). The water quantity is recorded and cumulated to provide the total water quantity after the last iteration, while the fuel and ullage state variables are fed into the next iteration as the initial values.

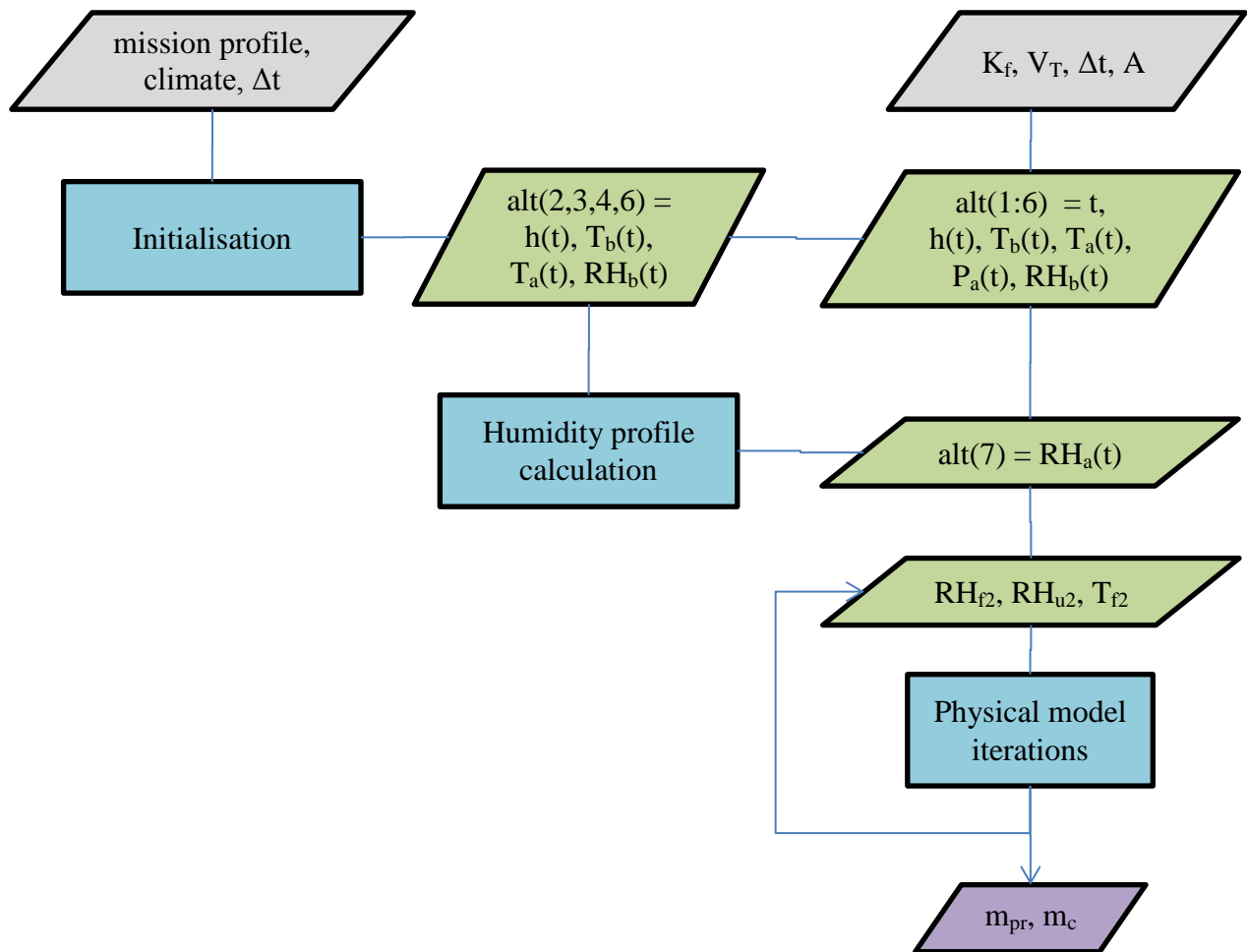


Figure 44: Schematic representation of the temporal model

### 12.1.1 Initialization

The “initialization” section performs several operations to convert the user inputs into the required format. A table (matrix “alt”) is generated with one row for each time step; the inputs are used to generate the time, altitude, base (sea level) temperature, ambient temperature, ambient pressure, base RH, and ambient RH for each time step.

An example of the matrix as provided to the iteration controller is given in Table 10 – this example corresponds to a time step  $\Delta t$  of 60 s.

Table 10: Example of MATLAB® matrix “alt”. The final column, giving the ambient humidity at the given altitude, is shown here for completeness but is actually calculated by the following section “humidity profile”.

Time (s)	h (ft)	T <sub>b</sub> (K)	T <sub>a</sub> (K)	P (Pa)	RH <sub>b</sub> (-)	RH <sub>a</sub> (-)
0	0	300.15	300.15	101325	0.94	0.94
60	0	300.15	300.15	101325	0.94	0.94
120	500	300.15	299.15	99500	0.94	0.95

The first column is filled simply using a linear series from 0 to the length of the supplied mission profile with a spacing corresponding to the time step length. Then, the mission profile is



interpolated to give the altitude at each time step. The base temperature is interpolated using the time and the STANAG 2895 climate series selected by the user, and the ambient temperature is simply determined using the ISA temperature lapse rate of  $0.0065 \text{ K m}^{-1}$  or  $0.002 \text{ K ft}^{-1}$ . Also using the ISA relationship, the ambient pressure is determined based on the current altitude. The base relative humidity once again is interpolated from the STANAG 2895 profile. Finally, the ambient relative humidity at the current altitude is calculated; this is a rather complex calculation warranting its own section.

### 12.1.2 Humidity profile

The ambient relative humidity is calculated based on the method presented by Parameswaran et al. [22], discussed in chapter 3.4. In order to calculate the humidity, the four coefficients  $C$ ,  $h_0$ ,  $H_1$  and  $H_2$  are needed. The sea-level vapour mixing ratio  $C$  can be easily calculated from the temperature and relative humidity given by the NATO climate categories.

The remaining coefficients are “characteristics of the local area” [23] as well as varying to some degree during the course of a day; for the purpose of this study, they have been generalized such that each NATO climate category is assigned one set of best-fit coefficients that are considered constant over the entire day due to the limited data available. These coefficients were chosen so that the vertical humidity profile calculated by the Parameswaran equation matches the data presented in the appendix. Table 11 provides an overview of the selected parameter values.

**Table 11: Overview of the humidity profile parameters selected for the four climate categories considered by the model. C0 parameters are selected to maintain 100% relative humidity at all times as suggested by NATO; absolute humidity is very low due to the low temperatures so no significant condensation occurs.  $h_0$  = transition altitude,  $H_1$  = humidity gradient below  $h_0$ ,  $H_2$  = humidity gradient above  $h_0$ .**

Climate	A3	B2	M2	C0
Location	Germany	Japan	Papua New Guinea	Japan
Time of year	September	September	--	December
Time of day	midday	midnight	midday	evening
Base temp. (°C)	20	30	31	-18
$h_0$ (km)	1.1	2.0	0.6	1.0
$H_1$ ( $\text{km}^{-1}$ )	10.0	3.5	6.0	1.9
$H_2$ ( $\text{km}^{-1}$ )	1.0	1.5	2.05	1.7

Figure 45 shows, for each climate, the humidity data found in literature compared with the selected humidity profile used in the model. When a compromise was necessary, preference was given to an accurate representation of the humidity at low altitudes, where helicopters perform the majority of their missions.

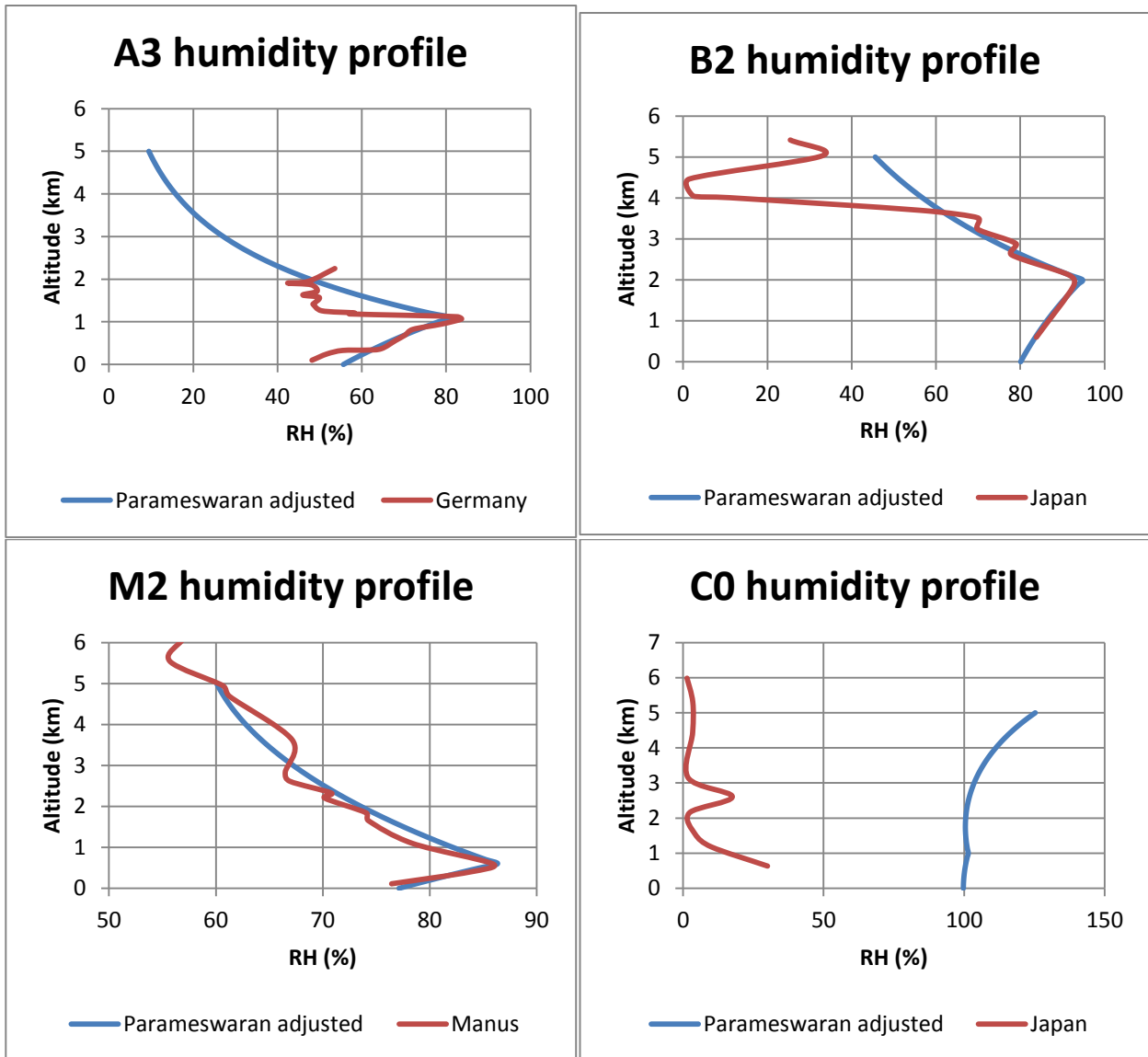


**Figure 45: Vertical humidity profiles for climates A3, B2, M2, and C0. Measured or simulation data shown in red, AHWAS inputs in blue. Relative humidity is capped at 100% in AHWAS.**

Climate C0 (mild cold) is a special case. The measured data does not conform to the Parameswaran profile at all, and furthermore, appears to contradict STANAG 2895 which states that sea-level relative humidity is 100% at all times in climate C0. In practice the impact of this difference is very small, as the absolute humidity air can carry at the temperatures (ranging from -19 to -6°C) does not lead to significant water accumulation, a fact which is supported by empirical observations that no water accumulation occurs in winter. Therefore, coefficients were chosen that lead MATLAB® to provide (close to) 100% relative humidity at all altitudes in climate C0. RH is capped at 100% in the model, so no supersaturation is considered (which is theoretically possible in the absence of condensation nuclei, but practically unlikely in the earth's atmosphere).

As previously mentioned, the sea-level vapour mixing ratio,  $C$ , is directly dependent on the relative humidity and temperature. Therefore, this value is calculated individually for each time step. As the sea-level temperature and humidity change over the course of a day (as per STANAG 2895),  $C$  therefore also varies, resulting in different vertical humidity profiles during

the day, even though the remaining coefficients of the Parameswaran equation have not been changed. This is shown in Figure 46.

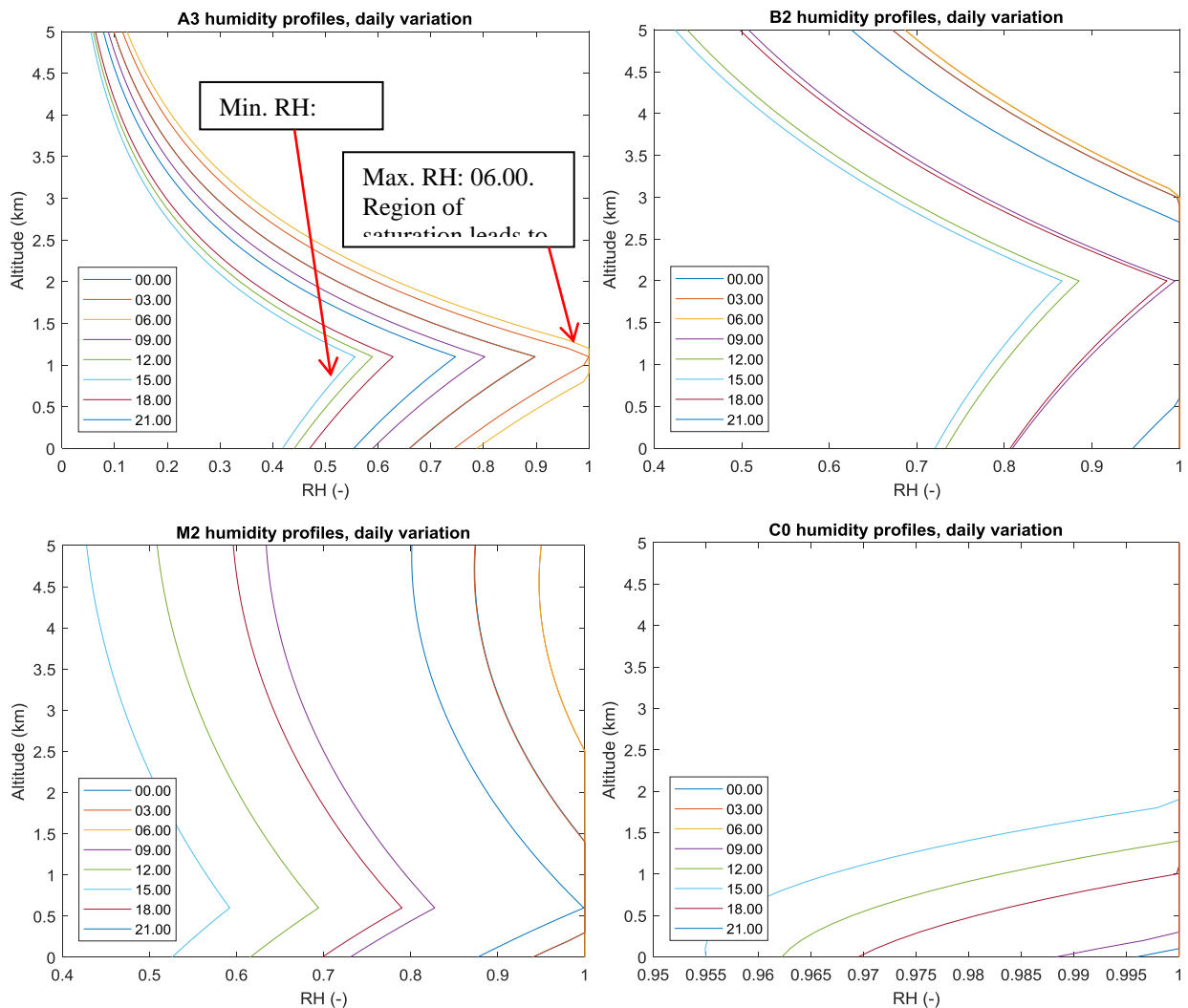


**Figure 46: Vertical humidity profiles for each of the four climates. Profiles differ throughout the day as sea-level relative humidity changes, which changes the value of C in the Parameswaran equation. Note the creation of a saturation region around the transition altitude in climate A3, even though the ground humidity never reaches saturation. A flight through this region will encounter condensation even though relative humidity is moderate at sea level.**

Best accuracy (especially above the transition altitude) would be achieved if different gradients were used depending on time of day, however as previously discussed, this is limited by the availability of data. Additionally, accuracy of the humidity profile increases close to the ground, which is where most helicopter missions take place.

## 12.2 Assumptions

### 12.2.1 Fuel consumption

The main helicopter model of study is the H135; performance data is readily available for this type. At maximum gross weight, the fuel consumption is approximately  $290 \text{ l h}^{-1}$  at maximum cruise speed and  $260 \text{ l h}^{-1}$  at the slightly lower economical cruise speed [61]. High-speed cruise corresponds to the maximum continuous power setting of the engines, which is also used during climb; therefore the model considers the climb and cruise fuel consumption figures as  $290$  and  $260 \text{ l h}^{-1}$  respectively.

During descent the fuel consumption rate depends strongly on the rate of descent so it is not possible to make a generalized statement of fuel consumption. However, descent phases are very short due to the fact that rate of descent is greater than rate of climb; an assumption that fuel consumption in descent equals approximately half of cruise ( $130 \text{ l h}^{-1}$ ) is therefore employed in the model. The contribution of fuel consumption to water accumulation is insignificant during descent, because a very large rate of air ingress is caused by the increasing ambient pressure, in excess of  $2000 \text{ l h}^{-1}$ . The change in fuel volume also does not significantly impact water accumulation as the change is very small during the short descent phase, regardless of fuel consumption rate.

### 12.2.2 Climb and descent

The maximum rate of climb of the H135 at sea level and maximum gross weight is  $1500 \text{ ft min}^{-1}$  ( $7.6 \text{ m s}^{-1}$ ) [61]. Climb performance decreases with altitude due to decreasing air density, so that at approximately  $16000 \text{ ft}$  ( $4900 \text{ m}$ ), the achievable rate of climb is only  $200 \text{ ft min}^{-1}$  ( $1.0 \text{ m s}^{-1}$ ).

The maximum possible rate of descent is greater than the maximum rate of climb; this phase of flight is (in unpressurised aircraft) limited by physiological as well as technical factors. However, operational reasons appear to limit the descent rate much more strongly: the data in chapter 6.2 show a typical rate of climb of around  $1000 \text{ ft min}^{-1}$  ( $5.1 \text{ m s}^{-1}$ ) and descent rates below  $500 \text{ ft min}^{-1}$  ( $2.5 \text{ m s}^{-1}$ ). These two values are therefore selected as the baseline climb and descent rates.

### 12.2.3 Refueling

Refueling processes are modelled very simply: it is considered that the helicopter is refueled immediately upon landing, and thus its fuel tanks are always filled to 95% when it is on the ground. The 5% ullage space accounts for the presence of a legally mandated expansion space of 2%, among other factors.

The actual refueling behavior will depend strongly on the type of operation; for applications where immediate response at short notice is necessary (air ambulance, law enforcement) it stands to reason that the helicopter is stored with sufficient fuel on board to perform a mission without first requiring refueling.

## 12.3 Limitations

The vertical humidity profiles employed by the model rapidly deteriorate in accuracy with altitude; having been chosen such that the result is conservative (higher assumed humidity than realistic), this leads to an overestimation of water production.

Another limitation results from the fact that the state variables must be initialized, including the initial fuel temperature and relative humidity. Due to the absence of better options, these two parameters are set equal to the initial ambient condition. However, results of simulating one day show that the final values are significantly discontinuous to the initial values; in all observed cases, the result remains conservative as the assumed initial relative humidity was higher than the final relative humidity, leading to a higher water accumulation figure than in reality.

When refueling, there is currently no provision to specify the relative humidity or temperature of the fuel being added; it is just assumed that the humidity is the same as that of the fuel already present inside the fuel tank. This is considered a reasonable assumption, as the fuel stored at the airfield should encounter similar conditions as the fuel remaining inside the helicopter, but it does not account for the possibility that the fresh fuel is saturated with water due to the presence of significant free water at the bottom of the storage tank.

Finally, it is currently only possible to simulate the four specified climate types. This is due to the necessity of one measured vertical humidity profile to calibrate the Parameswaran function; if a different climate is to be simulated, hourly sea level temperature and humidity data must be provided as well as a measured vertical humidity profile.

# 13

## Validation

Due to the absence of physical, measured data to validate the entire model on a system level, alternative validation methods are required. Sargent [62] provides an overview of the possibilities for verifying and validating a computational model. Verification refers to “ensuring that the ... computerized model and its implementation are correct”, while validation addresses the question of whether the model correctly and accurately represents the real system. To achieve these two aims, Sargent lists 15 possible techniques.

The object of study is effectively a non-observable system, as it is not possible within the project scope to perform experiments and collect data from real helicopter fuel tanks; only limited partial data is available from past measurements. Therefore many of the techniques can be applied only in a qualitative context. Considering this constraint, methods to be considered are:

- Animation (graphical representation of input/output relationships, checked against expectations)
- Similarity to other models
- Degeneracy tests (checking whether internal parameters exhibit the expected relationship to inputs)
- Event validity (qualitatively replicating the conditions of known events to ensure that a plausibly correct outcome is produced)
- Face validity (static check of model logic by persons knowledgeable about the real system)
- Internal validity (check of result stability/consistency under repeated calculations)
- Sensitivity analysis (do outputs vary with the expected magnitude and direction when inputs are varied?)

Validation is an iterative process. Animation, degeneracy tests, event validity and face validity checks are an integral part of the evolutionary development process; the examples presented in this chapter represent only a small sample of all the checks performed.

### 13.1 Similarity

In this section, the modelling method will be compared to the data produced by Wetterwald's model. Knowing the assumptions taken by Wetterwald (chapters 8.3 and 11.2), it is possible to

apply the same assumptions to AHWAS to ensure the two models produce the same results. This is described in the following section.

### 13.1.1 Recreating Wetterwald's data

Wetterwald provides data from a simulation of a Boeing 747 center wing tank while neglecting the effects of the inerting system. This case is similar in concept to the situation on helicopters, so confidence in AHWAS can be increased by recreating the circumstances to observe similarity.

To recreate Wetterwald's experiment, AHWAS was run with the mission profile specified (a trilinear altitude and fuel temperature profile, shown in Figure 47). The fuel thermal model was deactivated and replaced by a table of fuel temperature against time for each time step. The time step was set at one second to match the simulation parameters.

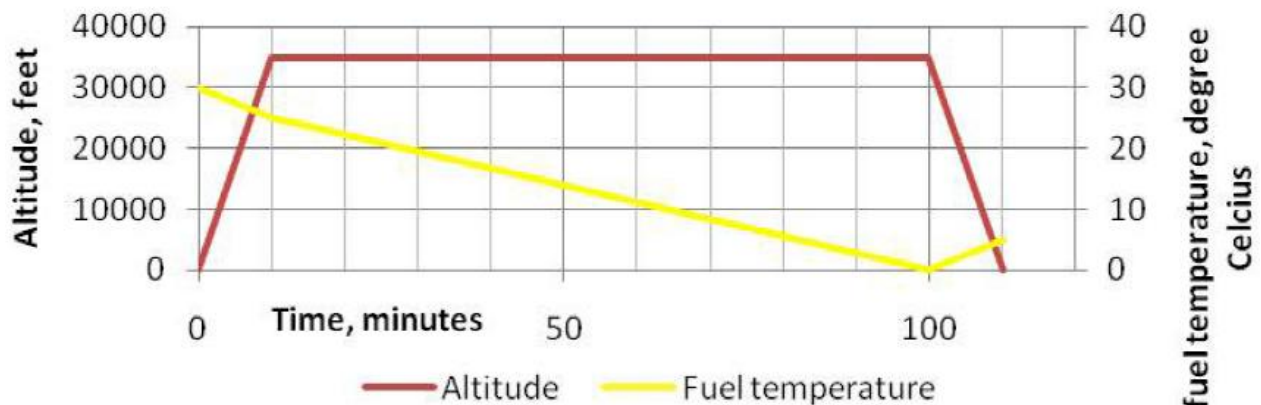
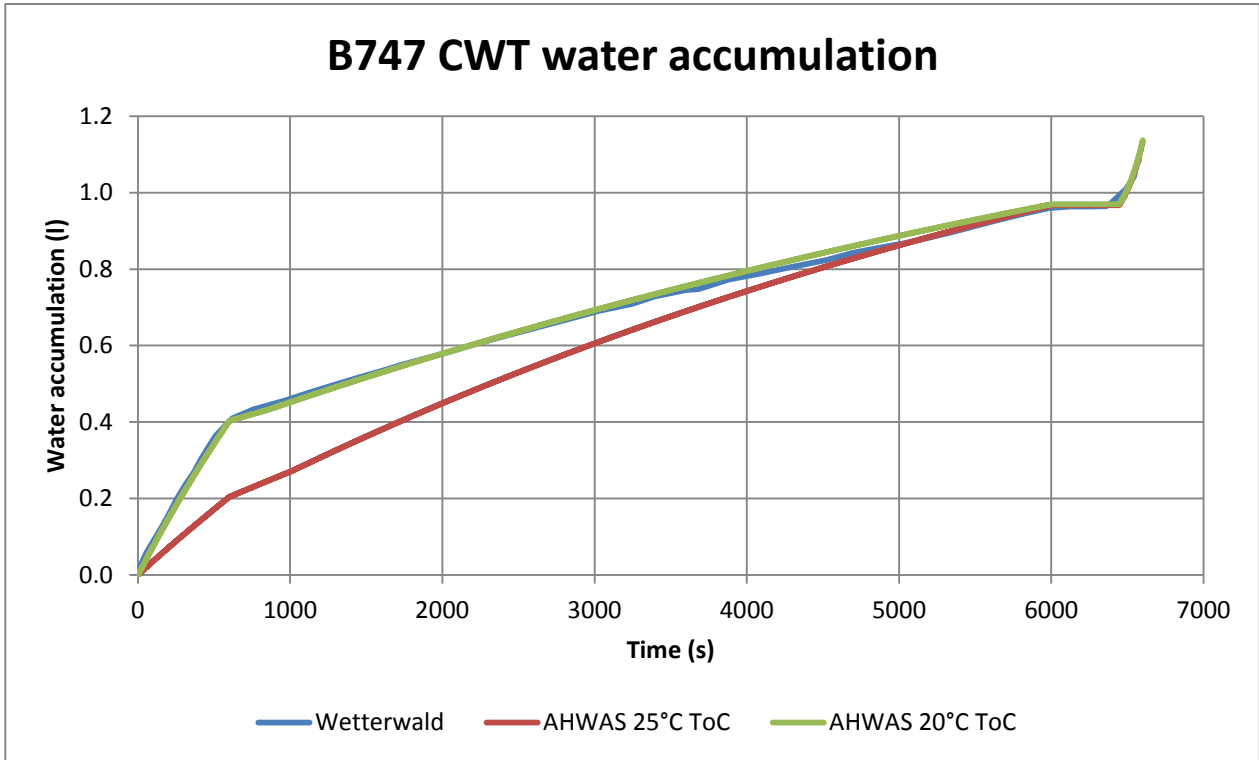


Figure 47: Wetterwald model mission profile [9]

In order to match assumptions, the exchange of humidity between fuel and ullage was disabled for this comparison. Wetterwald uses the altitude-dependent humidity profile proposed by Parameswaran (chapter 3.4); the same parameter values were used to recreate the results.

Wetterwald provides water accumulation over time for a Boeing 747 center wing tank (CWT) of  $52.5 \text{ m}^3$ ; although this is far from representative of a helicopter fuel tank, the data can be used to evaluate AHWAS. This is shown in Figure 48; the results using the above temperature profile are shown in red.



**Figure 48: Boeing 747 CWT water accumulation from Wetterwald and AHWAS**

The final results agree very closely and exhibit a very similar profile. Nevertheless, Wetterwald’s model shows a more rapid precipitation process during climb, where there is a faster fuel cooling rate. As the results agree very well in the latter half of the time span, it may be that the fuel temperature profile given by Wetterwald as an example (Figure 47) is not the same as that used to produce the results. Changing the fuel temperature at top of climb from 25 to 20°C (while keeping the initial and final temperatures the same) results in a near-perfect agreement between the two datasets, as should be expected given the replication of input parameters (shown in green).

**Table 12: Comparison of temporal model results with Wetterwald results**

Fuel tank	% fuel load	Wetterwald (l)	AHWAS (l)	% difference
<b>A320 CWT</b> <b>8.0 m<sup>3</sup></b>	0	0.04	0.05	32
	25	0.10	0.11	12
	50	0.16	0.17	8
	75	0.22	0.23	4
	95	0.27	0.27	-2
<b>B747 CWT</b> <b>52.5 m<sup>3</sup></b>	0	0.25	0.35	39
	25	0.64	0.73	15
	50	1.06	1.13	7
	75	1.47	1.54	4
	95	1.80	1.86	3

Comparing the results produced by the temporal model to those given by Wetterwald (Table 12, Figure 49), the results converge when the tank is full. This points to the temporal model producing a higher value for condensation, which is consistent with the differing assumptions



between the two, specifically that Wetterwald does not account for surface condensation, which as he states, leads to an underestimation of total condensation quantity. Both models used fuel solubility and density curves given by the 1983 edition of the CRC handbook (which differs from the current edition), so that only condensation can possibly be responsible for the discrepancy.

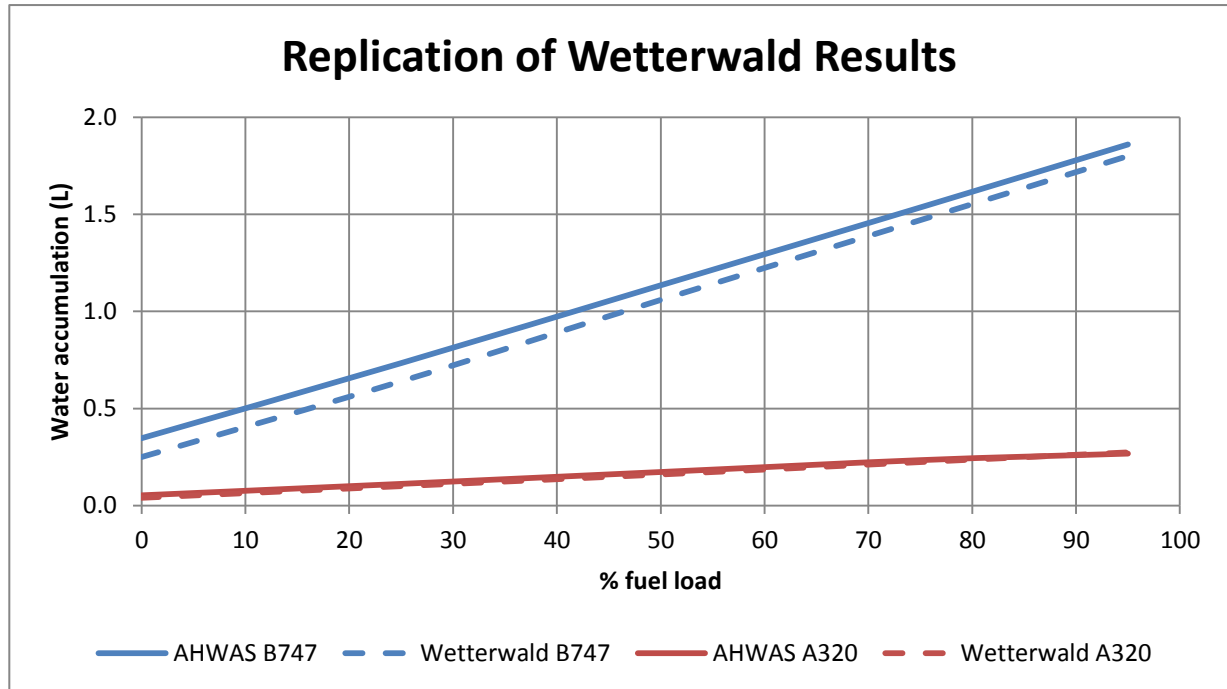


Figure 49: Comparison of AHWAS results with Wetterwald

In summary, the two models produce very similar final results, regardless of the intermediate fuel temperature, as shown in Figure 49, so the similarity check is considered passed.

### 13.1.2 Scaling Effects

The Boeing 747 fuel tank considered by Wetterwald is two orders of magnitude larger than the tanks of small helicopters, raising the question of whether scaling effects limit the relevance of this validation. Particularly the very different ratios of surface area to volume (of both ullage and fuel) can be expected to lead to significant non-linearities.

However, under the specific modelling assumptions employed by Wetterwald, this is not the case. The assumptions of perfect mixing in both fuel and ullage phases, as well as the usage of a fixed temperature profile instead of a calculation relying on heat transfer and fuel mass, lead to a calculation output that is independent of scale, even though the real system most likely does display scaling effects.

As an example, multiplying the fuel tank volume and fuel volume of the B747 by 0.5 yields 0.6033 l of water accumulated (compared to 1.2067 l for the standard configuration), or exactly half. As previously discussed, the outcome is not dependent on the fuel surface area in a statistically relevant magnitude. Finally, the fact that the fuel temperature pathway between the initial and final temperatures (Figure 48) does not affect the final outcome further indicates model linearity.

## 13.2 Degeneracy

Degeneracy checks consist of examining the relationship between inputs or outputs and key internal parameters (state variables) used in the analysis, to determine whether their relationship conforms to expectations based on logical reasoning and empirical observation. Degeneracy checks are the primary method employed during the development of this analysis when checking for the presence of errors and locating their source. Selected examples are presented below.

### 13.2.1 Surface Condensation

As discussed in chapter 11, surface condensation is estimated based on the relationship between the ullage dew point and the bladder surface temperature. Any dew point has an associated saturation vapour pressure; therefore, if the actual vapour pressure in the ullage exceeds the saturation vapour pressure associated with the bladder surface temperature, condensation will occur on the surface.

Figure 50 shows the volume of condensation (left) and the vapour pressures in the ullage (right) over the course of three days in climate B2 (hot and humid).

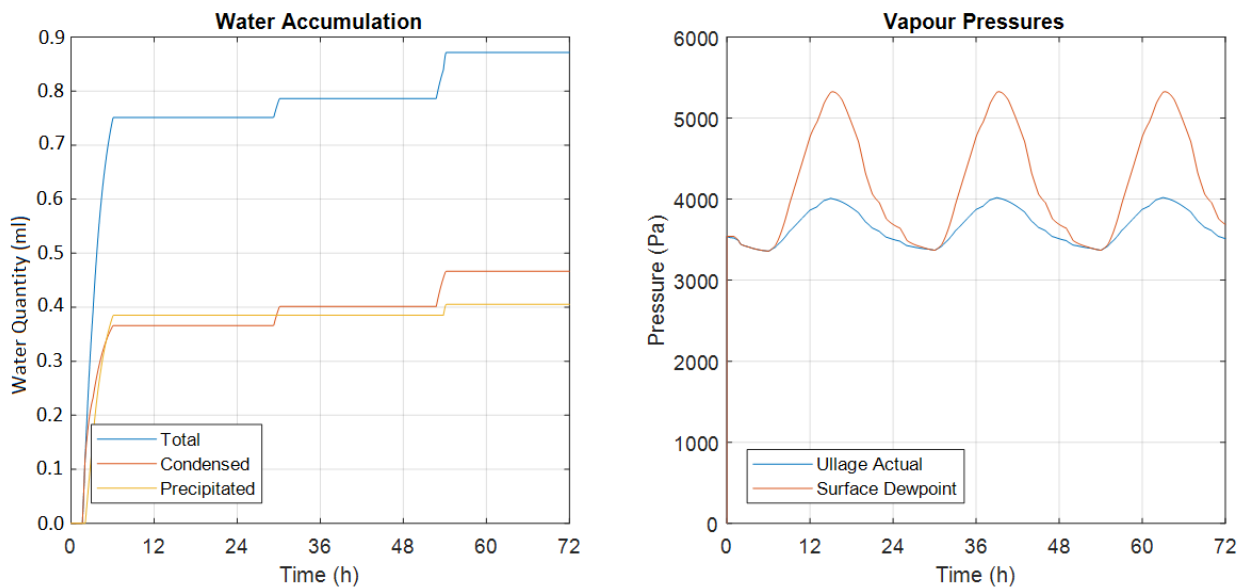


**Figure 50: Degeneracy check of condensation accumulation and vapour pressures**

Comparison of the two graphs shows that each time the ullage vapour pressure meets the surface dew point vapour pressure, condensation occurs (the quantity of water increases). Additionally, knowing that the three day sample interval begins and ends at midnight, it can be concluded that condensation occurs exclusively in the early hours of the morning, corresponding to empirical observations of dew on cold surfaces outdoors after a cool night.

## 13.2.2 Fuel-Ullage Humidity Exchange

During model development, a degeneracy check of the relative humidities of the fuel and ullage compared to the water mass transfer between the two phases (evaporation / hygroscopic absorption) was conducted multiple times to ensure correct directionality. A negative mass transfer indicates evaporation while a positive figure indicates absorption.

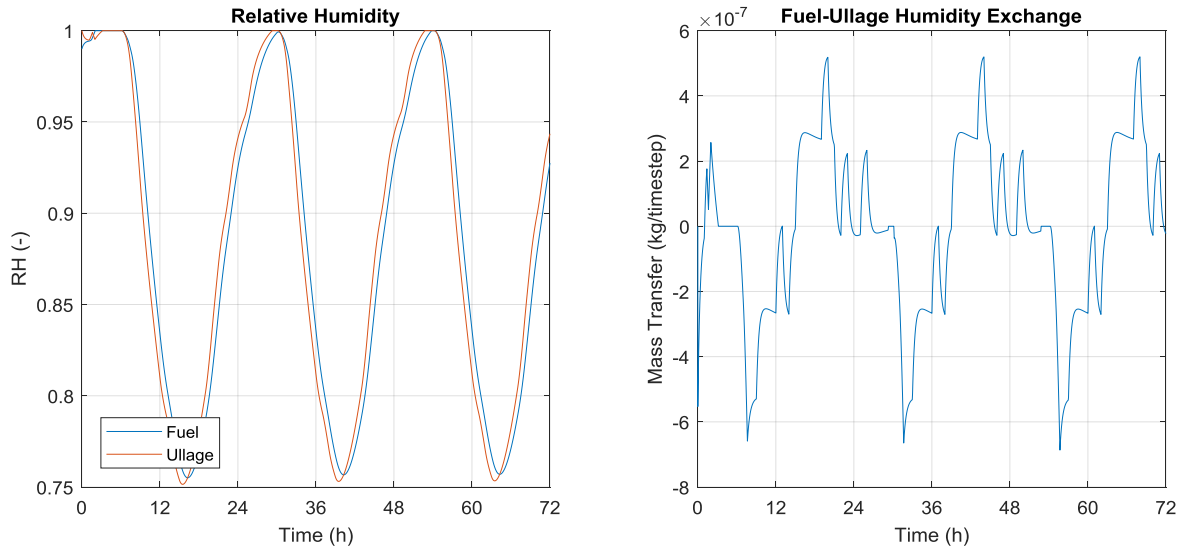


**Figure 51: Comparison of fuel and ullage relative humidity (left) and interphase humidity exchange (right)**

In Figure 51, it can be seen that the rate of water transfer between fuel and the ullage is correlated to the difference in relative humidity (only if both phases are at equal temperature, which they were during this test). Furthermore, the correct directionality is confirmed, as the transfer of water is negative at times between 09:00 and 15:00 each day, during which interval the relative humidity of the ullage is lower, causing the more humid fuel to release moisture to the air.

## 13.3 Face validity

Face validity involves presenting and discussing the model (focusing on the logic and assumptions) to persons knowledgeable about the real system and/or subject matter [62]. Apart from the project supervisors, Vincent Pommé (the Airbus Helicopters expert for environmental control systems) was consulted.

The definition of bladder surface and ullage temperatures was raised as a source of significant uncertainty. Both  $T_s$  and  $T_u$  must lie between the ambient and fuel temperature, and are interpolated during each time step. A sensitivity analysis was conducted to determine the effect of these temperatures on the calculated water quantity, the results of which are shown in Table 13. Each was assigned one of 5 interpolation locations, leading to 25 simulations in total, of one day each (the mission profile and other conditions are discussed in section 13.4.1).

**Table 13: Calculated water accumulation (ml), depending on definition of bladder surface temperature  $T_s$  and ullage temperature  $T_u$ .**

		$T_s$				$T_f$
		$T_a$	25%	50%	75%	
$T_u$	$T_a$	1.02	1.02	1.02	1.02	2.11
	25%	2.58	0.60	0.60	0.70	2.10
	50%	3.55	2.05	0.19	0.70	2.11
	75%	3.87	2.63	1.75	1.04	2.39
	$T_f$	4.97	4.11	3.24	2.51	2.50

The results in Table 13 indicate that the case when  $T_u = T_f$  and  $T_s = T_a$  is the most conservative (the largest quantity of water is calculated). This was confirmed for other mission profiles and climates using a statistical analysis with a random mission profile generator. One example of this analysis (random missions, climate M2) is shown in Figure 52; the four colours correspond to the four corners of Table 13. The analysis showed that  $T_u = T_f$  and  $T_s = T_a$  is the most conservative case for any mission altitude and duration.

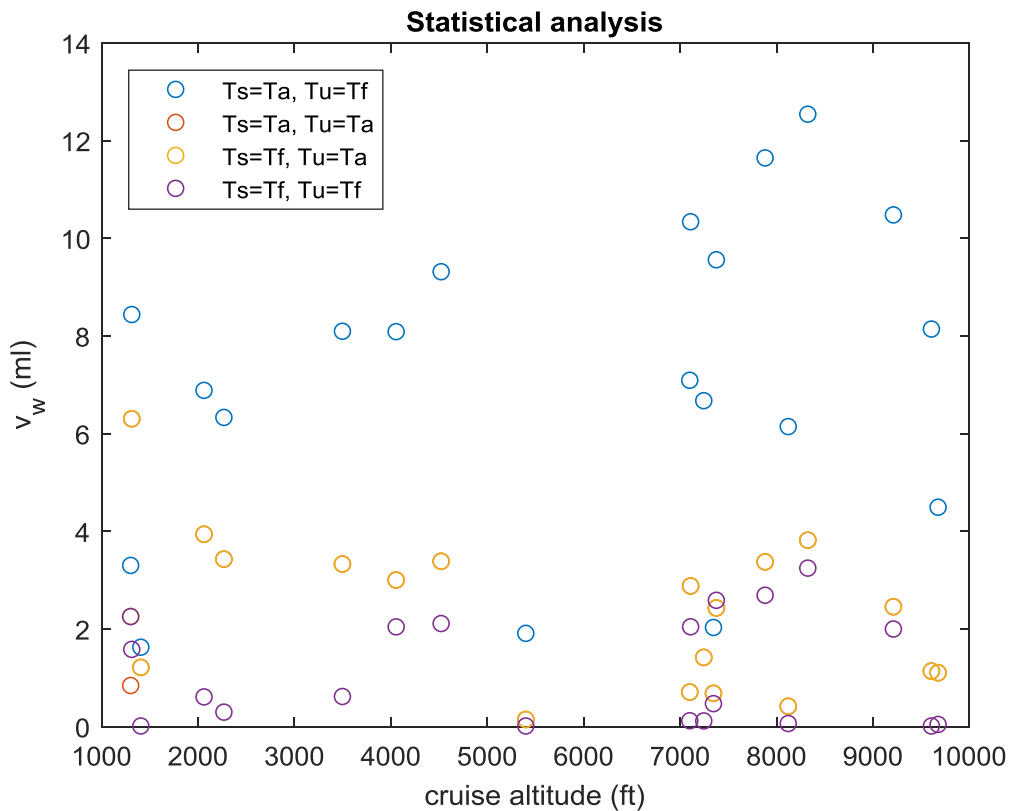


**Figure 52: Results of a statistical analysis, showing that  $T_s = T_a$  and  $T_u = T_f$  generate the largest water quantities independent of mission profile (the mission durations and time of day were also random).**

The advantage of using the most conservative case possible, even if this combination of temperatures is physically impossible, is certainty: the actual water quantity accumulating in the fuel tank must be below the calculated value.

However, in discussion it was concluded that an acceptable balance between conservatism and certainty would be achieved by considering the ullage to be at fuel temperature, while the bladder

surface should also be close to fuel and ullage temperature rather than ambient; its entire interior surface is in contact with air or fuel at  $T_f$ , and the bladder's exterior is well insulated from the ambient conditions. It was decided to consider  $T_s$  as 75%  $T_f$  and 25%  $T_a$ , or  $T_s = \frac{3T_f + T_a}{4}$ . As discussed in chapter 11.2.1, cross-venting is not considered, which is why the ullage temperature is considered to so closely follow fuel temperature.

The remainder of the logic was accepted as reasonable, and the assumptions correct and conservative where necessary. Uncertainties are covered by a sufficient level of conservatism to produce a high degree of confidence in the conservatism of the final result (V. Pommé, personal communication, 4<sup>th</sup> September 2019).

## 13.4 Sensitivity analysis

Sensitivity analysis refers to checking a model or simulation by varying its inputs and observing whether the outputs change in the expected way; this can occur quantitatively, qualitatively or both. It is not just physical inputs (such as the ambient temperature) that can or should be investigated; model-internal parameters such as the time step also influence precision and accuracy.

Input parameters will be varied one by one except where multiple parameters are known to be linked. The time step is an example of an independent input, while the tank volume, cross-sectional area and thermal constant are particular to a certain helicopter design and thus are linked. Specifically, the model will be analysed on its sensitivity to:

- Time step
- Mission profile (altitude, time of day)
- Refuelling behaviour
- Climate
- Fuel blend

### 13.4.1 Baseline configuration

Table 14 gives the baseline parameter values. In the following sections, when the model's sensitivity to one parameter is being investigated, the remaining parameters will be kept constant and corresponding to the values presented here.

Table 14: Model input parameter values in the baseline configuration.

Parameter	Value	Explanation
mission profile	one 2-hour flight per day. Figure 53.	
time step (s)	1.0	
fuel thermal constant $K_f$ ( $\text{kJ K}^{-1} \text{s}^{-1}$ )	0.035	
tank volume (l)	701	Linked to helicopter model: H135
fuel surface area ( $\text{m}^2$ )	2.43	
fuel consumption ( $\text{l h}^{-1}$ ), ground/climb/cruise/descent	0/290/260/130	
refuelling	tanks always 95% filled on ground	refuelling immediately on landing
climate	M2	
fuel water solubility curve	Jet A-1: CRC average	

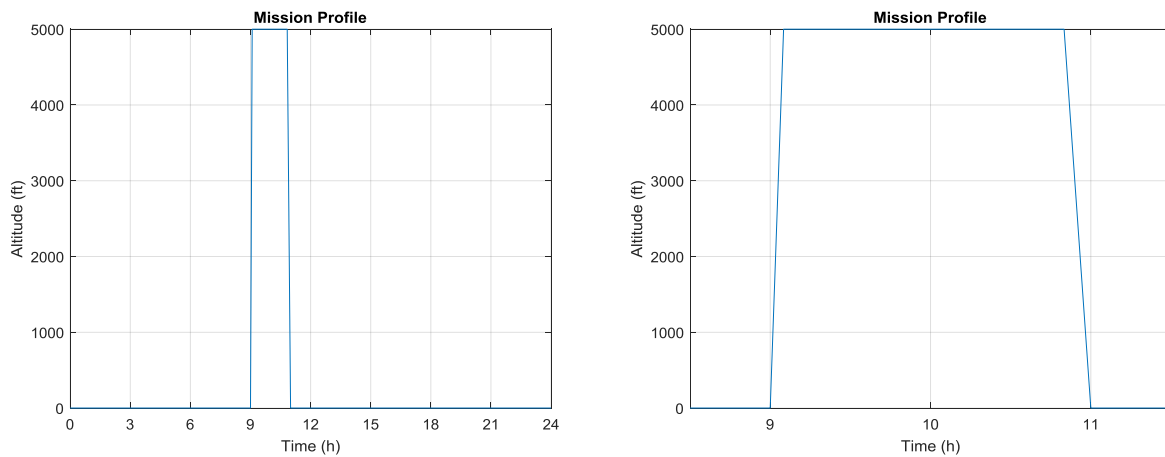


Figure 53: Baseline mission profile including one flight per day (left) and detail view (right). The flight takes off at 09:00, cruises for 01:45 at 5000 ft (1500 m), and lands at 11:00 for a total flight time of two hours. Climb and descent rates are  $1000$  and  $500 \text{ ft min}^{-1}$  ( $2.5 \text{ m s}^{-1}$ ) respectively.

### 13.4.2 Sensitivity to time step

The model was run in the baseline configuration with several time step lengths.

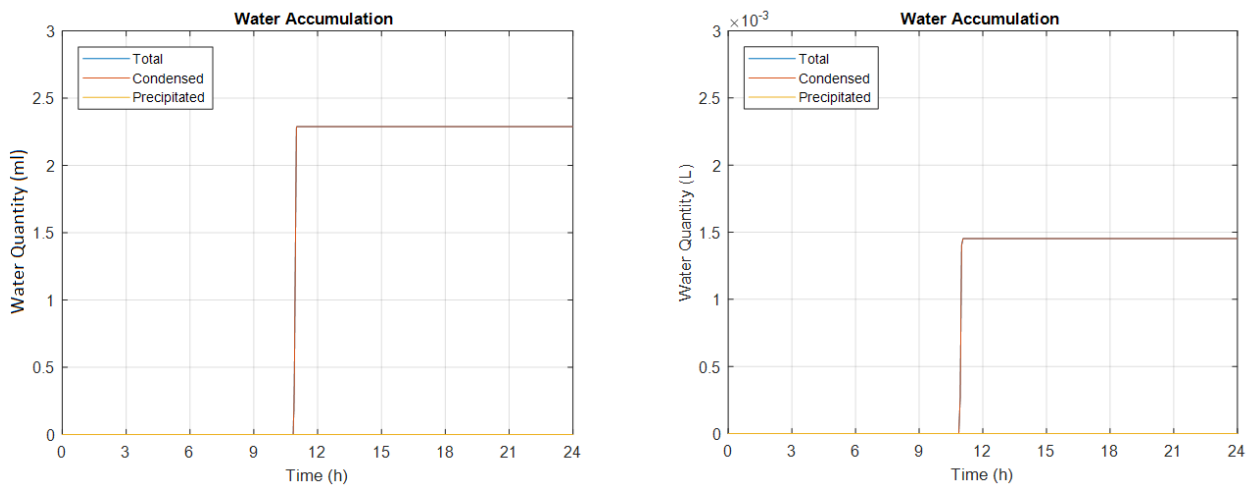
Table 15: Sensitivity analysis results for differing time step

time step (s)	0.2	1	10	60	240	300
time to simulate one day (s)	2494	83	5.9	3.5	2.8	2.9
relative simulation speed	35	1041	14580	24372	30758	29886
generated free water (ml)	2.5470	2.5435	2.5046	2.2885	1.4521	1.1902
% difference in result	0	-0.1	-1.7	-10.1	-43.0	-53.3

Table 15 shows that the analysis is able to tolerate time steps of up to one minute while (almost) staying within an accuracy band of 10%, and that the result converges towards smaller time steps. Depending on the required accuracy, a time step between 1 and 10 seconds is likely to provide the best balance of fidelity and speed. Missions with rapid changes in conditions (e.g. large rate of descent) require smaller time steps to provide appropriate fidelity; the user should keep this in mind and if in doubt, choose a smaller time step.

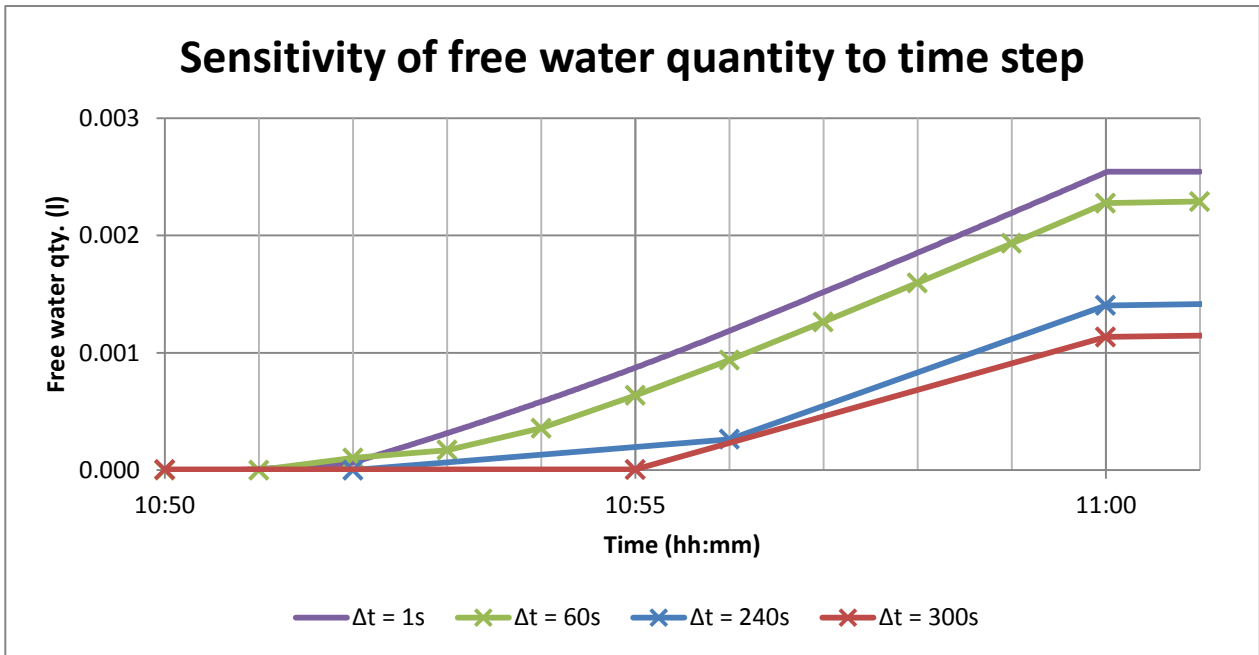
With larger time steps, the result accuracy decreases until the interval reaches 4 minutes (240 seconds); at this point the analysis begins to show unstable behaviour so the result should not be trusted (this is discussed further below).

Figure 54 shows that a large proportion of the accumulated water forms during descent (refer to Figure 53). In this situation, warm low-altitude air meets cool fuel, causing surface condensation. As the descent phase is very short (10 minutes), it is natural that a larger time step leads to this important contributor to water accumulation being inaccurately modelled.



**Figure 54: Water accumulation using a time step of 60 (left) and 240 seconds (right)**

Taking a closer look at water accumulation during descent in Figure 55, the cause of this disparity becomes clear:



**Figure 55: Closeup of free water accumulation during descent phase, with different time step lengths. The descent begins at 10:50:00 and ends at 11:00:00.**

The first time step of the descent phase, regardless of the time step length, does not produce any free water. This is because the ambient conditions are considered constant within each iteration. The longer the time step, the more of the descent phase is neglected due to the lack of fidelity; this limitation is inherent to the time step discretization approach used to model a continuous process. In practice, this does not pose a significant problem as the model can easily employ much shorter time steps which reduce the impact on the final result to well within the acceptable range.

The limit of stability appears to lie around 240 seconds: the ullage humidity begins to oscillate. This is illustrated in Figure 56.

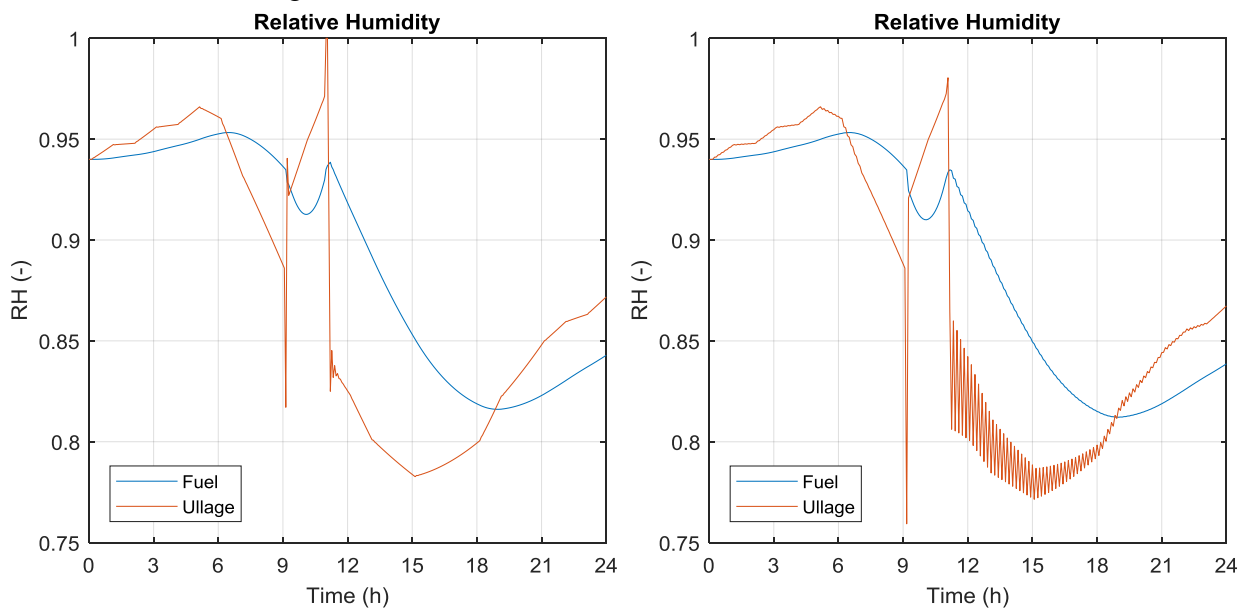


**Figure 56: Fuel and ullage relative humidity in the baseline configuration with time steps of 240 (left) and 300 seconds (right).**



This oscillation is once again inherent to the time step approach. The rate of water mass transfer between the fuel and ullage is calculated once during each time step and assumed to be a constant rate during the entire step, which is an acceptable assumption only when the time step is small. If the interval is too large, the transferred water quantity has the effect of reversing the vapour pressure gradient at each iteration; an oscillation is produced which may or may not subside depending on the time step length. The dependence of water quantity on the time step is therefore an artefact of the simulation rather than a physical phenomenon. This can be seen in Figure 57.

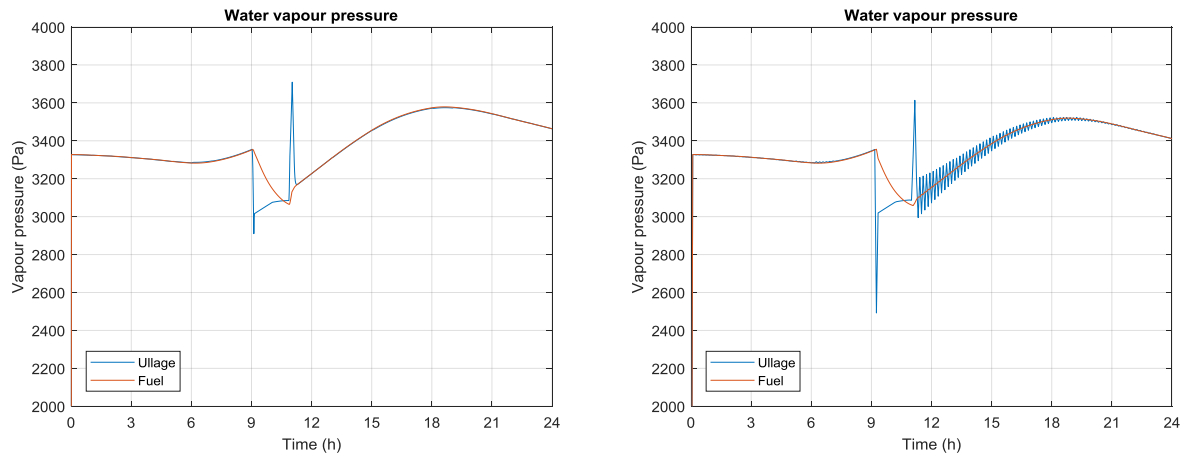


**Figure 57: Water vapour pressure over time with a time step of 60 (left) and 300 seconds (right). Ullage water vapour pressure begins to oscillate about the fuel water vapour pressure.**

If an even longer time step is used, the instability worsens; using a time step of 10 minutes (600 seconds), the oscillations reach a magnitude such that the calculated ullage relative humidity becomes negative.

### 13.4.3 Sensitivity to mission profile

There are endless possibilities for the mission profile: factors include takeoff time, flight duration, cruise altitude, rate of climb and descent, and the number of flights in a given period of time. The purpose of the sensitivity analysis is to ensure the correct functioning of the model, so only a small selection of those parameters needs to be investigated.

Firstly, the effect of only reducing the cruise altitude will be investigated, keeping all other aspects the same. This simulates a situation where on two different days, the same route is flown at different altitudes due to weather or traffic reasons. As the ambient humidity and temperature are dependent on altitude, this should accordingly impact water accumulation. Specifically, the cruise altitude will be reduced from 5000 ft (1500 m) to 2000 ft (600 m), which corresponds to the transition altitude in climate M2. In practice, this might be necessary to remain below the cloud ceiling (which would be expected in the region of maximum humidity).

Secondly, the takeoff time will be changed. Once again, the ambient humidity and temperature depend on the time of day, so accordingly a change in the generated water quantity is expected. Ambient humidity is highest early in the morning, so the baseline takeoff time of 09:00 will be moved forward to 04:00.

**Table 16: Water accumulation - sensitivity to cruise altitude and time of day**

Case	Baseline	Decreased altitude	Earlier start
<b>Generated free water (ml)</b>	2.5435	4.5053	5.5069

In both cases, the accumulated quantity of free water increased over the baseline, as expected due to the higher ambient humidity. This higher ambient humidity increases the mass of water vapour contained in the ullage, and thus increases the quantity of condensation that is released when the ullage reaches saturation.

In the case of an earlier takeoff time, the ullage spends much less time in a saturation condition; however, the bladder surface (which is still much cooler, having not yet warmed up after the cool night) causes local saturation near the surface and thus condensation. Figure 58 shows the relative humidity profiles of both cases.

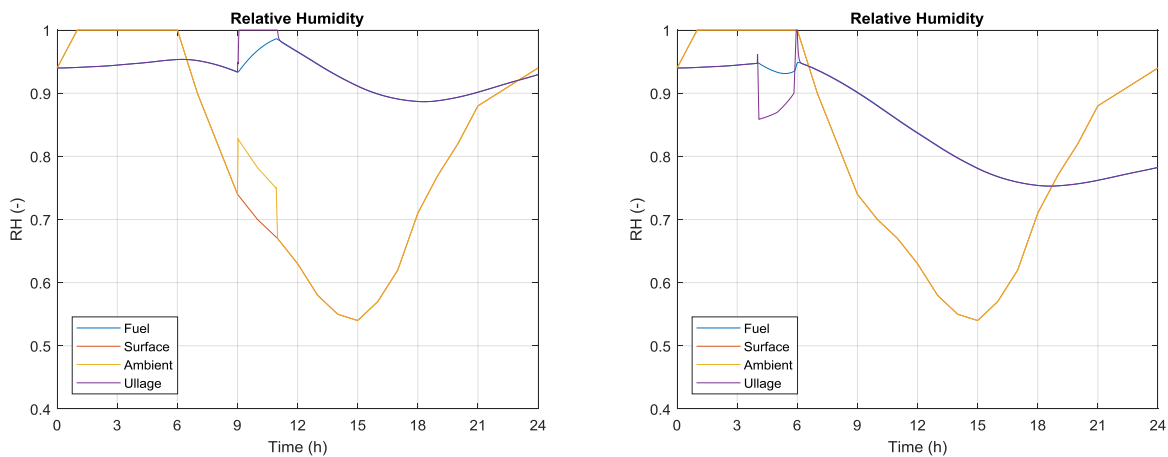


**Figure 58: Fuel, sea level (surface), ambient and ullage relative humidity for the lower-altitude case (left) and the earlier takeoff time case (right). The latter produces approximately double the baseline free water quantity, despite less time spent in saturation conditions, due to surface condensation and increased ambient humidity during flight.**

Comparing Figure 58 to the baseline data given in Figure 59, the higher ambient humidity effects of both modified cases can be clearly seen; a lower cruise altitude increases ambient humidity by moving the flight into the transition altitude, while an earlier takeoff time moves the flight into a more humid part of the day.

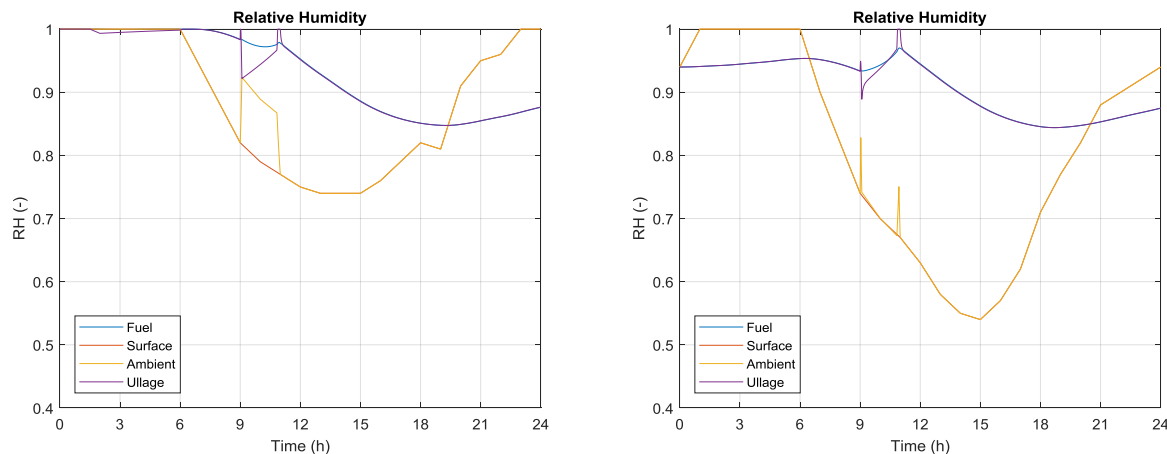
### 13.4.4 Sensitivity to climate

Table 17 gives the quantities of free water generated using the baseline configuration in the four different climates considered. As expected, the two warm, humid climates B2 and M2 produced by far the most water, while those climates found in continental Europe produced little to none.

**Table 17: Water accumulation - sensitivity to climate type**

Climate	A3	B2	M2	C0
<b>generated free water (ml)</b>	0.0000	7.0251	2.5435	0.6308

Figure 59 gives the relative humidity profiles for climates B2 and M2:



**Figure 59: Fuel, sea level (surface), ambient and ullage relative humidity profiles in climates B2 (left) and M2 (baseline, right). B2 shows a much higher average ambient humidity and longer duration spent in saturation conditions.**

Climate B2 shows a much higher average ambient humidity than M2, and is the only climate in which the fuel itself reaches saturation, allowing for the generation of free water by precipitation from the fuel. However it is possible that this effect will not occur on subsequent days (at least not when the fuel mass is large), as the fuel and ullage relative humidity at the end of the day is discontinuous from the values at the beginning (this applies to both climates); the fuel may not reach saturation the following day. However, the ullage will still reach saturation during flight and therefore some condensation will always be produced in these two climates.

The impact of the vertical humidity profile as discussed in section 12.1.2 is displayed in Figure 59: during flight (from 09:00 to 11:00), in climate B2 the ambient humidity is higher than at sea level, while in climate M2 the flight merely passes through a region of high humidity during climb and descent. This is because the latter climate possesses a lower transition altitude (which is the region of highest humidity), so that the flight takes place above transition altitude where humidity is once again lower (Figure 46).

### 13.4.5 Sensitivity to refuelling behaviour

The baseline refuelling behaviour considered is that the fuel quantity is set equal to 95% of the tank volume at all times when the helicopter is on the ground. However, depending on the application, several different behaviours could be considered, among them:

- Full refuelling immediately before the flight
- Filling only to the required level for the next flight
- Flying multiple short missions, refuelling at the end of the day or as needed between missions
- Keeping the tanks partially filled in anticipation of a sudden short-range, high-payload mission (emergency response role)

The refuelling behaviour affects the quantity of fuel in the fuel tanks when the helicopter is parked, and the accumulation of free water while the helicopter is on the ground is dependent on the quantity of fuel within the tanks.

When the helicopter does not fly at all, free water can still be generated under specific conditions. In order for free water to be generated by precipitation from the fuel, the fuel must reach saturation. As the only source of fuel hydration is the ullage (the conditions of which are linked to the ambient conditions), the likelihood of precipitated free water increases with the average daily ambient humidity and the length of time the ambient air is saturated. Additionally, the less fuel exists within the tank, the faster its relative humidity will follow the ullage conditions, meaning that a partially-filled tank has a much higher probability of forming precipitated water than a completely full tank. A smaller fuel mass will also change temperature more quickly, increasing the probability that saturation will be reached by sudden cooling.

In the model, the bladder surface temperature is considered to lie between the ambient and fuel temperatures; the daily temperature range of the bladder surface is therefore greater than that of the fuel. This means that (as far as the model is concerned), condensation will more readily occur than precipitation in edge cases such as when the helicopter does not fly at all. An example of such a situation is shown in Figure 60.

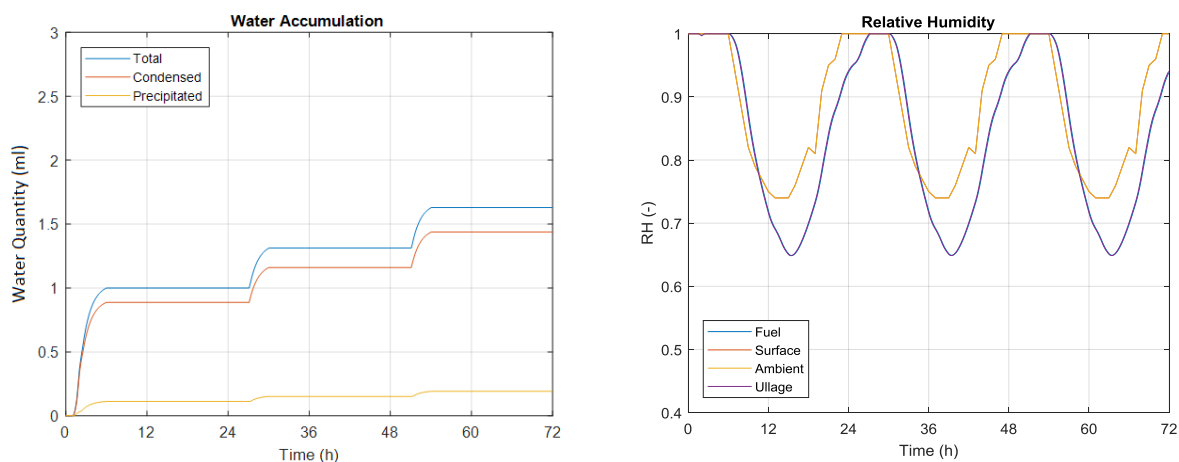


**Figure 60: Water accumulation and relative humidities in climate B2 over three days with no flights, and the tank filled 15% with fuel.**

In climates B2 and M2, free water can be produced continuously when the tank is mostly empty of fuel, such as might be the case if the helicopter is not refuelled after a flight. This continuous phenomenon does not occur in the other climates tested, or if the tank is filled above 50%.

In summary, the factors increasing the probability of free water accumulation on the ground are:

- High average ambient humidity
- Long duration of ambient saturation
- Large daily temperature range
- Low fuel quantity

These results suggest that the accumulation of free water in a helicopter fuel tank while the helicopter is parked or stored can be effectively prevented by storing it with nearly full tanks. This also represents event validity, as this technique is practiced in the automotive world when vehicles are to be stored for extended periods of time.

## 13.4.6 Sensitivity to fuel blend

As discussed in chapter 2.1, the exact composition of the fuel blend in use affects the ability of water to dissolve in the fuel. The absolute value of how much water can be dissolved in a fuel blend at a particular temperature is not relevant, as dissolved water in itself is harmless. The parameter of interest is the sensitivity of water solubility to temperature, or “what quantity of free water is released when the fuel is cooled from temperature X to temperature Y?”. This is often (see chapter 2.1) but not always linked to the absolute value of water solubility.

In this sensitivity analysis, three water solubility curves will be considered: the CRC average for Jet A/A-1, and experimental curves for Coryton high aromatics and Sasol. Importantly, experimental results indicate that Sasol has a lower water solubility across most of the temperature range, but crosses the CRC average curve at 25°C, so that it exhibits a slightly higher solubility than the CRC average at all times in climates M2, B2 and A3. The three solubility curves are shown in Figure 61:

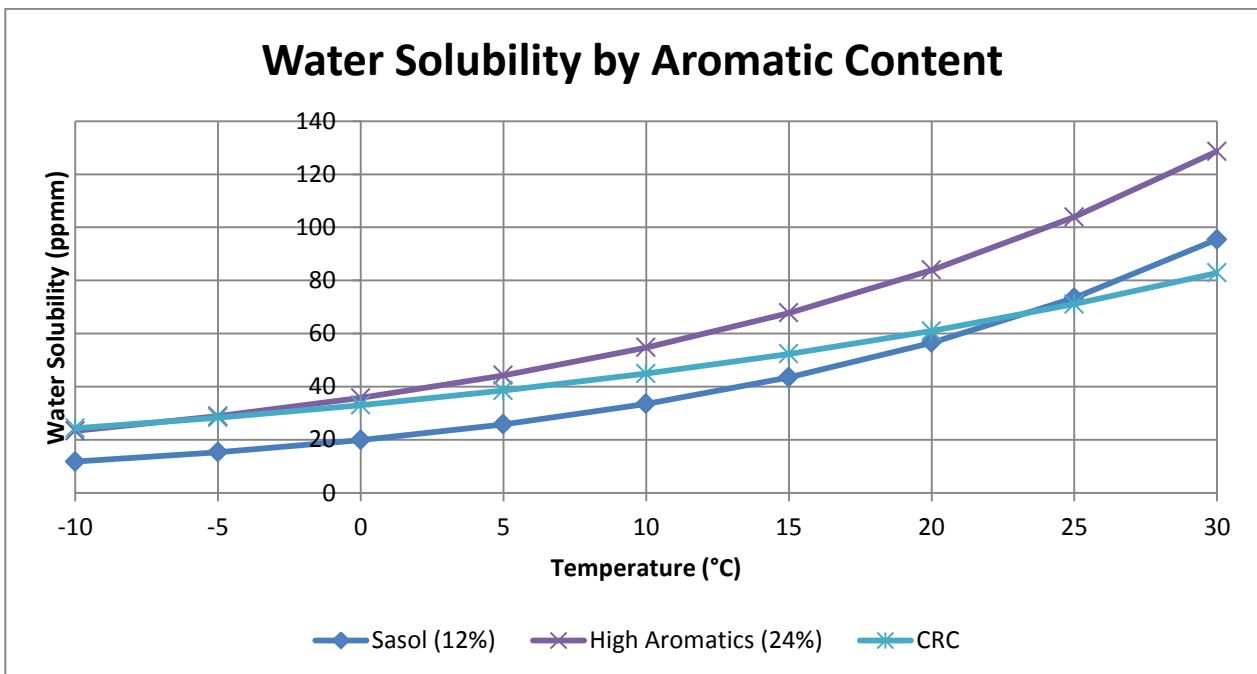


Figure 61: Three solubility curves considered for determining the sensitivity of water accumulation to solubility curve. Extract from Figure 4.

Table 18 shows the results of changing the water solubility curve used by the model.

Table 18: Comparison of generated free water quantities using the CRC average water solubility curve, and the experimentally-determined curves for a high-aromatic (high water solubility) and low-aromatic (low solubility) blends.

Condition	Generated water quantity (ml) by solubility curve		
	CRC avg.	High Aromatics	Sasol
Baseline	2.5435	2.7281	2.7884
3-day ground storage in B2, 15% fuel	1.6700	1.8695	1.8286

Both the high aromatics (24% aromatic content) and Sasol (12%) curves increased the water accumulation in similar magnitude over the CRC average. As both alternative curves exhibit higher solubility at the 26-35°C temperatures encountered (Figure 4), it is expected that both increase water accumulation. However, the results of the high aromatics and Sasol blends lie unexpectedly close together.

The solubility curves for both of these fuel blends were determined experimentally and therefore have an uncertainty band associated with them. Although the data given here cannot prove the relationship between aromatic content and water solubility (other research has already proven this), it does strongly support the hypothesis that higher water solubility leads to more water accumulating in the fuel tank.

### **13.5 Summary of Validation**

Section 13.1 found that the results produced by AHWAS correspond well with those presented by Wetterwald. This not only increases confidence in the reliability of AHWAS but also shows that it is not limited to only simulating helicopters, Wetterwald having chosen the fuel tank of a Boeing 747 to simulate.

Degeneracy checks (chapter 13.2) showed correct and reasonable relationships between internal parameters within the model, as such proving that the physical first principles which form the basis of the model are correctly interpreted and implemented; additionally, the degeneracy checks give the opportunity to compare predicted situations with empirical observations and to thus gain an element of event validity.

This was furthered by consulting with an expert on these physical principles for face validity (chapter 13.3), to whom the logic and assumptions employed by AHWAS were presented and explained. The suggested improvements were taken into account and the logic was approved.

Finally, the sensitivity analysis (chapter 13.4) showed the model behaving as expected in all cases, or in other words, the way in which the model reacted to the differing inputs was in accordance with the underpinning physical processes.

On the basis of the above, AHWAS is considered validated within the scope of the research project. Despite extensive effort in investigating the model's performance, no indication of any incorrect behaviour or error was found. Having passed this milestone, the model is used to simulate real missions and estimate the quantity of water produced; this is described in the following chapter.

# 14

## Results, Conclusions and Recommendations

### 14.1 Results

Given the nearly infinite possible combinations of helicopter type, mission and climate, it is impossible to provide a comprehensive set of results here. Instead, this section is intended to give an overview of what range of water quantities should be expected, and in what relation these stand to safety margins.

A summary of the findings generated by the sensitivity analysis is useful in order to decide which types of helicopter flights are the most critical in terms of water accumulation. This then informs the cases to be studied in the following section and leads to the conclusion of whether or not the water quantities encountered warrant an extension of the drainage interval.

In chapter 13.4.3 (sensitivity to mission profile) it was found that any change in the mission profile that leads to the helicopter spending more time in highly humid air masses increases the water accumulation – specifically, low altitude flights, in humid climates, during humid times of the day. All climates display periods of high humidity in the early morning, so this is the time of day in which the greatest risk of water accumulation exists.

Section 13.4.5 (sensitivity to refuelling behaviour) concluded that a low fuel quantity in the tank is conducive to water accumulation, so the most at-risk operations are those where the helicopter is not refuelled until the fuel level is quite low – most commonly because the flight is long and the destination is remote.

Synthesising all of the findings, the most at-risk helicopter operation is one in which the helicopter performs multiple flights per day (or multiple altitude steps in one flight), at moderate altitude, in a humid environment and is not refuelled until the tank is relatively empty. The individual flight duration does not play a major role.

This corresponds very well to typical oil & gas platform transfer missions, so this case will be examined in further detail in the following section. Additionally, having found that most water accumulation occurs during descent, high-altitude missions will also be investigated.

### 14.1.1 Oil & Gas platform transfer missions

The airbus helicopters H160 is similar in size and intended role to the H175, and as such can be expected to perform similar missions. An insight into the water quantities to be expected in everyday use can be gained by replicating known H175 missions with the H160, for which sufficient data is available to confidently model fuel temperature (section 6.1).

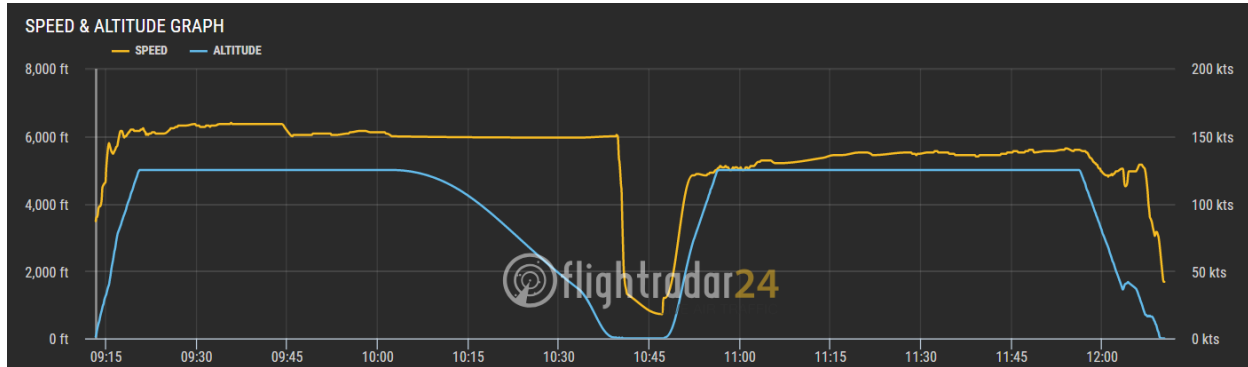


Figure 62: Typical oil & gas platform transfer mission profile [50]

The most feasible climate category for the North Sea in summer is M2 (marine intermediate). Using this climate and simulating the above flight exactly as it was performed, an accumulated water quantity of 5.8 ml is calculated on a H160 (the helicopter is assumed not to refuel on the platform).

However, based on the findings of the sensitivity analysis, it is possible to produce far more water if the conditions are adjusted slightly: more flights in the same day, lower cruise altitude, and a more humid climate. By lowering the cruise altitude to 2000 ft (600 m) and performing two round trips (instead of one) in a day, the simulation arrives at up to 36 ml in climate B2 (which might be expected in more tropical oil & gas fields); a summary is given in Table 19.

Table 19: Calculated water accumulation in a H160 oil & gas platform transfer flights. Low cruise altitude is 2000 ft (600 m), high cruise altitude is 20000 ft (6100 m).

Mission	Water accumulation, H160, by climate (ml)			
	M2	B2	A3	C0
as flown	5.8	15.9	0.0	1.5
two return trips	9.4	32.2	0.0	3.6
two return trips, low cruise altitude	18.0	36.0	0.0	5.0
two return trips, high cruise altitude	8.1	21.5	0.0	3.6

The maximum concentration of water in fuel is 180 ppmv in the worst case; although this is still below the certification limit of 200 ppmv, the calculated concentration would rise if there were less fuel in the tank (the lowest fuel volume was 200 l).

However, in the applicable CS29 certification specification, a sump volume of at least 0.1% is prescribed, which is equivalent to 1.45 l in the H160. In the worst case of 36 ml per day, this still allows 40 days of such flights before the accumulated water escapes the sump.



At the beginning of the project, it was assumed that the lower cruise altitudes favoured by helicopters would lead to less water accumulation due to smaller heat cycle magnitude. Table 19 suggests that this assumption was incorrect, and that in fact the high ambient humidity found at low altitudes is the dominant parameter.

### 14.1.2 High altitude operations

So far, all results have assumed takeoff and landing both occur at sea level. However, helicopters are also frequently used to access mountainous terrain not otherwise (quickly) reachable – a mountain rescue operation, for example. A (fictional) mission profile for such a flight is given in Figure 63.

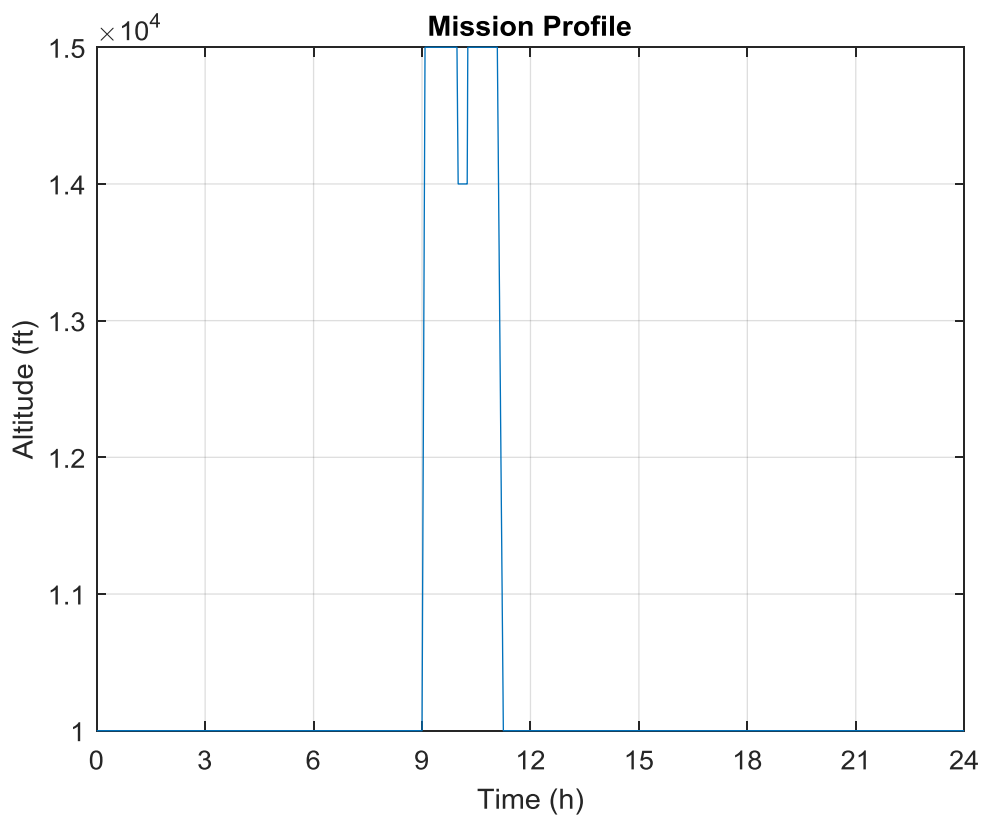


**Figure 63: Fictional mountain rescue mission. Origin heliport at 10000 ft (3000 m), cruise at 15000 ft (4600 m), rescue site at 14000 ft (4300 m). Flight duration each way is one hour.**

The above mission profile generated a maximum of 0.21 ml of water in climate C0 (all other climates produced less) for both helicopters. Evidently, high-altitude missions are not a concern. Lowering the field elevation to sea level does significantly increase the quantities of water produced (up to 11.8 ml in the worst case – climate B2), but it is still significantly below that produced during the oil & gas missions.

## 14.2 Conclusions

The aim of this research project was to investigate the possibility of computationally predicting the quantity of water accumulating in a helicopter fuel tank. This was done by first reviewing available literature on the types, generation pathways and consequences of water accumulation, as well as a review of associated modelling efforts of similar problems (primarily focused on fixed-wing aircraft).

By this literature review, it became apparent that there was a substantial lack of both understanding and modelling effort focusing on rotorcraft. Only one analysis previously existed to estimate water accumulation in helicopters, the Airbus Helicopters step 1 model. This only allowed a unidirectional analysis of water generation, for one time step, and under the assumption that the fuel is always saturated, which is both conservative and unrealistic. Therefore it was decided to develop AHWAS from the ground up. The model improves on each of these limitations, enabling the analysis of water accumulation over an unlimited time period with any mission profile.

During and after the development process, several validation techniques were applied to AHWAS to both inform development decisions and verify correct operation of the model. Comparison between the results produced by AHWAS to those originating from associated models yielded the conclusion that the model performs satisfactorily.

As part of the aforementioned validation procedure, a sensitivity analysis was performed to determine the influence of relevant model input variables on the quantity of water which accumulates in the fuel tank. It was determined that the most important factor is the ambient humidity and the fuel load; the worst case for water accumulation is a flight in humid surroundings with a nearly empty fuel tank. Contrary to the initial assumption, more water accumulates during flights at low altitude than at high altitude because the relative humidity is higher closer to the surface.

As with any simulation of a real system, there is a balance to be struck between certainty and accuracy: the more conservative the assumptions are, the greater the certainty is that the calculated water quantity is on the safe side (greater than reality). If the worst-case assumptions are taken at every step, this leads to a significant overestimation of water accumulation and to unnecessarily frequent drainage operations. Such an abundance of conservatism is theorized to have contributed to the presently prescribed daily interval, without any formal calculation or simulation having taken place. In the present study, assumptions were made such that they are closer to reality, yet still on the conservative side – as an example, all condensed water is assumed to enter the fuel without considering the possibility of re-evaporation which exists in practice. The worst case result shows that it would take 40 days for water to fill the tank sump; therefore the author would personally consider a weekly drainage interval safe and acceptable on the basis of this study. The model delivers reasonable and conservative results to the best of the author's knowledge as well as that of Airbus experts; however, for absolute certainty, it must be validated against physical measured data from real helicopter flights.

With regards to the impact of biofuels, this can be split into two hypotheses:

1. The solubility of water in fuel is determined primarily by aromatic content
2. Greater solubility of water in fuel leads to greater (risk of) water accumulation in the fuel tank.

Hypothesis 1 has been independently proven; hypothesis 2 appears to be true based on the limited analysis performed for this study. The two hypotheses are independent, however due to the limited data available and the limited accuracy thereof, it is not possible to conclusively determine the degree of impact. Additionally, experimentally gathered solubility curves are only applicable to the specific samples investigated and may not be representative of the fuel type as a whole; especially in biofuels, the composition is likely to change depending on the source. Finally, the impact of other non-aromatic substances on water solubility is unknown. The solubility of each new alternative fuel blend must be individually determined to gauge its effect on water accumulation. However, given the water solubility curve of a given fuel blend, the model may be used to estimate the relative difference between two blends, for example a traditional fossil-based one and a proposed biofuel to be introduced.

Ultimately it was found that, depending on the climate, mission profile, refuelling behaviour and fuel blend, the water accumulating in the fuel tank of a medium helicopter may vary from 0.0 to 36.0 ml per day, using the Airbus Helicopters H135 and H160 as reference helicopters. Other helicopter types may produce small variations from these values.

The main research question of the study was:

*Is it possible to improve understanding of the physical phenomena causing water accumulation in helicopter fuel tanks, by developing a computational prediction model?*

On the basis of the results produced by AHWAS, it was found to a high degree of certainty that a drainage interval longer than one day but no more than seven days is feasible from a safety perspective, with the caveat that the model must first be checked against physical measured data from real helicopter flights.

### **14.3 Recommendations**

Validation against physical measured data is an important next step in the development of AHWAS. Data collected after actual helicopter flights would be preferable to include any effects caused by forward flight speed (which is not considered by AHWAS), but data generated in a laboratory climate chamber may be more reliable due to the controlled environment.

Additionally, the effect of cross-ventilation (where one fuel tank is fitted with multiple vent connections to the outside atmosphere) is not currently considered by AHWAS. This is not possible due to the way in which condensation was modelled; however, the effect is not expected to be very large as discussed in section 11.2.1. Nonetheless, this should be verified experimentally before the drainage interval of any helicopter type with cross-venting is changed.

The certification regulations are not clear on the actual limit for free water content of a fuel tank; only the 200 ppmv fuel system functionality requirement provides any indication for how much water is tolerable. A limitation citing water in fuel concentration is not useful when considering multi-day drainage intervals, as the concentration changes along with the fuel quantity present in the tank. The author recommends that a new definition be developed referring to the maximum fraction of the tank sump which may be filled with water at any given time.

For the application of alternative fuel blends, preliminary investigation during the present study has shown that it is not sufficient to generalise a conclusion based on a maximum or minimum content of certain substances in the fuel (this was not the goal); for each new fuel blend, the water solubility curve must be determined and provided to AHWAS to estimate the effect on water accumulation. This curve is generally supplied by the fuel manufacturer.

# 15

## Bibliography

- [1] S. Baena, S. L. Repetto, C. P. Lawson and J. K. W. Lam, "Behaviour of Water in Jet Fuel: A Literature Review," *Progress in Aerospace Sciences*, vol. 60, pp. 35-44, 2013.
- [2] Robinson Helicopter Company, *R22 Pilot's Operating Handbook*, 2004, pp. 4-4.
- [3] L. Lollini, "List of Fuels and Additives Potentially used on AH Helicopters," Airbus Helicopters, Marignane, 2019.
- [4] Eurocopter Deutschland GmbH, *EC 135 T2+ Approved Rotorcraft Flight Manual*, 2006, pp. 4-3.
- [5] S. Baena, "Triton Simscape Model of A330-200. KLM Flights with Biofuel.," Airbus Group, 2015.
- [6] D. King, "Report on the accident to Boeing 777-236ER, G-YMMM, at London Heathrow Airport on 17 January 2008," Department for Transport - Air Accidents Investigation Branch, 2010.
- [7] N. A. Ragozin, *Jet Propulsion Fuels* (translated from the russian by W.E. Jones), London: Pergamon Press, 1961.
- [8] M. Smith, *Aviation Fuels*, Henley-on-Thames: G. T. Foulis & Co Ltd, 1970.
- [9] M. Wetterwald, C. P. Lawson and J. K.-W. Lam, "Feasibility Study of OBIGGS for Water Contamination Control in Aircraft Fuel Tanks," 10th AIAA Aviation Technology, Integration, and Operations (ATIO) Conference, Fort Worth, Texas, USA, 2010.
- [10] Coordinating Research Council, *Aviation Fuel Properties Handbook*, vol. 663, 2014, pp. 2-59.
- [11] J. K.-W. Lam, M. D. Carpenter, C. Williams, J. Hetherington, L. Lao, D. Hammond, C. Ramshaw and H. Yeung, "WAFCOLT - Water in Aviation Fuel Under Cold Temperature Conditions," EASA, 2013.
- [12] V. L. Zherebtsov and M. M. Peganova, "Water solubility versus temperature in jet aviation fuel," *Fuel* 102, pp. 831-834, 13 June 2012.
- [13] C.-J. Tien, Y.-Y. Shu, S.-R. Ciou and C. S. Chen, "Partitioning of Aromatic Constituents into Water from Jet Fuels," *Archives of Environmental Contamination and Toxicology*, vol. 69, pp. 153-162, 2015.
- [14] *Lecture 9: Surface Energy, Surface tension and Adhesion energy*, The University of Nottingham.
- [15] Z. J. West, T. Yamada, C. R. Bruening, R. L. Cook, S. S. Mueller, L. M. Shafer, M. J. DeWitt and S. Zabarnick, "Investigation of Water Interactions with Petroleum-Derived and Synthetic Aviation Turbine Fuels," *Energy & Fuels*, vol. 32, pp. 1166-1178, 2018.

- [16] P. Schatzberg, "Solubilities of Water in Several Normal Alkanes from C7 to C16," *Journal of Physical Chemistry*, vol. 67, no. 4, pp. 776-779, 1963.
- [17] J. Polak and B. C.-Y. Lu, "Mutual Solubilities of Hydrocarbons and Water," *Canadian Journal of Chemistry*, vol. 51, pp. 4018-4023, 1973.
- [18] J. L. Monteith and M. H. Unsworth, *Principles of Environmental Physics*, Amsterdam: AP, 2008.
- [19] Deutscher Wetterdienst, "ICAO-Standardatmosphäre (ISA)," [Online]. Available: [https://www.dwd.de/DE/service/lexikon/begriffe/S/Standardatmosphaere\\_pdf.pdf](https://www.dwd.de/DE/service/lexikon/begriffe/S/Standardatmosphaere_pdf.pdf). [Accessed 29 March 2019].
- [20] A. J. Melo Correia, "NATO STANAG 2895: Extreme Climatic Conditions and Derived Conditions for use in Defining Design/Test Criteria for NATO Forces Materiel," 1990.
- [21] T. Gelas, "Sub System Specification SSS for H160 Environment Control System," 2017.
- [22] K. Parameswaran and B. V. Krishna Murthy, "Altitude Profiles of Tropospheric Water Vapor at Low Latitudes," *Journal of Applied Meteorology*, vol. 29, pp. 665-679, 1990.
- [23] C. H. Reitan, "Surface Dew Point and Water Vapor Aloft," *Journal of Applied Meteorology*, vol. 2, pp. 776-779, 1963.
- [24] R. Sander, "Compilation of Henry's Law Constants for Water as Solvent," *Atmospheric Chemistry and Physics*, vol. 15, pp. 4399-4981, 2015.
- [25] Y. Terada, C. P. Lawson and A. Z. Shahneh, "Analytical Investigation into the Effects of Nitrogen Enriched Air Bubbles to Improve Aircraft Fuel System Water Management," *Journal of Aerospace Engineering*, 2017.
- [26] O. Merkulov, V. Zherebtsov, M. Peganova, E. Kitanin, J. K.-W. Lam and A. Sartori, "OBIGGS for Fuel System Water Management - Proof of Concept," SAE International, 2011.
- [27] M.-G. Medici, A. Mongruel, L. Royon and D. Beysens, "Edge Effects on Water Droplet Condensation," *Physical Review Online Archive, American Physical Society*, vol. 90, no. 6, p. 062403, 2014.
- [28] "PXhere," [Online]. Available: <https://pxhere.com/en/photo/595620>.
- [29] D. R. Durran and D. M. Frierson, "Condensation, Atmospheric Motion, and Cold Beer," *Physics Today*, vol. 66, no. 4, pp. 74-75, 2013.
- [30] H. Mendick, "R&D Learning Path - Fuel Systems - Airframe & Vehicle Integration," Donauwörth, 2019.
- [31] H. Mendick, "EC135 Improved Fuel Sensor - Reduction of Water Susceptibility," Airbus Helicopters, Donauwörth, 2018.
- [32] M. J. Behbahani-Pour and G. Radice, "Fuel Contamination on the Large Transport Airplanes," *Journal of Aeronautics & Aerospace Engineering*, vol. 6, no. 4, 2017.
- [33] P. Krebs, "EC135 Fuel System Water Contamination Tests AHD TN ETVDFG- 13/14," Airbus Helicopters, 2014.
- [34] C. McGregor, "Fuel Contamination: Prevention and Maintenance Actions," *FAST Flight Airworthiness Support Technology*, vol. 38, pp. 26-30.
- [35] International Air Transport Association (IATA), Montreal - Geneva, 2011.
- [36] ASTM International, "Standard Guide for Microbial Contamination in Fuels and Fuel Systems D6469," 2014.
- [37] L. Aris, "Fuel System Water Management - A330/A340 Enhancements," *FAST Flight*

*Airworthiness Support Technology*, vol. 42, pp. 21-25, July 2008.

- [38] M. Yahyaoui, "State of the Art of Water Detection and Management," Airbus Group Innovations, Suresnes, 2016.
- [39] S. L. Repetto, R. Patel, T. Johnson, J. F. Costello, J. K.-W. Lam and C. J. Chuck, "Dual Action Additives for Jet A-1: Fuel Dehydrating Icing Inhibitors," *Energy & Fuels*, vol. 30, pp. 9080-9088, 2016.
- [40] L. M. Balster, E. M. Strobel, M. D. Vangsness, D. D. Pike and D. L. Dalrymple, "Effect of FSII on Microbial Contamination in Jet Fuel: DiEGME and TriEGME," *11th International Conference on Stability, Handling and Use of Liquid Fuels*, vol. 3, pp. 1437-1482, 2009.
- [41] BASF SE & Lufthansa Group, "BASF and Lufthansa start the In-Service-Evaluation of Kerojet® Aquarius - an innovative water scavenger for jet fuels," 2018.
- [42] M. Frank and D. Drikakis, "Draining Water from Aircraft Fuel Using Nitrogen Enriched Air," *Energies*, vol. 11, pp. 908-923, 2018.
- [43] J. K.-W. Lam, D. Parmenter and S. Masters, "Aircraft Fuel Tank Ventilation". United States of America Patent 8,753,429 B2, 17 June 2014.
- [44] T. Godwin, "Investigation of Free Water Detection of NH90 Logic Fuel Probe," NHIndustries, 2017.
- [45] Engineering ToolBox, "Thermal Conductivity of Common Materials and Gases," 2003. [Online]. Available: [https://www.engineeringtoolbox.com/thermal-conductivity-d\\_429.html](https://www.engineeringtoolbox.com/thermal-conductivity-d_429.html). [Accessed 24 04 2019].
- [46] National Bureau of Standards, "Thermal Conductivity of Selected Materials," U.S. Department of Commerce, Washington DC, 1966.
- [47] N. Certain, "H160-B Certification Sheet - CS29.961 Fuel System Hot Weather Operation with TS-1 Fuel - Flight Test Report," Airbus Helicopters, 2017.
- [48] R. Joven, R. Das, A. Ahmed, P. Roozbehjavan and B. Minaie, "Thermal Properties of Carbon Fiber-Epoxy Composites with Different Fabric Weaves," in *SAMPE International Symposium*, Charleston, 2012.
- [49] European Aviation Safety Agency, "Type Certificate Data Sheet No. EASA.R.150 for EC 175," 2019.
- [50] FlightRadar24, "FlightRadar24," [Online]. Available: [www.flightradar24.com](http://www.flightradar24.com). [Accessed 24 04 2019].
- [51] P. McLoughlin, "Report on the Accident to Eurocopter (Deutschland) EC135 T2+, G-SPAO, Glasgow City Centre, Scotland on 29 November 2013," Air Accidents Investigation Branch, Aldershot, 2015.
- [52] European Aviation Safety Agency, "Certification Specifications and Acceptable Means of Compliance for Small Rotorcraft CS-27," 2018.
- [53] European Aviation Safety Agency, "Certification Specifications and Acceptable Means of Compliance for Large Rotorcraft CS-29," 2018.
- [54] Federal Aviation Administration, "FAR part 29 Amdt. 29-10," 1974.
- [55] Federal Aviation Administration, "Notice of Proposed Rulemaking No. 71-12," 1971.
- [56] European Aviation Safety Agency, "Certification Specifications and Acceptable Means of Compliance for Large Aeroplanes CS-25," 2018.
- [57] P. Blanquet, "Rapport d'Activité de la 2ème Année d'Alternance à Airbus Helicopters," 2016.

- [58] A. V. Oreshenkov, "Accumulation of Water in Jet Fuels. Mathematical Modeling of the Process," *Chemistry and Technology of Fuels and Oils*, vol. 40, no. 5, pp. 320-325, 2004.
- [59] A. B. Lambe and J. R. R. A. Martins, "Extensions to the Design Structure Matrix for the Description of Multidisciplinary Design, Analysis and Optimization Processes," *Structural and Multidisciplinary Optimization*, vol. 42, no. 2, pp. 273-284, 2012.
- [60] A. Tiwari, J.-P. Fontaine, A. Kondjoyan, J.-B. Gros, C. Vial and C.-G. Dussap, "Investigation of Interfacial Phenomena During Condensation of Humid Air on a Horizontal Substrate," *Oil & Gas Science and Technology - Revue d'IFP Energies nouvelles*, vol. 69, no. 3, pp. 445-456, 2014.
- [61] Eurocopter, "Eurocopter EC135 Technical Data," 2006.
- [62] R. G. Sargent, "Verification and Validation of Simulation Models," in *Proceedings of the 2011 Winter Simulation Conference*, Phoenix, AZ, USA, 2011.
- [63] S. Duesing, B. Wehner, P. Seifert, A. Ansmann, H. Baars, F. Ditas, S. Henning, N. Ma, L. Poulain, H. Siebert, A. Wiedensohler and A. Macke, "Helicopter-borne observations of the continental background aerosol in combination with remote sensing and ground-based measurements," *Atmospheric Chemistry and Physics*, vol. 18, pp. 1263-1290, 2018.
- [64] H. Yu, P. E. Ciesielski, J. Wang, H.-C. Kuo, H. Voemel and R. Dirksen, "Evaluation of Humidity Correction Methods for Vaisala RS92 Tropical Sounding Data," *Journal of Atmospheric and Oceanic Technology*, vol. 32, pp. 397-411, 2015.
- [65] T. Sakai, T. Shibata, S.-A. Kwon, Y.-S. Kim, K. Tamura and Y. Iwasaka, "Free tropospheric aerosol backscatter, depolarization ratio, and relative humidity measured with the Raman lidar at Nagoya in 1994-1997: contributions of aerosols from the Asian Continent and the Pacific Ocean," *Atmospheric Environment*, vol. 34, pp. 431-442, 2000.
- [66] European Aviation Safety Agency, "Acceptable Means of Compliance and Guidance Material," 2012.
- [67] E. Clinton Wilcox and A. M. Trout, "Analysis of Thrust Augmentation of Turbojet Engines by Water Injection at Compressor Inlet Including Charts for Calculating Compression Processes with Water Injection," NASA, 1950.
- [68] D. L. Deggett, "Water Misting and Injection of Commercial Aircraft Engines to Reduce Airport NO<sub>x</sub>," Boeing Commercial Airplane Group, Seattle, 2004.
- [69] H. Jahani and S. R. Gollahalli, "Characteristics of Burning Jet A Fuel and Jet A Fuel-Water Emulsion Sprays," *Combustion and Flame*, vol. 37, pp. 145-154, 1980.
- [70] International Panel on Climate Change, "Global Warming Potential Values," 2014.
- [71] A. H. Lefebvre and D. R. Ballal, *Gas Turbine Combustion: Alternative Fuels and Emissions*, Boca Raton, FL, USA: CRC Press, 2010.



# Appendix

This appendix provides vertical humidity profile data for Germany, warm marine islands, Japan and India, which exhibit distinctly different magnitudes of humidity and vertical gradient thereof, while also showing similarity in the general trend with altitude.

## Germany

Düsing et al. [63] measured RH and temperature by helicopter up to an altitude of 2300 m at Melpitz, Germany (a rural site in the east of the country). As shown in Figure 64, the ground-level ambient temperature and humidity classify it as climate category A3.

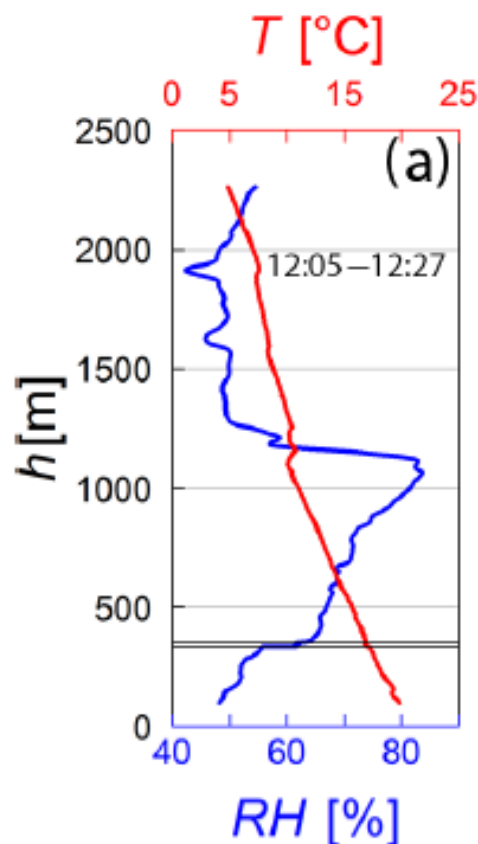


**Figure 64: Measured RH and temperature vertical profiles in Melpitz, Germany, September 2013 [63]**

The measured temperature lapse rate of  $-0.0065 \text{ K m}^{-1}$  corresponds exactly to the value given by ICAO. RH initially increases linearly with altitude from ground level up to approximately 1100 m, inversely proportional to the temperature, indicating a constant specific humidity. There is then a step change to a lower RH of 50%, which subsequently remains almost constant at higher altitude. This altitude will be referred to as the transition altitude henceforth; the transition altitude frequently coincides with the cloud ceiling. In this particular case, a small inversion can be spotted: just at the step change in RH, the temperature gradient is briefly inverted. This indicates a very stable weather condition with no significant turbulence which might affect low-level humidity.

The reliability of this data is limited by the absence of multiple measurements; a single measurement typically cannot be relied upon to be accurate. Nonetheless it does provide a useful indication of the general vertical profile, which could be used as an initial modelling input.

## Tropical Oceans

Yu et al. [64] give some data from humidity prediction models, based on three locations: Gan (Maldives), Manus (Papua New Guinea) and Nauru. All three are small islands surrounded by large bodies of water, in close proximity to the equator; the most plausible climate category is therefore M1 or M2 (marine hot or marine intermediate). One example is shown in Figure 65.

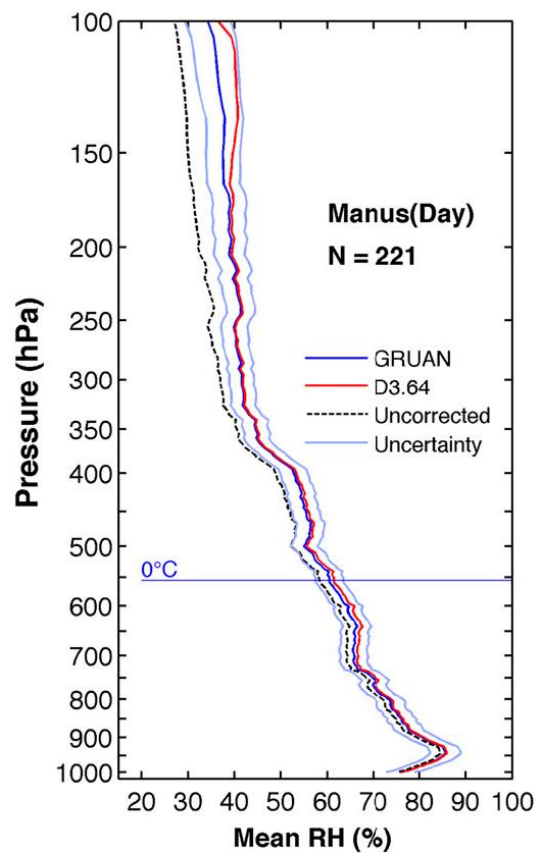


**Figure 65: RH altitude profile from models, for Manus (Papua New Guinea) [64]. Data fits best within climate category M2 “marine intermediate”.**

The RH profile at low altitude exhibits a similar pattern to the measurements taken in Germany: a steady increase up to around 1000 m altitude, followed by a rapid decrease (refer to Figure 9 to convert between pressure and altitude), even though the RH values differ in magnitude.

This result suggests that above the initial peak in RH, a linear progression of RH could be considered for the altitude range relevant to helicopters. The transition altitude is slightly lower than that in the results from Germany, suggesting a lower cloud ceiling.

## Japan

Sakai et al. [65] provide vertical RH profiles measured throughout the year 1994 over Nagoya, Japan (Figure 66). Nagoya falls into climate categories A3, B2 and C0 depending on season. These data are especially interesting as they also provide the mixing ratio (equivalent to specific humidity). When specific humidity is very low (i.e. at low temperatures), it becomes very difficult to accurately measure, which increases the uncertainty in the relative humidity. This is the case in the December measurement below.

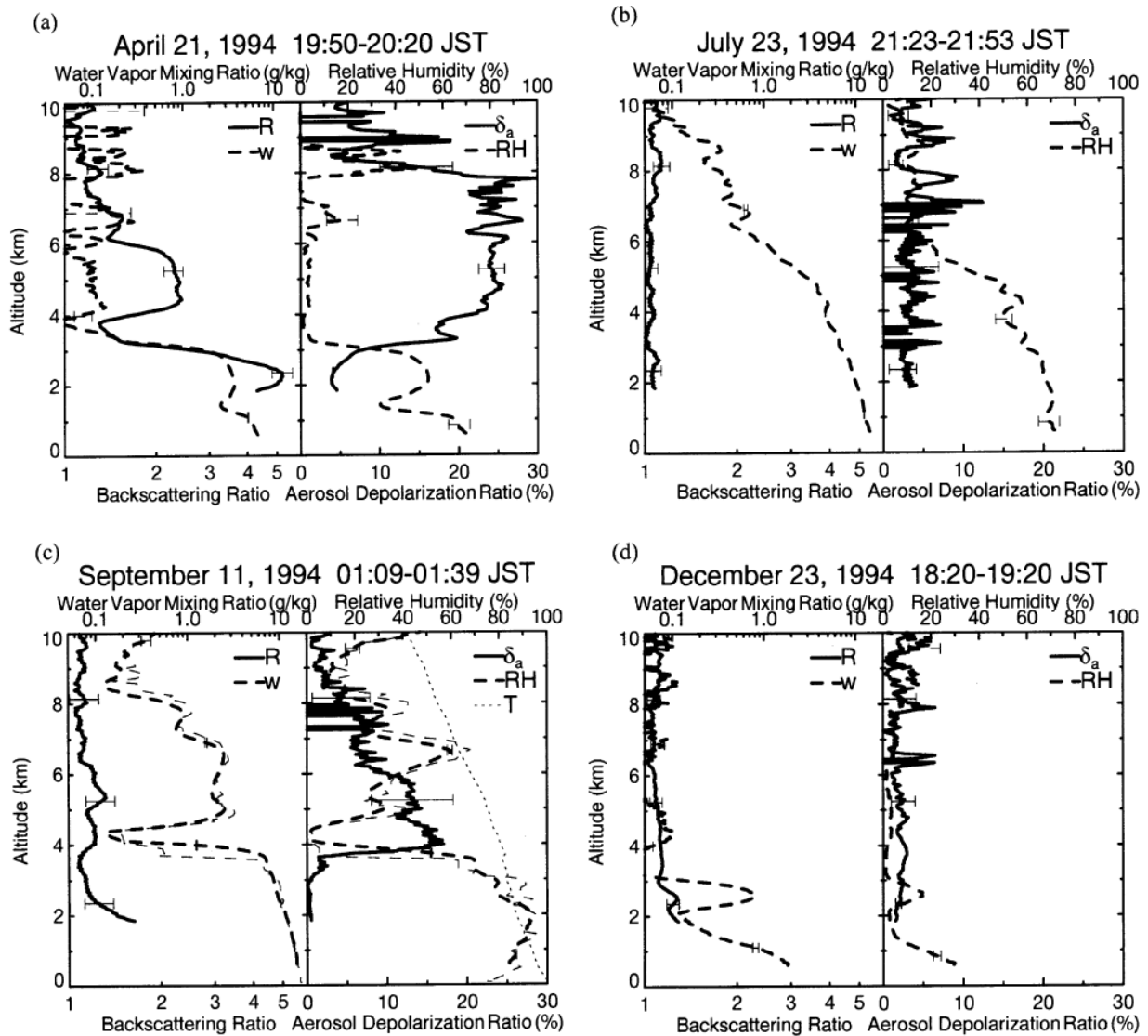


Figure 66: Measured vertical RH profile over Nagoya in 1994 [65], in all 4 seasons.

All 4 measurements show RH generally decreasing with altitude; the lowest altitude for which data are given is approximately 800 m. The December measurement suggests that RH is very low in climate category C0; this contradicts NATO, which gives 100% RH in this condition. However, the saturation specific humidity at  $-6^{\circ}\text{C}$  is 10 times lower than at  $+30^{\circ}\text{C}$ . Minor fluctuations and measurement errors therefore deliver wild variations in measured RH.

These results indicate a transition altitude between 1.5 and 6 km depending on the season: warmer seasons produce higher transition altitudes. This poses an interesting contrast to the data for both Germany and tropical oceans, which indicate higher temperature produces lower transition altitudes. Wind might be a factor that unfortunately was not recorded in any of the papers.